THE JOURNAL
OF
CHEMICAL PHYSICS

VOLUME 2 APRIL, 1934 NUMBER 4

Concerning the Structure of N-Alcohol Solutions of Lithium Chloride

G. W. STEWART, *University of Iowa*
(Received January 23, 1934)

Since in x-ray diffraction both experimental results and theoretical considerations are in agreement as to the presence of structure in liquids, an x-ray study is made of concentrated solutions of LiCl in the three normal alcohols, ethyl, propyl and butyl. A definite but tentative conclusion is that in these concentrated solutions of a strong electrolyte, both Li^+ and Cl^- participate with the molecules of the solvent in forming a common liquid cybotactic or quasi-crystalline structure. This is a new conception which may be made to include what have been described as "ionic clouds" and as "association." A conclusion of secondary importance is that the solutions are in fact solutions of the alcoholates of LiCl, although above the corresponding transition temperatures.

THE problem of the structure of concentrated electrolytic solutions is both interesting and difficult. Great advances have been made, but so far removed is a satisfactory understanding that additional evidence secured by every method of approach possible is highly desirable. The study of the structure of liquids by the diffraction of x-rays has shown beyond reasonable doubt that liquids generally have an orderliness in the arrangement of their molecules. One would expect that the x-ray method of investigation, though crude, could shed valuable light for, after all, it is a very direct approach to the nature of the structure of a liquid.

Since the x-ray results are only statistical time averages, the nature of the structure of a liquid cannot be obtained with the uniqueness possible in crystals. At the present time either one of two conceptions of the liquid structure seem to be plausible. One is that immediately about any point of observation, for a distance of from 10A to 20A, the arrangement of scattering centers approximates very closely to that of a crystal. If the liquid is near the freezing temperature, the crystal structure referred to is that of the solid. This approximately regular structure may change materially with temperature. An important feature of the picture is that the point of observation specified is any scattering center. The liquid is therefore assumed to be homogeneous. This conception could be only approximately correct, for this homogeneity would demand a repetition of like structure or a crystalline structure in fact, which obviously is not the case. It is in the approximation that allowance is made for temperature effects and the relative movement of the molecules. So the conception may be regarded as representing really a statistical mean rather than an instantaneous condition. The other plausible conception is not so clearly stated but is an instantaneous picture. It assumes that, at any instant, the liquid is spotted throughout with regions which are quite orderly, as assumed in the other view, fading away into regions with little orderliness. There is a constant shifting of position with the result that a given molecule does not continue to remain in a well-defined group. At any instant, then, part of

the molecules participate in one or the other of these regions. An orderly region may be called a "group," though of course without sharp boundaries. The name "cybotactic group" has been given to it for convenience. The liquid is not homogeneous in detail. The latter conception is probably nearer the truth though the x-ray observations do not distinguish between the two views. But the former one has the advantage of being easily applied to computation. This has been done and reasonable structures have been found[1] to give approximately the observed diffraction curves. It is fair to say that in view of the large number of consistent experimental results[2] and of the satisfactory comparison with theoretical considerations, liquids generally do have a structure and that these results, which give a clearer conception of solutions, may become of quantitative importance. To this structure the name "cybotaxis" has been given because it is neither fluid nor crystalline but yet a crude and unstable imitation of the latter. At times reference has been and will be herein made to cybotactic "groups," by using thereby the second conception given above of the liquid structure.

By interpreting the results now presented through the use of previous x-ray studies of liquids, the following tentative conclusion seems evident. In a concentrated solution of a strong electrolyte, LiCl, both the ions and the molecules of the solvent, n-alcohol, participate in the same liquid (cybotactic) structure and there is no significant change in the liquid structure as the unsaturated liquid passes through the solute's temperature of transition to an alcoholate. The importance of the conclusion, if true, is evident, for it gives a new relationship of ions with ions and ions with solvent.

[1] For water, Bernal and Fowler, J. Chem. Phys. **1**, 518 (1933); for para-azoxyanisol, Buchwald, Ann. d. Physik **10**, 558 (1931); for n-paraffins, Warren, Phys. Rev. **44**, 969 (1933); for ethyl ether near the critical point, Warren, Phys. Rev. **44**, 969 (1933). These computations follow the method of Zernike and Prins, Zeits. f. Physik **41**, 184 (1927) and Debye and Menke, Phys. Zeits. **31**, 797 (1930) and Ergebnisse der Technischen Röntgenkunde, Vol. II, p. 1, Akad. Verlagsgesell., Leipzig, 1931.

[2] For the lines of experimental evidence see Stewart, Indian J. Physics **7**, Pb. 6, 603 (1933).

Previous Conclusions

Prins[3] investigated water solutions of LiBr, LiI and KI. He applied the Debye-Hückel ionic cloud theory to ascertain the probability distribution of the anions and found certain qualitative agreement but also quantitative disagreement. Later he[4] investigated water solutions of KCl, NaBr, $SrBr_2$, $BaCl_2$, $AgNO_3$ and $Pb(C_2H_3O_2)_2$. He concluded (1) that the ions are arranged in the solutions in a more orderly manner than would be expected according to the geometrical Spielraum, and (2) that the ionic cloud computations do not agree with experiment. Prins[5] also remarks that one may account for the absence of the typical gas diffraction picture by assuming that the ions have about them solid water shells which are independent of concentration and approximately monomolecular.

Meyer[6] has investigated the water solutions of NaCl and LiCl. The Cl^- ions were sufficient in number to give a definite effect if arranged at corners of a cube 6 A on a side or scattered at random throughout the liquid. The diffraction curve gave no evidence either of this structure or of gaseous scattering from Cl^-.

Good[7] has used aqueous solutions of LiCl, NH_4SO_4, CaCl, KCl, KB, KI, and finds in the case of the sulphate a new inner ring which he suggests might be formed by complexes of water molecules and NH_4^+.

Experimental Method

Mo $K\alpha$ radiation, Soller slits, methyl bromide ionization chamber and differential readings with $SrCO_3$ and ZrO_2 screens[8] 0.036 g/cm² and 0.0025 g/cm²,[9] respectively, were used. By this method the elimination of all but the Mo $K\alpha$ radiation was effected. This is shown by the diffraction curve of an aluminum rod 3 mm in diameter for

[3] Prins, Zeits. f. Physik **56**, 617 (1929).

[4] Prins, Zeits. f. Physik **71**, 445 (1931).

[5] Prins, Naturwiss. **21**, 435 (1931).

[6] Meyer, Ann. d. Physik **5**, 701 (1930).

[7] Good, Physica Acta **4**, 205 (1930).

[8] Ross, Phys. Rev. **28**, 425 (1926); J.O.S.A. **16**, 443 (1928).

[9] The number of g/cm² were chosen so that the transmission of wave-lengths other than the Mo $K\alpha$ would be equal for the two screens and yet the difference in transmission for the Mo $K\alpha$ would be an optimum.

which the readings with the filters were alike in all but the $K\alpha$ region. The Soller slits were those previously described[10] and gave a peak width at half height of approximately 26 seconds with crystal diffraction.

The solutions were those of LiCl in n-ethyl, n-propyl and n-butyl alcohols. The percentage of saturation was obtained by dissolving the correct weight in the solvent. The saturated solution was secured by heating the base of a test tube containing the solvent and an excess of LiCl for two weeks, the temperatures of the base being maintained at 50°C. The solubility of LiCl in grams per 100 grams of the solvent was determined at 25°C and found to be 12 percent for n-butyl. This is in slight disagreement with other recorded values[11] for the same temperatures which are respectively 42.3 at 50°C and 10.6 at 25°C. The values of 24.7 percent for n-ethyl and 16.0 for n-propyl, quoted in Seidell, were verified and adopted. The solubility of the salt in n-butyl was redetermined after the solution had been standing in contact with excess LiCl for more than seven months, and the result obtained was 12.2 grams, an increase of less than two percent.

The solutions were placed in the path of the x-ray beam in a very thin-walled cylindrical glass container, having a diameter about 0.8 of the "optimum" thickness,[12] although the optimum thickness precaution is not so important with the differential filter readings as when using a zirconium filter only.

The temperature regulation of the solution in the path of the x-ray beam was obtained by the circulation of air in a heat insulated enclosure having very thin mica windows. For temperatures in the neighborhood of 0°C, the air was passed through a copper tube immersed in a bath of salt, ice, and water. For much lower temperatures, a current of cold air was obtained by evaporating liquid air from a special vessel containing an electric heater. The flow of the air and thus the temperature of the air bath was controlled by the supply of heat through current regulation.

The following are possible corrections of the readings:

1. The effective difference in thickness of the fluid in the container at different angles of diffraction.
2. The variation in the absorption of the container and mica windows and in their scattering at different angles of diffraction.
3. The lack of parallelism of the x-rays and the penetration of the Soller slits.
4. The incoherent radiation.

For the small angles of diffraction used in this report, less than 15°, corrections 1 and 4 are not important, for as will be shown, no use is made of the exact position of diffraction peaks and great accuracy is not required. Corrections 2 and 3 were approximated as follows. The readings were taken throughout the range with the container empty. These were reduced because of absorption of Mo $K\alpha$ when the liquid is in place, and then used as corrections for the actual observations. In taking readings the current in the ionization chamber was always read first with one filter in position and then the other. Then the spectrometer setting was altered to an equal angle on the other side of 0°.

Results

Figs. 1, 2 and 3 show the experimental curves for the x-ray ionization current with n-ethyl, n-propyl and n-butyl alcohols after correction is made for slit penetration, container and mica window scattering. Each point is the average of two, one on each side of $\theta = 0°$. The percentage of saturation is shown for each curve, all being taken at 24°C. Each curve has a different zero ordinate, as indicated on the left-hand margin, and all are altered to have the same maximum ordinate.

Fig. 4 shows the chief lithium chloride alcoholate crystal diffraction peaks obtained with samples secured by plunging a saturated solution of each into liquid air, the purpose being a very rapid formation of the crystals and thereby a lack of preferred orientation. Measurements were made on two solidifications in each instance and the readings were in sufficient agreement to assert that the chief diffraction peaks of each alcoholate have approximately the relative values

[10] Stewart, Phys. Rev. **30**, 232 (1927).

[11] Seidell's *Solubilities of Inorganic and Organic Compounds*, 2nd Ed., D. Van Nostrand, 1919.

[12] This optimum thickness was computed from the following value of μ.

$$\mu/\rho = (1.36\times10^{-2}\lambda^3\Sigma N^4 + \Sigma.32N)/\Sigma A$$

wherein N is the atomic number and A the atomic weight.

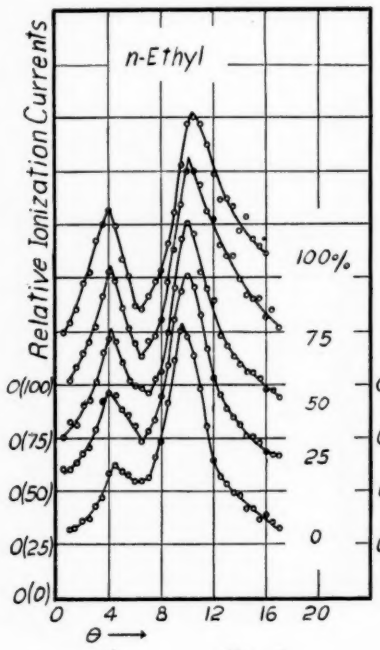

FIG. 1.

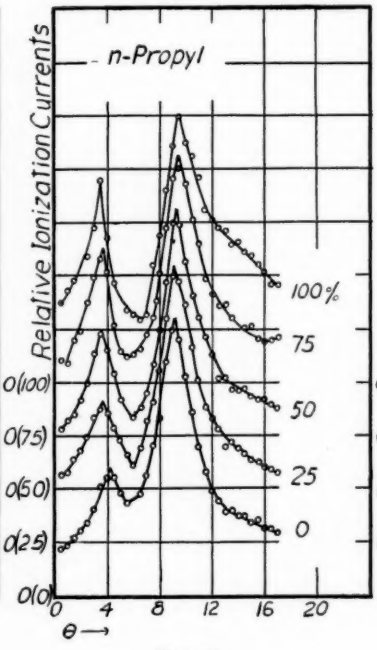

FIG. 2.

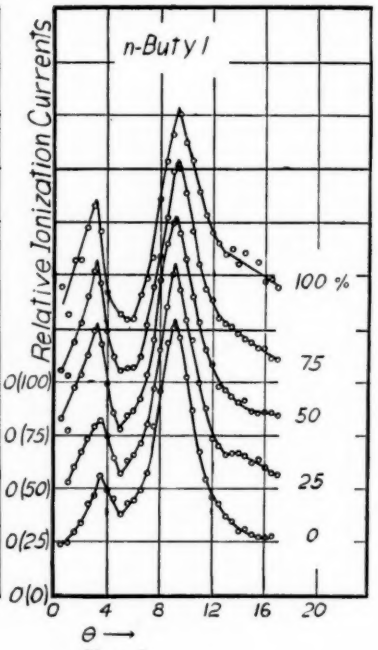

FIG. 3.

FIG. 1. Relative diffraction intensities, Mo $K\alpha$ radiation, n-ethyl alcohol solutions of lithium chloride.
FIG. 2. Relative diffraction intensities, Mo $K\alpha$ radiation, n-propyl alcohol solutions of lithium chloride.
FIG. 3. Relative diffraction intensities, Mo $K\alpha$ radiation, n-butyl alcohol solutions of lithium chloride.

indicated. The complete curve in each case was not obtained because, as will be seen, the discussion involves only the chief intensity peaks. The temperature of observation for the alcoholates was kept at -15°C which was well below the temperature for the solubility curve in each case. The temperature of the transition point or of the junction of the alcoholate and salt solubility curve is 17.4°C for the n-ethyl,[13] $+3$°C for n-propyl and -3°C for n-butyl as determined within 1° or 2° in these experiments.

In Fig. 5 a diffraction curve for each alcohol is taken several degrees below its transition temperature. Again zero ordinates are shifted for convenience and the maxima are reduced to the same scale. The solutions were 75 percent saturated at 24°C, and then cooled. The solid alcoholates would appear with these solutions at 10°C with the n-ethyl, at -9°C to -10°C with the n-propyl and at -20°C to 25°C with the n-butyl alcohol. The temperatures of observation are respectively 12°C, -7°C and -10°C and are in each case below the transition temperature with the samples wholly liquid. Under this condition of temperature and concentration the solution is in each case that of the alcoholate.

DISCUSSION

A reasonable deduction can be made directly by comparison of Fig. 5 with Figs. 1, 2 and 3, without the use of any assumptions. Each of the curves in Fig. 5 is closely like the curve for the same solution at 24°C as shown in the other figures. The ratio of major and minor peak intensities for a curve in Fig. 5 was computed and then compared with the like ratio in the corresponding curve in Figs. 1, 2 or 3. In the solutions with each alcohol the ratios are the same within 8 percent and the peak positions are alike within measurement error. There is a small difference in a noticeable lessening of the minor peak width at the lower temperature, which, other experiments show, may readily be only a direct temperature effect. But since the solutions at the lower temperatures in Fig. 5 are obviously alcoholate solutions, then because of the likeness of diffrac-

[13] Obtained by Turner and Bissett, J. Chem. Soc. **103**, 1904 (1913).

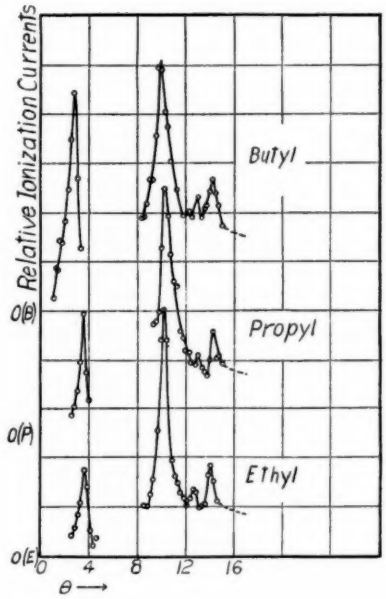

FIG. 4. Most prominent Mo $K\alpha$ diffraction peaks with powdered lithium chloride alcoholate crystals.

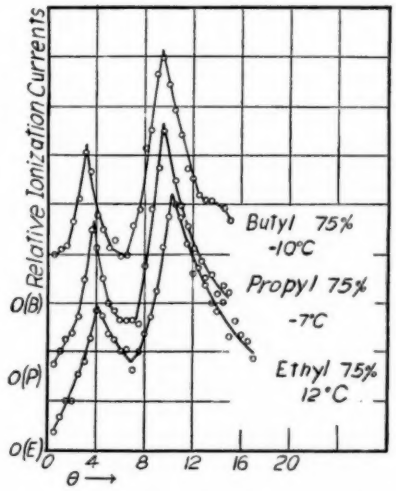

FIG. 5. Relative diffraction intensities, Mo $K\alpha$ radiation, n-ethyl, -propyl, and -butyl solutions of lithium chloride at temperatures below the respective alcoholate transition points.

tion, or the same arrangement of scattering centers, those in Figs. 1, 2 and 3, at the higher temperatures, would appear to be also the same alcoholate solutions.

A second conclusion can be obtained by reference to previous experiments with miscible solutions. It is that the ionic LiCl alcoholate forms a liquid structure with the solvent molecules and that the diffraction curves arise from this structure or grouping. This is fundamentally important, if true. For it is a conception of the rôle of the solvent molecules, of the ionic cloud and of association, all in one. It has been conclusively shown[14] that when two thoroughly miscible liquids are mixed, one does not get two corresponding sets of x-ray diffraction peaks for the solution, but only one, this corresponding to a cybotactic structure in which both constituents participate. Indeed, the evidence is that the case in liquids is analogous to that in solid solutions.[15] Thus one would expect that varied mixtures of a hypothetical liquid alcoholate and a n-alcohol would give shifting peaks with the pattern altering from that of the n-alcohol to that of the alcoholate as the amount of alcoholate in the solution is varied. The position of the diffraction peaks for the hypothetical liquid alcoholate can be judged from the diffraction with the crystal form. For it is well known in liquid diffraction experiments that the liquid curve has its broad diffuse bands approximately in the regions of the greatest "density" of peak energies on the crystal diffraction curve. With increasing concentration of the alcoholate in the n-alcohols, the peaks shift as if the liquid solute alone would have peaks at the small angle of 2° or 3° and in the region greater than 10°. But this is just what the crystal alcoholate diffraction curves would suggest on the ground of the peak density rule already stated. Thus the change in diffraction curves with concentration is clearly consistent with the tentative conclusion that the ionic alcoholates of LiCl forms a liquid (cybotactic) structure with the solvent molecules. It would seem that the conclusion from miscible liquids is justified whether or not the alcoholate may exist as a separate liquid. It is upon the effect of the final mixture and the crystal itself that the argument is based.

[14] Meyer, Phys. Rev. **38**, 1083 (1931).

[15] Of course the reference here is to the simple case of like crystals in the solid solutions. Experiments with liquids have not proceeded far enough to obtain analogies with all the cases found in solid solutions.

One justification of the selection of the alcoholate as the solute in reaching the second conclusion has been expressed in the first conclusion above. Another is that the chief peaks for LiCl crystal for Mo $K\alpha$ radiation would occur at 13.9° and 16°[16] and liquid peaks in this region could not, according to the above argument, give the observed effect of the concentration of LiCl. The solute must be the alcoholate. It thus seems that, from our present knowledge of x-ray diffraction in liquids, one is led to the definite but of course tentative conclusion that the liquid groupings in the solutions are those of the alcoholates in normal alcohol. The important feature is, however, that there is a liquid structure in which both Li^+ and Cl^- participate with the alcohol molecules.

A confirmation of this view is that there is no evidence whatever for gaseous scattering due to Cl^- near 0°.[17] If there were random ions of Cl^- and if they were in sufficient number this gaseous scattering would be found. But in the case of the saturated solution of n-ethyl alcohol the number of chlorine ions is approximately one-fourth the number of alcohol molecules, and hence the number of scattering electrons in the former is about one-fifth of the latter. If the Cl^- ions give incoherent scattering as in a gas, there would be a noticeable relative increase in scattering near 0°. (The relative intensities in the various curves have been reduced to the same value at the higher peaks.) In Figs. 1, 2 and 3, one finds no evidence whatever for gaseous scattering near the zero, for in Fig. 1 the curve for normal ethyl alcohol, if extended, would meet $\theta = 0°$ at a point about 20 percent of the intensity of the chief maximum. For 20 percent saturation this is slightly increased but for 80, 75 and 100 percent saturation the corresponding value is actually decreased. In n-propyl and n-butyl alcohol the differences are negligible. Although these curves have not been corrected and presented so the diffraction with the same number of alcohol molecules is shown, yet the effect of the Cl^- ions, if at random, would clearly be in evidence.

Judging from these consistent evidences, one may then regard the conclusion as at least strongly indicated that the LiCl occurs in liquid cybotactic groups, in which both the alcoholate and alcohol participate. Presumably the LiCl is ionized and hence these temporary cybotactic structures may be regarded as analogous to ionic crystals. Indeed, it is already known that conduction in ionic crystals has definite similarities to conduction in electrolytes. Just how far this conception of the structure of concentrated electrolytic solutions will be found general one can only surmise. Experiments by the author in water solutions are at present in entire harmony with the view here expressed, but the details will be presented in a subsequent paper.

I wish to acknowledge with appreciation my indebtedness for the observational work recorded herein to Dr. R. M. Zabel, research assistant.

[16] According to the measurement of Davey, Phys. Rev. **21**, 143 (1923).

[17] Attention has already been called by Prins (reference 5) to this same absence of scattering in aqueous solutions.

An X-Ray Study of the Structure of Liquid Benzene, Cyclohexane and Their Mixtures*

HERBERT K. WARD, *Pennsylvania State College*

(Received January 15, 1934)

Carefully purified benzene and cyclohexane exhibit x-ray diffraction peaks corresponding to preferred spacings of 4.68A and 5.09A, respectively, which are interpreted as the effective thicknesses of the respective rings. Mixtures of these two hydrocarbons give rise to two independent diffraction peaks indicating emulsion-type solutions, in which the disperse phase is too small to show even a Tyndall effect.

INTRODUCTION

STUDIES of the x-ray diffraction effects exhibited by liquids have given much information concerning the nature of the liquid state. These studies, at least in the case of liquids composed of molecules not having spherical symmetry, appear to substantiate Stewart's cybotactic theory.[1]

The spacings corresponding to the diffraction peaks exhibited by liquids composed of disk shaped molecules, such as benzene and cyclohexane, have been shown[2] to correspond to the effective thicknesses of the respective rings or disks. The positions of the diffraction peaks given by these two liquids have been measured also by other workers[3] with fairly concordant results.

Several binary liquid systems have been studied.[4, 5, 6] The earlier work of Wyckoff[6] indicates a pure addition of the diffraction effects of the components. Krishnamurti[4] finds some cases belonging to this class and postulates the coexistence of the original groupings, as: *AAAA*, *BBBB*. For other solutions he finds one halo or diffraction peak for the solution located at a continuously variable position between those corresponding to the components; for this (second) class, groupings such as *ABABAB*, A_mB, A_mB_n, AB_n are postulated. Meyer,[5] however, finds all of the systems studied by him, excepting phenol-water below the critical solution temperature, belonging to Krishnamurti's second class. Other studies of liquid solutions include, in addition to binary liquid systems, also cases of solid solutes in various solvents, chiefly water.[7]

Krishnamurti[4] suggests that the action of a solution toward the salting out effect (he here refers to aqueous solutions) might serve to indicate to which class the solution belongs. Meyer,[5] however, perhaps more logically, places

* From a thesis submitted to the Graduate School of the Pennsylvania State College in partial satisfaction of the requirements for the degree of Ph.D. in Physical Chemistry and Chemical Physics.

[1] G. W. Stewart, Chem. Rev. **6**, 483 (1929); Rev. Mod. Phys. **2**, 116 (1930).

For other reviews see: C. Brucker, Phys. Zeits. **29**, 373 (1928); W. Good, Helv. Phys. Acta **3**, 205 (1930).

[2] G. W. Stewart, Phys. Rev. **33**, 889 (1929).

[3] P. Debye and P. Scherrer, Nachr. Kgl. Ges. Wiss. Göttingen (1916); p. 1.

E. D. Eastman, J.A.C.S. **46**, 917 (1924).

C. W. Hewlett, Phys. Rev. **22**, 688 (1922).

J. R. Katz, Zeits. f. Physik **45**, 97 (1928).

W. H. Keesom and J. de Smedt, Proc. Amst. Acad. Sci. **25**, 118 (1922); **26**, 112 (1923).

P. Krishnamurti, Ind. J. Phys. **4**, 104 (1928).

C. V. Raman and C. M. Sogani, Nature **119**, 601, (1927).

S. S. Ramasubramanyam, Ind. J. Phys. **3**, 127 (1928).

W. C. Pierce, Phys. Rev. **38**, 1413 (1931).

C. M. Sogani, Ind. J. Phys. **1**, 357 (1927); **2**, 97 (1927).

E. W. Skinner, Phys. Rev. **36**, 1625 (1930).

[4] P. Krishnamurti, Ind. J. Phys. **3**, 331 (1929); **3**, 507 (1929).

[5] A. W. Meyer, Phys. Rev. **38**, 1083 (1931).

[6] R. W. G. Wyckoff, Am. J. Sci. **5**, 455 (1923).

[7] K. Banerjee, Ind. J. Phys. **3**, 399 (1929).

W. Good, Helv. Phys. Acta **3**, 305 (1930).

P. Krishnamurti, Ind. J. Phys. **2**, 501 (1928); **3**, 209 (1928).

W. C. Pierce, Phys. Rev. **38**, 1413 (1931).

J. A. Prins, Nature **123**, 84 (1929); Phys. Zeits. **30**, 525 (1929).

H. Shiba and T. Watanabe, Sci. Papers. Inst. Phys. Chem. Research (Tokyo) **10**, 187 (1929).

M. Ishino, S. Tanaka and A. Tsuji, Mem. Coll. Sci. Kyoto Imp. Univ. **13**, 27 (1930).

solutions into the two classes: emulsion type and true solution type. In the former, two distinct types of cybotactic groups are postulated to exist, while in the latter both components enter into the same cybotactic groups, supposedly the groups have about the same composition as the macro-composition of the solution.

There is no reason to doubt the technique, results, or interpretation of any of the workers as there is little duplication in the systems studied by the different workers. However, only qualitative agreement exists between the work of Meyer and of Krishnamurti on the two systems: phenol-water and tetranitromethane-cyclohexane.

Apparatus

X-radiation

A molybdenum anode Coolidge type x-ray tube (G. E. X-ray Corp.) was operated at 20 milliamperes and at about 30 kilovolts r.m.s. The usual zirconium oxide in celluloid filter (supplied by G. E. Company) transmits selectively the $K\alpha$ group of molybdenum (7.10A), however, there is an appreciable transmission of the white radiation at about 0.4A. This was corrected for by the use of a balanced strontium oxide filter[8] made by soaking several pieces of blotting paper, free from filler containing heavy atoms, in strontium nitrate solution, drying, and assembling with the use of Duco Household Cement. The whole filter was then impregnated with celluloid.

Spectrometer

The spectrometer was constructed with an horizontal axis of rotation in order that it may be used for certain studies planned for the future. Essential features of the spectrometer are given by Fig. 1. The scale given in the figure applies only in directions parallel to the x-ray beam. Dashed lines have been used to indicate an alternative position of the spectrometer arm. The mirror, lamp and scale used for the measurement of the angles of diffraction have not been indicated. The Soller slits[9] used for both collimator and ionization chamber each consist of ten parallel slits 19.7 cm long by 0.0795 cm wide by 1.27 cm, with lacquered iron foil 0.0076 cm thick as separators.

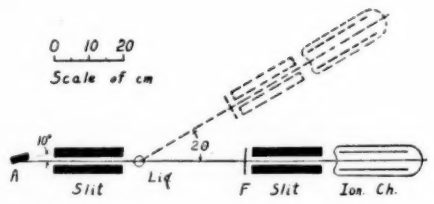

FIG. 1. Diagram of spectrometer. (Scale applies only to directions parallel to the x-ray beam.) *A*, Mo anode of Coolidge type x-ray tube. *Slit*, Soller type slit (see text). *Liq.*, Liquid being measured. *F*, ZrO_2 or SrO filter (see text). *Ion.Ch.*, ionization chamber.

Sample holder

The sample holder was made of nickel plated brass with cellophane windows, cemented on with Duco Household Cement. The sample holder could be filled, emptied and washed without removing it from its position on the spectrometer. The spacing (1.3 cm) between the two cellophane windows is definitely less than the optimum thickness (about 1.6 cm) in order to avoid undue filtration effect on the x-ray beam by the sample.

Ionization chamber

The ionization chamber used (see Fig. 2) was blown from Pyrex with a Pyrex window about 0.1 to 0.2 mm thick and was filled with methyl bromide at 74 cm pressure. Electrodes made from

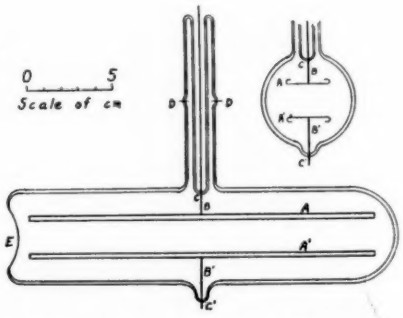

FIG. 2. Ionization chamber. *A*, *A'*, Electrodes made of 10 mil (0.25 mm) sheet nickel (polished). *B*, *B'*, 40 mil (1.0 mm) stub nickel leads electrically welded to electrodes (*A*, *A'*) and to 40 mil tungsten leads used to make the metal-to-Pyrex seals. *C*, *C'*, Tungsten-to-Pyrex seals. *DD'*, Copper disk-to-Pyrex seals (see text). *E*, Thin Pyrex window.

[8] P. A. Ross, Phys. Rev. **28**, 425A (1926).
W. C. Pierce, ibid. **38**, 1409 (1931).
[9] W. Soller, Phys. Rev. **24**, 159 (1924).

polished sheet nickel each 20 cm long by 2.6 cm wide and about 2.0 cm apart were used. A copper disk sealed[10] into the Pyrex side tube provides electrical guarding for the collector electrode and lead. The side tube used for preliminary evacuation, testing for leaks, filling of the chamber is not shown; this was later sealed off.

Vacuum tube electrometer

The vacuum tube electrometer used to measure the ionization currents is shown schematically in Fig. 3. This amplifier uses the General Electric

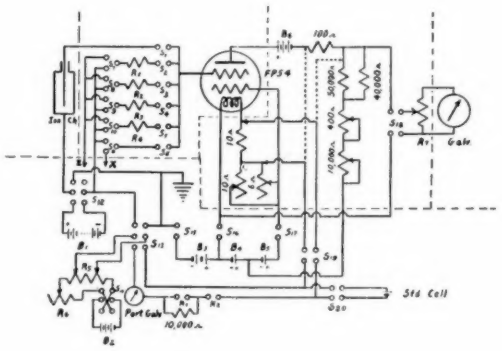

FIG. 3. Vacuum tube electrometer. R_1, 7×10^{11} ohms. R_2, 2.5×10^9 ohms. R_3, 10 megohms. R_4, 1.0 megohm. R_5, L. and N. student potentiometer. R_6, L. and N. dial decade resistance box 9(100+10+1+0.1) ohms. R_7, Galvanometer shunt—10+100+1000+10,000 ohm fixed resistors in series with an inductance switch connected to all junctions. S_1 to S_6, Sealing wax insulated switches with mercury-copper contacts. S_7 to S_{20}, Switches of suitable mechanical construction—"jack" knife, and Pyrex insulated mercury copper contacts (these in the filament circuit).

electrometer tube—Pliotron FP54.[11] A number of circuits using this tube have been described recently,[12] being used for various purposes. The overall sensitivity of the amplifier here described is about 6×10^{-16} amperes per division using a rugged galvanometer* having a sensitivity of 1.3×10^{-8} amperes per division. This has been accomplished without recourse to rate of deflection technique, usually used for the higher current sensitivities.

The several sections of the circuit have been separately shielded as indicated by the dashed lines. The ionization chamber battery (B_1) is also separately shielded, similarly the several storage batteries (B_2 to B_6) are shielded as a unit. Shielded flexible wires are used between the several shield boxes. All shielding and electrical guarding are connected together and jointly grounded.

Sealing wax insulators made from a tested supply of sealing wax have been used throughout the high insulation part of the circuit. For measuring currents of various magnitudes any one of several grid leaks (R_1, R_2, R_3, R_4) may be selected by suitable switches (S_2 to S_{10}). Resistors supplied commercially† have been found satisfactory for use as grid leaks. Good quality commerical wire wound resistors have been used elsewhere in the circuit, excepting those used for protection purposes only. Potential for the ionization chamber is supplied by a number of large radio B batteries in series (B_1), while other voltages required are supplied by storage batteries of large capacity (B_2 to B_6).

Leads X and Z, normally connected to ground, have been provided for test purposes and the intercomparison of the several grid leaks when using the FP54 as the indicating instrument.[13] The filament current of the FP54 may be measured with the potentiometer (R_5) by the IR drop through a 10 ohm resistor in the filament circuit. When desired the plate (anode) current may be measured by transferring these leads to the 100 ohm resistor in the plate circuit as indicated by the dotted lines.

MATERIALS

Benzene

Benzene was purified by successive treatments with sulfuric acid, treating with mercury, washing with water, drying, distillation, and several fractional recrystallizations. This method is

[10] W. G. Housekeeper, Trans. Am. Inst. Elect. Eng. **42**, 870 (1923).

[11] G. F. Metcalf and B. J. Thompson, Phys. Rev. **36**, 1489 (1930).
A. W. Hull, Physics **2**, 409 (1932).

[12] A. DuBridge, Phys. Rev. **37**, 392 (1931).
Heil and Edwards, Phys. Rev. **43**, 1 (1933).
S. E. Hill, Science **73**, 529 (1931).
F. J. Moles, Genl. Elec. Rev. **36**, 156 (1933).
W. Soller, Rev. Sci. Inst. **3**, 416 (1932).

* Leeds and Northrup—Catalog number 2400a.

† S. S. White Dental Supply Co., 154 W. 42nd St., New York, N. Y.

[13] G. M. Rose, Rev. Sci. Inst. **2**, 810 (1931).

similar to that used by Richards and coworkers.[14] It had a boiling point of 80°C (uncorrected), a freezing point of 5.49°±0.02°C, and an index of refraction (n_0^{20}) of 1.5008 as determined by an Abbe refractometer.

Cyclohexane

Cyclohexane was thought to contain benzene as one of its impurities, so it was first nitrated (cyclohexane is not affected) with an equal volume of a mixture consisting of two parts of sulfuric acid and one part of nitric acid to one part of water. Then the cyclohexane was given several successive treatments with sulfuric acid, washed with water, dilute sodium hydroxide solution, and several more water washes. At this stage a test portion did not discolor clean mercury upon prolonged shaking. The cyclohexane was then dried with calcium chloride, distilled, and further purified by several fractional recrystallizations. It had a boiling point of 80°C (uncorrected), a freezing point of 6.45°±0.05°C, and $n_0^{20}=1.4262$.

Solutions

Three solutions (or mixtures) of benzene and cyclohexane were made up by volume from the purified components. The refractive index of each was determined at 20°C by means of an Abbe refractometer. Table I gives the composition and refractive index of each. Weight and mol percentages are calculated from the volume percentages and the densities of the components.

TABLE I.

Liquid	Percent Cyclohexane Volume	Weight	Mol	Refractive Index
Benzene	0.0	——	——	1.5008
Solution No. 1	25.0	22.8	21.5	1.4790
Solution No. 2	50.0	47.0	45.2	1.4595
Solution No. 3	75.0	72.8	71.3	1.4413
Cyclohexane	100.0	——	——	1.4262

EXPERIMENTAL PROCEDURE

The amplifier was warmed up by operation for about one hour before use in the measurement of ionization currents. During this period the amplifier was balanced by the adjustment of the variable 10,000 ohm and 400 ohm resistors in the plate circuit, after adjusting the filament current of the FP54 Pliotron to 0.110 ampere. The ionization current for the zero beam was checked periodically using low sensitivity at this time; however, no appreciable change was found over the period of this work. Then for the rest of the warm-up period, the collector electrode was tied to the control grid of the FP54 and the rest of the grid circuit connected for highest sensitivity, i.e., grid connected to ground through R_1 and R_5 in series. After the warm-up period the initial current was balanced out with the use of R_5; this initial current is due in part to the grid current of the FP54 and in part to the natural ionization in the ionization chamber in the absence of x-rays.

Ionization currents were then measured by direct deflection of the galvanometer, waiting a period of one minute between readings. This wait is required since the relaxation time RC, (where R is in ohms and C is in farads the time unit will be seconds) of the grid circuit is longer than the galvanometer period and hence determines the speed of response of the system. This method of operation is speedier than the null method under these conditions (namely, with a grid leak of over 10^{10} ohms), and introduces no errors since the galvanometer deflection-grid voltage curve is linear over the range involved. The drift after the first hour of operation (warm-up) is negligible over a period of fifteen minutes or more under the worst conditions encountered during the work.

At each setting of the spectrometer the intensity of the diffracted x-rays passed by each of the filters was measured by the vacuum tube electrometer and ionization chamber. The ionization current obtained using the strontium oxide filter was then subtracted from that obtained using the zirconium oxide filter giving that due to the molybdenum $K\alpha$ radiation alone. This follows since they have the same transmission factor for the white radiation and the ZrO_2 filter selectively transmits this spectral group. Zero readings in each were obtained by inserting a lead screen in the path of the x-ray beam. At least three checking deflections were obtained at each setting of the spectrometer arm with each filter, and the three sets of readings were averaged.

[14] T. W. Richards, J.A.C.S. **36**, 1825 (1914); **41**, 2019 (1919).

In measuring the diffraction curves, the spectrometer arm was moved to the several positions. The angles were measured by a lamp and scale, and determined by calculations on the basis of the geometry of the lamp and scale system.

Each diffraction curve was measured both in the direction of increasing and in the direction of decreasing angles. Both of the curves checked within the precision of measurement in all cases. The curves given herewith (Fig. 4) are the average curves obtained from these pairs.

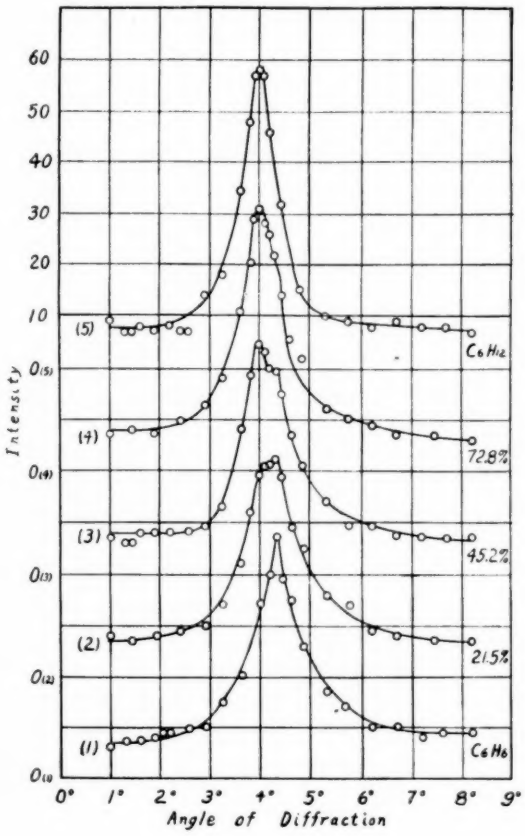

FIG. 4. Diffraction curves.

Over the range included in this study the correction for scattering by the collimator slit and the cellophane windows of the sample holder is negligible as determined by experiment. At smaller angles the correction is not negligible and at larger angles has not been determined.

RESULTS AND DISCUSSION

Diffraction curves for benzene, cyclohexane, and their solutions are given in Fig. 4. All curves have been plotted to the same scale, hence comparisons may be made between the several curves. The angles of diffraction as given are one-half the respective angles of deviations and are thus equivalent to θ in the Bragg formula

$$n\lambda = 2d \sin \theta. \quad (1)$$

The x-ray diffraction curves for the solutions indicate the presence of each peak, although they are close enough together so that the resolution is not perfect. The curves for the 21.5 and 45.2 mol percent cyclohexane solutions show clearly both peaks in both of the original experimental curves for each solution. In the case of the 71.3 mol percent cyclohexane solution, the top of the peak is identical in position with that of the pure cyclohexane while the central portion is asymmetrical with respect to the top. This asymmetry is present in both of the original experimental curves while none of the curves for pure benzene or cyclohexane is asymmetrical in this region. This shows that the diffraction curves for the solutions arise from the combined effects of two preferred spacings, which are identical with those of the two pure components.

Positions of the diffraction peaks for benzene, cyclohexane, and their mixtures are given in Table II. The positions of the secondary peaks

TABLE II.

Liquid	Main Peak θ	Main Peak d	Side peak θ	Side peak d
Benzene	4.33°	4.68A	——	——
Solution No. 1	4.33	4.68	4.00°	5.09A
Solution No. 2	4.00	5.09	4.33	4.68
Solution No. 3	4.00	5.09	4.33	4.68
Cyclohexane	4.00	5.09	——	——

are, of course, not so well defined as those of the main peaks but are given as those of the components from which they arise, with which the curves are consistent. Table III gives the peak limits and widths (half intensity used arbitrarily). The values given in parentheses for the mixtures are the corresponding values for curves calculated by assuming that the diffraction effects of the

TABLE III.[1]

Liquid	Peak limits (at half intensity)				Peak width (at half intensity)
Benzene	3.73°		4.93°		1.20°
Solution No. 1	3.53	(3.50)*	5.04	(5.00)	——
Solution No. 2	3.50	(3.50)	4.78	(4.70)	——
Solution No. 3	3.48	(3.50)	4.63	(4.65)	——
Cyclohexane	3.52		4.48		0.95

* Values in parentheses are from curves calculated by assuming strict addition of the diffraction effects of the components.

[1] Quotation from laboratory notebook.

			Synthetic		
θ	C_6H_6	C_6H_{12}	1–1	1–3	3–1
1.0	7	8	8	8	7
1.5	7	8	8	8	7
2.0	8	8	8	8	8
2.5	9	9	9	9	9
3.0	12	14	13	14	12
3.3	16	21	18½	20	17
3.6	20	32	26	29	23
3.8	26	45	35½	40	31
3.9	30	55	42½	49	36
4.0	33	58	45½	52	39
4.1	36	55	45½	50	41
4.2	40	46	43	44	42
4.3	46	39	42½	41	44
4.4	44	33	38½	37	41
4.5	38	28	33	31	35
4.6	34	18	26	22	30
4.8	28	15	21½	18	25
5.0	23	12	17½	15	20
5.5	16	9	12½	11	14
6.0	12	9	10½	10	11
6.5	10	8	9	8	10
7.0	9	8	9	8	9
7.5	9	8	8	8	9
8.0	9	8	8	8	9

Column 1 headed θ represents various selected angles of the spectrometer. Column 2 headed C_6H_6 gives values of the intensity of the diffracted beam for the angles given in column 1. These intensities are read from the smooth curve drawn through the experimental points found for benzene. Column 3 gives corresponding values of the intensity of the diffracted beam from cyclohexane. Columns 4, 5 and 6 give the calculated values for 3 mixtures. In column 4 the values are obtained by adding 50 percent of the values in column 2 to 50 percent of the value in column 3. Column 5 is obtained by adding $\frac{1}{4}$ of the values in column 2 to $\frac{3}{4}$ of the value in column 3. Column 6 is obtained by adding $\frac{3}{4}$ of the values of column 2 to $\frac{1}{4}$ of the value of colume 3. The values in parentheses in Table III come from plots of the values in the last three columns which were then treated as if they were real data.

two components are strictly additive. These differences are more apparent than real as may be shown by plotting the experimental points on top of the synthetic curves. Trial shows no difference in any portion of any of the curves large enough to be significant.

It will be noted that the peak for cyclohexane is distinctly higher and its width is distinctly less than in the case of benzene. There are over seventeen percent less molecules per unit volume of cyclohexane than of benzene, and since the same thickness of sample was used in each case, it means that there were less cyclohexane molecules in the diffracting volume. While the comparative diffracting power of the benzene and cyclohexane molecules acting as diffracting centers is not known, it is probable that the diffracting power of the cyclohexane molecule is not more than about fifteen percent greater than that of the benzene molecule. The sharper peak means that the semi-orderly arrangement in cyclohexane is more orderly than in the case of benzene and that probably a greater fraction of the cyclohexane molecules (more intense diffraction) are included in the cybotactic groupings. It was noticed that during the recrystallization the crystal nuclei of cyclohexane were much more persistent above the melting point than those of benzene. This is consistent with theory.[15]

The spacings corresponding to the diffraction peaks exhibited by benzene and cyclohexane have been shown[2] to be the effective thicknesses of the respective rings. This is an intermolecular spacing as contrasted with an intramolecular spacing.* Hence it may be seen that the cybotactic groups of both benzene and cyclohexane coexist in their mixtures. Thus we may picture benzene-cyclohexane solutions as submicroscopic emulsions. The minimum size of the groups which are able to give rise to regular x-ray diffraction is smaller than the limit of resolution of an ultramicroscope even for the case where the difference of refractive indices is larger than for the liquids used here. The extreme smallness of the cybotactic groups in the present experiments is shown

[15] W. P. Davey, Trans. Am. Soc. Steel Treating (1933).

* If, as it seems unlikely, the peak corresponds to an intramolecular spacing, the following interpretation of the data taken on the solutions is not demanded, but it is still not inconsistent with the data.

by the fact that the ordinary rough tests showed no Tyndall effect in any of the solutions. It is believed that such emulsions are described here for the first time.

The independent existence of the cybotactic groups of benzene and cyclohexane molecules in their solutions may be possibly connected with their deviations from the laws of perfect solutions in very dilute solution. Professor M. R. Fenske and Mr. M. R. Cannon[16] have found that the cryoscopically determined molecular weight of benzene in cyclohexane is nearly twice normal. It is here suggested that some of the cybotactic groups may have a regular enough structure to act as single molecules in their effects on the thermodynamic (vapor pressure connected) properties of solutions, thus making it appear that the solute molecules are associated. True association should give rise to secondary peaks corresponding to distances in the associated molecule such as has been found, for example by Stewart[1, 17] in the case of some polar compounds such as certain of the aliphatic alcohols.

Summary

1. Carefully purified benzene and cyclohexane give x-ray diffraction peaks at 4.68 and 5.09A, respectively.

2. A possible connection between the shape and intensity of the x-ray diffraction peaks given by liquids and the persistence of crystal nuclei above the melting point has been suggested.

3. Solutions of benzene and cyclohexane have an emulsion type structure, in which the disperse phase is considerably too small to be seen with a microscope, and too small to show a perceptible Tyndall effect.

4. A possible connection between the deviations from the laws of perfect solutions and the x-ray diffraction patterns of solutions has been suggested.

5. A vacuum tube electrometer has been designed and tested, which has a direct deflection (or null method if desired) sensitivity of 6×10^{-16} ampere per division.

Acknowledgment

The author wishes to thank Dr. Wheeler P. Davey, Research Professor of Physics and Chemistry, for his continued interest and suggestions throughout the progress of this research. He is also indebted to Professor M. R. Fenske, Petroleum Refining Research Laboratory for valuable suggestions concerning the benzene-cyclohexane system and to the General Electric Company, Schenectady, New York for making available certain equipment, without which the work would have been difficult, if not impossible.

[16] Private communication, July, 1933.

[17] G. W. Stewart, Phys. Rev. **35**, 296 (1930).

The Lattice Energies of the Ammonium Halides and the Proton Affinity of Ammonia

WILLARD E. BLEICK, *The Institute for Advanced Study, Princeton, New Jersey*

(Received January 23, 1934)

The lattice energies of NH_4F and of the CsCl-type lattices of the other ammonium halides are computed by the method of Born and Mayer, assuming ionic crystals with a van der Waals potential. The calculations appear to be quantitatively satisfactory for the chloride, bromide and iodide. The method fails, however, for the asymmetrical fluoride lattice, and another method is employed. The theoretically calculated lattice energies in kilocalories are, NH_4Cl, 161.6; NH_4Br, 154.0; NH_4I, 145.5. From these lattice energies by means of a thermal cycle the energy change at 0°K of the reaction $NH_{3gas}+H^+_{gas}\rightarrow NH_4^+{}_{gas}$, which may be called the proton affinity of ammonia, is found to be -206.4 kcal. With this proton affinity and the same cyclic process the lattice energy of NH_4F is calculated to be 191.4 kcal.

INTRODUCTION

THE ammonium halides, with the exception of the fluoride, are dimorphic, crystallizing in the CsCl-type lattice at low temperatures and in the rocksalt-type lattice at elevated temperatures. The fluoride possesses a Wurzite-type lattice. The interest in the anomalous behavior of the ammonium halides has created during recent years a considerable literature describing the physical properties of these salts. These data now make it possible to evaluate the lattice energies with some degree of accuracy. This calculation is carried out here following the method of Born and Mayer.[1] Reference should be made to their paper since the detailed equations and notations will not be given here. The lattice energies, U, of these uniunivalent ionic crystalline salts, namely the energy changes at 0°K of the reactions $NH_4X_{cryst.}\rightarrow NH_4^+{}_{gas}+X^-{}_{gas}$, are given by

$$-U=\Phi(r_0)=-\frac{\alpha e^2}{r_0}-\frac{C}{r_0^6}-\frac{D}{r_0^8}+B(r_0)+\tfrac{1}{2}h\nu_0. \quad (1)$$

The term varying inversely with the lattice distance, r_0, is the electrostatic energy. The terms varying as r_0^{-6} and r_0^{-8} are, respectively, the dipole-dipole and the quadrupole-dipole contributions to the van der Waals potential. $B(r_0)$ is the repulsive potential and $h\nu_0/2$ is the zero-point energy.

[1] M. Born and J. E. Mayer, Zeits. f. Physik **75**, 1 (1932).

CALCULATION OF THE VAN DER WAALS POTENTIAL

The evaluation of the constants C and D from the polarizabilities, α, and from certain energies, ϵ, of the ions *in the lattice* has been discussed by Mayer.[2] ϵ is an energy corresponding to a weighted average frequency of absorption of the ion in the crystal. The values of ϵ for the negative ions of the ammonium halides are taken to be the same as the values found by Mayer[2] for the negative ions of the rubidium halides. The values used for the matrix elements, Q_{00}^2, of the negative ions are the average values found by Mayer[2] for the negative ions of the alkali halides. The polarizabilities, α, of the negative ions are then calculated from the relation

$$Q_{00}^2=(3/2)(\alpha\epsilon/e^2). \quad (2)$$

The energy, ϵ, of the positive ammonium ion is given the value 90 percent of the ionization potential (the potential required to produce a doubly charged ion) of the gaseous ammonium ion. This ionization potential of NH_4^+ is estimated to be 31.7 volts by proportion from the ionization potentials of its electronic isomers CH_4, Na^+ and Ne, which are, respectively, in volts, 14.5,[3] 47.0[4] and 21.47.[4] The polarizability,

[2] J. E. Mayer, J. Chem. Phys. **1**, 270 (1933).

[3] T. R. Hogness and H. M. Kvalnes, Phys. Rev. **32**, 942 (1928).

[4] R. F. Bacher and S. Goudsmit, *Atomic Energy States*, McGraw-Hill, New York, 1932.

α, of the ammonium ion in the lattice is calculated from its molar refractivity given by Wulff and Cameron[5] as 4.30. The matrix element, Q_{00}^2, of the ammonium ion is then computed by means of Eq. (2).

The sums of the polarizabilities of the negative and positive ions, $\Sigma\alpha$(calc.), Table III, row 9, have been compared with the experimental values, $\Sigma\alpha$(yellow), row 10, calculated from the indices of refraction, n_D^{25}, for yellow light.[5] The experimental values of $\Sigma\alpha$(yellow) will be lower than those which would be calculated were the index of refraction extrapolated to $\lambda = \infty$, because of the infrared vibrations of the ammonium ion. An estimated value of $\Sigma\alpha(\lambda = \infty)$, calculated from the dielectric constants[6] measured at radiofrequencies, is given in row 11.

The electron numbers, p, of the ions, which are needed to compute D, are taken as the geometric mean of the number of outer electrons, assumed here to be 8 for all ions, and the value calculated from the energy, ϵ, and from the polarizability, α, by the method of Herzfeld and Wolf.[7] The lattice constants S_6', S_6'', S_8' and S_8'', needed in the calculation of C and D, and the Madelung constant, α, needed in the calculation of the electrostatic energy, are given in Table I. These

TABLE I. *Lattice constants.*

Crystal type	Wurzite	CsCl	Crystal type	Wurzite	CsCl
α (Madelung constant)	1.638	1.763	S_8''	0.253	2.148
S_6'	4.354	8.709	a	1.633	1.155
S_6''	0.762	3.545	M	4	8
S_8'	4.104	8.208	M'	12	6

constants as given for the Wurzite-type lattice are in reality those for the very slightly different Zincblend-type lattice. This approximation introduces no error in the final results, however, since it will be shown later that the lattice energy of NH_4F must be calculated by a different method.

[5] P. Wulff and H. K. Cameron, Zeits. f. physik. Chemie **B10**, 347 (1930).

[6] *International Critical Tables*, Vol. VI, p. 99.

[7] K. F. Herzfeld and K. L. Wolf, Ann. d. Physik **78**, 195 (1925).

The Repulsive Potential and the Lattice Energy

To calculate the repulsive potential, $B(r_0)$, it is necessary to approximate the ionic radii. In Table II the lattice distances r_0, the distance

TABLE II. *Rocksalt-type lattice distances.*

Salt	$r_0 \times 10^8$ cm	Salt	$r_0 \times 10^8$ cm
NH_4Cl	3.266	RbCl	3.267
NH_4Br	3.45	RbBr	3.427
NH_4I	3.622	RbI	3.662

between the centers of closest ions, of the NaCl-type lattices of the ammonium and rubidium halides are compared. These lattice distances, taken from the *Strukturbericht*,[8] agree closely, and hence the ionic radius of the ammonium ion is taken to be the same as that of the rubidium ion. The ionic radii given in Table III, rows 22 and 23, are taken from a paper of Huggins and Mayer.[9]

The various steps in the calculation of the repulsive potentials and of the lattice energies are given in Table III. The values in parenthesis are averages of the values for NH_4Cl and NH_4Br. The compressibility data are computed from the measurements of Bridgman.[10] The thermal coefficients of expansion are from the work of Simon and Bergman.[11] Both data are for atmospheric pressure and 273°K. The lattice distances, r_0, as determined from x-ray measurements[8] and as calculated from densities,[5] are given in Table III, rows 20 and 21, respectively. The x-ray values are used here to calculate the lattice energies, except in the case of NH_4F where the density value is used since the x-ray value appears to be of doubtful accuracy. The values of r_0 given for NH_4F represent weighted means since this crystal is so deformed that one of the four neighbors of any ion is closer than the other three. The constants a, M and M', needed in the calculation of the repulsive poten-

[8] P. P. Ewald and C. Hermann, *Strukturbericht 1913–1928*, Akad. Verlagsgesellschaft, Leipzig, 1931.

[9] M. L. Huggins and J. E. Mayer, J. Chem. Phys. **1**, 643 (1933).

[10] P. W. Bridgman, Phys. Rev. **38**, 182 (1931).

[11] F. Simon and R. Bergman, Zeits. f. physik. Chemie **B8**, 255 (1930).

TABLE III. *Calculation of the lattice energies.*

	Salt	NH_4F	NH_4Cl	NH_4Br	NH_4I
2	Crystal type	Wurzite	CsCl	CsCl	CsCl
3	Q_{00}^2 (neg. ion) $\times 10^{16}$ cm^2	1.44	3.40	4.08	5.27
4	Q_{00}^2 (pos. ion) $\times 10^{16}$ cm^2	5.08	——	——	——
5	ϵ (neg. ion) $\times 10^{12}$ ergs/molecule	18.5	15.7	13.8	12.0
6	ϵ (pos. ion) $\times 10^{12}$ ergs/molecule	45.3	——	——	——
7	α (neg. ion) $\times 10^{24}$ cm^3	1.18	3.29	4.49	6.66
8	α (pos. ion) $\times 10^{24}$ cm^3	1.70	——	——	——
9	$\Sigma\alpha \times 10^{24}$ (calc.) cm^3	2.88	4.99	6.19	8.36
10	$\Sigma\alpha$(yellow) $\times 10^{24}$ (exp.) cm^3	2.83	4.96	6.22	——
11	$\Sigma\alpha(\lambda = \infty) \times 10^{24}$ (exp.) cm^3	——	9.09	10.8	——
12	$c_{++} \times 10^{60}$ ergs cm^6	98	——	——	——
13	$c_{--} \times 10^{60}$ ergs cm^6	19	127	208	399
14	$c_{+-} \times 10^{60}$ ergs cm^6	40	98	121	161
15	$d_{++} \times 10^{76}$ ergs cm^8	150	——	——	——
16	$d_{--} \times 10^{76}$ ergs cm^8	24	266	510	1192
17	$d_{+-} \times 10^{76}$ ergs cm^8	55	177	240	363
18	$C \times 10^{60}$ ergs cm^6	217	1251	1597	2286
19	$D \times 10^{76}$ ergs cm^8	248	1898	2681	4423
20	$r_0 \times 10^8$ (from x-rays) cm	2.67	3.342	3.514	3.785
21	$r_0 \times 10^8$ (from density) cm	2.699	3.347	3.508	——
22	$r_- \times 10^8$ cm	1.133	1.503	1.624	1.810
23	$r_+ \times 10^8$ cm	1.294	——	——	——
24	$\beta \times 10^{12}$ (compressibility) barye^{-1}	——	5.76	6.13	——
25	$\beta^{-1}(\partial\beta/\partial T)_P \times 10^4$ degree^{-1}	——	14	9.5	——
26	$\beta^{-1}(\partial\beta/\partial P)_T \times 10^{11}$ barye^{-1}	——	−4.5	−5.3	——
27	$V^{-1}(\partial V/\partial T)_P \times 10^4$ degree^{-1}	——	1.42	1.61	——
28	$(3T/N\beta)(\partial V/\partial T) \times 10^{12}$ ergs/molecule	(1.30)	1.16	1.44	(1.30)
29	$r_0^2[d^2\Phi(r_0)/dr^2] \times 10^{12}$ ergs/molecule	——	99.3	89.2	——
30	$\alpha e^2/r_0 \times 10^{12}$ ergs/molecule	13 81	12.00	11.41	10.60
31	$C/r_0^6 \times 10^{12}$ ergs/molecule	0.56	0.90	0.85	0.78
32	$D/r_0^8 \times 10^{12}$ ergs/molecule	0.09	0.12	0.12	0.11
33	$\tau \times 10^{12}$ ergs/molecule	16.6	17.2	16.0	14.8
34	$\sigma \times 10^{12}$ ergs/molecule	——	170	156	——
35	σ/τ	——	9.87	9.75	——
36	$\rho \times 10^8$ cm	(0.359)	0.347	0.371	(0.359)
37	r_0/ρ calculated	7.52	9.63	9.47	10.54
38	$B(r_0) \times 10^{12}$ ergs/molecule	2.17	1.75	1.65	1.36
39	$\frac{1}{2}h\nu_0 \times 10^{12}$ ergs/molecule	0.20	0.12	0.10	0.08
40	$U \times 10^{12}$ (calc.) ergs/molecule	12.09	11.15	10.63	10.04
41	U (calc.) kcal.	175.2	161.6	154.0	145.5
42	U (thermal cycle) kcal.	191.4	——	——	——

tial, are given in Table I. The values of c_1 and c_2, which give the dependence of the repulsion on the charge, are computed from a theoretical equation of Pauling's[12] assuming 8 electron shell positive and negative ions. These values are 1.25 and 0.75, respectively. The small zero-point energy is easily estimated.

The values of the lattice energies in ergs per molecule and in kcal. calculated by means of Eq. (1) are tabulated in Table III, rows 40 and 41. The lattice energy thus found for NH_4F is more than 16 kcal. too small. The error is due to the fact that Eq. (1) holds only for perfectly symmetrical crystals, whereas NH_4F is deformed or asymmetrical. It is obvious for reasons of stability that the nature of the forces producing the asymmetry must be such as to increase the lattice energy above that of a symmetrical crystal of equal lattice distance. The correct lattice energy of NH_4F, as given in Table III, row 42, is calculated in the next section by using a thermal cycle involving the average proton affinity of ammonia found from the lattice energies of the other ammonium halides.

THE PROTON AFFINITY OF AMMONIA

In Table IV are given the energies of the reactions used to calculate the energy change at 0°K of the reaction $NH_{3_{gas}} + H^+_{gas} \rightarrow NH_4^+{}_{gas}$, which may be called the proton affinity of ammonia. The lattice energies are those of the salts calculated in Table III, and are the energies of the indicated reaction at 0°K. The heats of formation of the crystals are taken from the *International Critical Tables*, as are also the heats of formation of ammonia and of the halogen gaseous atoms. The heat of dissociation of fluorine is from the work of von Wartenberg and Taylor.[13] The energy changes of the crystals between 291°K and 0°K are calculated by integrating the heat capacities measured by Simon, von Simson and Ruhemann.[14] The small energy changes of the gases for this temperature change are estimated. The electron affinities of the halogen atoms are taken from a paper by Mayer and Helmholz[15] where they were calculated from the lattice energies of the alkali halides. The sum of the ΔH's of all of the first eleven reactions gives the ΔH, which at 0°K is the proton affinity of ammonia. The value in parenthesis in the NH_4F column is the average value of the proton affinity of ammonia found from the other three halides. From this average value of 206.4 kcal. the ΔH of the first reaction, or the lattice energy of NH_4F, is found to be 191.4 kcal.

[12] L. Pauling, Zeits. f. Krist. **67**, 377 (1928).

[13] H. v. Wartenberg and J. Taylor, Goett. Nachr., Math.-phys. Kl., p. 119 (1930).

[14] Simon, v. Simson and Ruhemann, Zeits. f. physik. Chemie **A129**, 339 (1927).

[15] J. E. Mayer and L. Helmholz, Zeits. f. Physik **75**, 19 (1932).

TABLE IV. *Calculation of the proton affinity of NH_3 and the NH_4F lattice energy. ΔH in kilocalories of the reactions.**

Reaction		NH_4Cl	NH_4Br	NH_4I	NH_4F
$NH_4X_{cr.} \rightarrow NH_4^+{}_{g.} + X^-{}_{g.}$	0°K	161.6	154.0	145.5	191.4
$NH_4X_{cr.}$ 291°K $\rightarrow NH_4X_{cr.}$ 0°K		−3.6	−3.8	−5.0	−2.7
$\frac{1}{2}N_{2g.} + 2H_{2g.} + \frac{1}{2}X_{2s.s.} \rightarrow NH_4X_{cr.}$	291°K	−75.1	−64.7	−48.5	−111.7
$NH_{3g.} \rightarrow \frac{1}{2}N_{2g.} + \frac{3}{2}H_{2g.}$	291°K	11.0	11.0	11.0	11.0
$H_{g.} \rightarrow \frac{1}{2}H_{2g.}$	291°K	−51.0	−51.0	−51.0	−51.0
$X_{g.} \rightarrow \frac{1}{2}X_{2s.s.}$	291°K	−28.8	−26.7	−25.5	−31.8
$NH_{3g.}$ 0°K $\rightarrow NH_{3g.}$ 291°K		2.3	2.3	2.3	2.3
$H_{g.}$ 0°K $\rightarrow H_{g.}$ 291°K		1.4	1.4	1.4	1.4
$X_{g.}$ 0°K $\rightarrow X_{g.}$ 291°K		1.4	1.4	1.4	1.4
$H_{g.} \rightarrow e^- + H^+{}_{g.}$	0°K	−312.0	−312.0	−312.0	−312.0
$X^-{}_{g.} \rightarrow X_{g.} + e^-$	0°K	86.5	81.5	74.2	95.3
Sum $= NH_{3g.} + H^+{}_{g.} \rightarrow NH_4^+{}_{g.}$	0°K	−206.3	−206.6	−206.2	(−206.4)

* Subscripts, cr. indicate crystal; s.s., standard state; and g., gas.

The values found here for the lattice energies and the proton affinity may be in error by as much as 3 kcal. due to uncertainties in the lattice distances and compressibilities.

DISCUSSION OF THE RESULTS

Two references concerning the proton affinity of ammonia have been found in the literature. By means of a similar cyclic process van Arkel and de Boer[16] find a proton affinity of 209 kcal., which is in good agreement with the value found here. The agreement is fortuitous, however, since they employ a lattice energy of 148 kcal. for NH_4Cl. This lattice energy is 14 kcal. less than the one found in this paper and must surely be in considerable error. By the method of molecular orbitals Mulliken[17] obtains an ammonia proton affinity of 9.0 volts or 207 kcal., again in good agreement with the value found here.

The good agreement obtained between the ammonia proton affinities deduced from the lattice energies of the ammonium halides is regarded as support for the accuracy claimed in the lattice energy calculations. It also shows that the ammonium halides are definitely ionic crystals to which the equations of Born and Mayer quantitatively apply.

The author is greatly indebted to Professor Joseph E. Mayer for suggesting the foregoing problem, and is very grateful to him for the advice received in working it out.

[16] A. E. van Arkel and J. H. de Boer, Physica **7**, 354 (1927).

[17] R. S. Mulliken, J. Chem. Phys. **1**, 492 (1933).

The Theory of the Electrolytic Separation of Isotopes

RONALD P. BELL, *Balliol College and Trinity College, Oxford*

(Received January 26, 1934)

(1) Gurney's treatment of overvoltage has been applied to the relative rates of discharge of two isotopes. As a first approximation it is found that the separation efficiency should be nearly independent of the electrode material and the current density. This agrees with the data at present available for the separation of the isotopes of hydrogen. (2) A more rigid treatment predicts small variations of the efficiency with the nature of the electrode and the current density, but is not at present able to predict these variations quantitatively. (3) The application of the theory to other isotopes is indicated, and a rough estimate given of the possibility of separating Li^6 and Li^7 by electrolysis.

SINCE the original discovery of the electrolytic separation of the isotopes of hydrogen by Washburn and Urey,[1] various suggestions have been made as to the mechanism involved. A difference in the behavior of the two isotopes may reasonably be expected at one or more of the following stages in the process of electrolysis

(a) The mobility of the hydrogen and diplogen ions.

(b) The rate of neutralization of the two ions by electrons.

(c) The rate of combination of hydrogen and diplogen atoms on the electrode.

In order to decide between these alternatives it is necessary to have some knowledge of the effect of various factors upon the separation, and it is only very recently that any work has been done in this direction.

Possibility (a) cannot be an important factor in the separation, since it can be carried out equally well in acid or in alkaline solution.[2] It is more difficult to decide between (b) and (c); however, it has recently been found by Bell and Wolfenden[3] and by Topley and Eyring[4] that the efficiency of separation is substantially the same for a number of different cathode materials, which makes it very improbable that the observed phenomena are due to the rate of combination of atoms on the electrode surface.[5] It is much more likely that the difference in the rates of discharge of hydrogen and diplogen is due to a difference in the rate at which their hydrated ions are neutralized by electrons. Gurney[6] has previously shown that it is this rate of neutralization which is chiefly responsible for hydrogen overvoltage, and has developed a quantitative theory of overvoltage which agrees well with experiment, notably with the fact that the variation of current density with applied potential is independent of the nature of the cathode. The author has previously pointed out[3] that Gurney's treatment can also be applied to the separation of the isotopes of hydrogen, when it predicts that the efficiency of separation will be independent of the cathode material, and gives a value of the right order of magnitude for the efficiency itself. The present paper deals with this point in more detail.

For the current density due to the discharge of a hydrated cation, Gurney derives the expression

[1] E. W. Washburn and H. C. Urey, Proc. Nat. Acad. Sci. **18**, 496 (1932).

[2] See C. H. Collie, Nature **132**, 568 (1933); K. F. Bonhoeffer and G. W. Brown, Zeits. f. physik. Chemie **B23**, 171 (1933).

[3] R. P. Bell and J. H. Wolfenden, Nature **133**, 25 (1934).

[4] B. Topley and H. Eyring, J. Am. Chem. Soc. **55**, 5058 (1933).

[5] As suggested, e.g., by A. Sherman and H. Eyring, J. Chem. Phys. **1**, 345 (1933).

[6] R. W. Gurney, Proc. Roy. Soc. **A134**, 137 (1932).

$$i \propto e^{(E_0/\gamma+\epsilon V-E_1)/kT} \int_{E_0}^{E_1-\epsilon V} \exp\left\{\frac{E}{kT}\left(1-\frac{1}{\gamma}\right)-\frac{4\pi x'(2mE)^{\frac{1}{2}}}{h}\right\}dE, \quad (1)$$

where E_0 is the energy of neutralization of the hydrated ion in its lowest energy state by an electron,
E_1 is the work function of the metal,
V is the applied cathodic potential,
x' is the mean distance from the electrode at which the ions are discharged,
ϵ and m are the charge and mass of the electron,
γ is a correction factor a little greater than unity, introduced to account for the repulsive potential energy of the discharged ion and the water molecule immediately after discharge.

If we apply this expression to the discharge of two isotopes X and Y under comparable conditions, the only factor which will not be the same in the two cases is E_0 which will differ on account of the effect of the mass on the lowest vibration-rotation state of the hydrated ions. Gurney has shown that Eq. (1) can be brought into the form

$$\log i = \frac{E_0 - E_1 + \epsilon V}{\gamma kT} + \log \frac{\gamma T}{\gamma - 1} + \Phi, \quad (2)$$

where Φ is a complicated function having the property that its variations with V and T are negligible compared with the variations of the rest of the expression. Similar considerations show that the variations of $\log i$ with E_0 are also determined essentially by the first term of Eq. (2), so that the relative rates of discharge of the two isotopes are given by

$$\log \alpha = \log (i_X/i_Y) = [(E_0)_X - (E_0)_Y]/\gamma kT. \quad (3)$$

α may be termed the efficiency of separation of the isotopes.

This equation predicts at once that the value of α should be independent of the nature of the cathode, and is thus in agreement with the experimental results for the separation of the hydrogen isotopes. It also agrees at least qualitatively with the actual magnitude of α. Taking the mean value as $\alpha = 0.2$[7] and putting $\gamma = 2$ (the value found by Gurney to give agreement with the observed values of $d \log i/dV$), Eq. (3) leads to $(E_0)_H - (E_0)_D = 1900$ cal. per mole. This is a reasonable figure for the difference between the zero-point energies of H and D in the ions H_3O^+ and DH_2O^+, and is not very different from the value of 1400 cal. given by Eyring and Sherman[5] for the links O–H and O–D. It might be possible to obtain an accurate value for this difference from the Raman spectrum of the ion H_3O^+, but the necessary data are not yet available.[8] It may be pointed out that any theory in which the zero point energy is regarded as contributing directly to a heat of activation will lead to the expression

$$\log \alpha = [(E_0)_X - (E_0)_Y]/kT,$$

which will only give the experimental value of $\alpha = 0.2$ by giving $(E_0)_H - (E_0)_D$ the improbably low value of 950 cal. per mole.

The above treatment assumes that γ has exactly the same value for the two isotopes, which would probably not be justifiable in a strict examination of the problem. The significance of γ appears from Fig. 1. The upper curve represents the potential energy of the ion H_3O^+ plotted against the distance of one of the hydrogen atoms from the center of gravity of the rest of the molecule, while the lower curve repre-

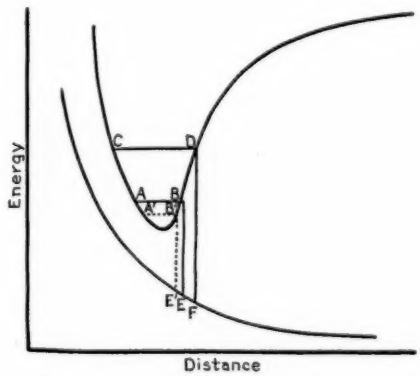

FIG. 1.

[7] See G. N. Lewis and Macdonald, J. Chem. Phys. 1, 341 (1933); Bell and Wolfenden, reference 3, Topley and Eyring, reference 4.

[8] The fundamental frequency in the Raman spectrum of H_2O leads to $(E_0)_H - (E_0)_D = 1600$ cal. per mole.

sents the potential energy of a discharged hydrogen atom at different distances from the center of gravity of an H_2O molecule. AB is the lowest vibrational level in the ion, and CD is the highest level to which an electron in the metal can make a transition. Gurney supposes that the curved portions EF and BD can be replaced by straight lines: if the ratio of the slopes of these straight lines is x, then $\gamma=1+x$. The potential energy curves in the figure will be unaltered for the systems DH_2O^+ and $D+H_2O$, but the lowest energy state will now be somewhat lower, say at $A'B'$. The curved portions to be replaced by straight lines are now $E'F$ and $B'D$, and it is obvious from the general shape of the curves that the value of γ will be slightly greater than in the first case. Eq. (3) should therefore be replaced in general by the equation

$$\log \alpha=\frac{(E_0)_X-E_1+\epsilon V}{\gamma_X kT}-\frac{(E_0)_Y-E_1+\epsilon V}{\gamma_Y kT}+\log\frac{\gamma_X(\gamma_Y-1)}{\gamma_Y(\gamma_X-1)}, \tag{4}$$

where γ_X and γ_Y are slightly different. Without a knowledge of the exact form of the potential energy curves it is impossible to predict the magnitude of the difference between γ_H and γ_D, but it may be pointed out that since $E_0-E_1+\epsilon V$ has a value of the order of 20,000 cal. per mole, a very slight change in γ will produce a considerable difference in the value of α. Eq. (4) predicts that the separation factor will vary slightly with the work function E_1 (and hence with the nature of the cathode), and also with the potential V, so that it should be possible to decide by experiment how far the simple Eq. (3) is applicable. Meanwhile it is probably unwise to attach much importance to the exact value obtained for $(E_0)_H-(E_0)_D$ from Eq. (3).

Both Eq. (3) and Eq. (4) give for the variation of α with temperature

$$d\log\alpha/dT=-\alpha/T. \tag{5}$$

For the separation of hydrogen and diplogen, Eq. (5) predicts a decrease in efficiency of about 35 percent over the temperature range 0°–100°. There are at present no accurate data on this point, but this figure is not incompatible with the results of Bell and Wolfenden.[3]

The above considerations will of course apply to the separation of any isotopes which can be discharged from a solvated ion. For a rough estimate of the efficiency of such a process for elements other than hydrogen, Eq. (3) will be sufficiently accurate and variations in γ may be neglected, so that the factor which essentially governs the separation is $(E_0)_X-(E_0)_Y$, the difference in the zero-point energies of the two isotopes in the hydrated ions. This quantity may be written

$$\begin{aligned}(E_0)_X-(E_0)_Y&=\tfrac{1}{2}h\nu_X-\tfrac{1}{2}h\nu_Y\\&=(h/4\pi)(f)^{\frac{1}{2}}\{1/M_X^{\frac{1}{2}}-1/M_Y^{\frac{1}{2}}\}\end{aligned} \tag{6}$$

where f is the force constant of the link between the ion and the water molecule and M_X, M_Y are the reduced masses of the two isotopes. It is immediately obvious that the separation will in no case be as efficient as it is for the hydrogen isotopes, since both the force constant and the value of the expression in $\{\ldots\ldots\}$ will be smaller for all other elements. There are no data available for any reliable quantitative predictions, but the point may be illustrated by a very rough investigation of the possibility of separating the isotopes Li^6 and Li^7 by electrolysis. The heat of hydration of the H^+ ion is about 200,000 cal. per mole. The corresponding quantity (per water molecule) for the Li^+ ion is not known directly, but is probably about 15,000 cal.[9] Assuming that the force constant is roughly proportional to the heat of hydration, Eq. (6) gives for the relative separation efficiencies

$$\frac{\log\alpha_{Li}}{\log\alpha_H}\approx\left(\frac{15{,}000}{200{,}000}\right)^{\frac{1}{2}}\left(\frac{1}{6^{\frac{1}{2}}}-\frac{1}{7^{\frac{1}{2}}}\right)\Big/\left(1-\frac{1}{2^{\frac{1}{2}}}\right)$$

which leads to $\alpha_{Li}=0.96$. Thus in this case separation by electrolysis will probably be less efficient than other methods, and conditions will be still more unfavorable for heavier elements.

[9] Estimated from the heat of hydration of the solid lithium halides.

The Limiting Gas Density Method for Molecular Weights

R. T. BIRGE AND F. A. JENKINS, *University of California, Berkeley*

(Received February 12, 1934)

In this, the first of a series of papers, we give a general discussion of the limiting gas density method for the determination of molecular weight. The various methods that have been used, or might well be used for the reduction of the data, are compared in a systematic way, and the most desirable methods for such work are pointed out. These methods are then applied to selected data given in the literature, and are compared with the actual published calculations and results. The paper closes with certain conclusions drawn from the preceding analysis.

INTRODUCTION

ONE of us[1] recently made a photometric measurement of the relative intensity of the $C^{12}C^{12}$ and $C^{12}C^{13}$ Swan bands. This result, combined with Aston's determination of the mass of C^{12} and with the known abundance of the oxygen isotopes, leads directly to an atomic weight of carbon of approximately 12.01, as contrasted with the international atomic weight 12.00.

In searching for the cause of this discrepancy, we have made a critical study of certain previous determinations of the atomic weight of carbon. Most of the recent work has been carried out by the "limiting gas density" method. We have found, in this study, that a number of different methods have been employed in the reduction of the data, and in many cases the logical basis for the method is not clear to us. We have, accordingly, made a certain number of recalculations, and have in some cases obtained results appreciably different from those published. It has not been possible to make a complete investigation of all previous data. In many cases the published information is too incomplete to allow a recalculation. It does seem desirable, however, to give at this time a general outline of the limiting gas density method, with illustrations of the various types of calculation that can be used and have been used in work in this field. From the calculations we have already made, it would appear that the best value of the atomic weight of carbon is appreciably higher than 12.00 and that the discrepancy with the band spectrum value, 12.01, may therefore not be serious.

The results that we have obtained will be presented in a series of papers. In this, the first paper of the series, we discuss the general principles of the limiting gas density method. The second paper of the series will be devoted to the limiting gas density of oxygen, and the resulting value of R, the normal mole volume. In the third paper we shall discuss the atomic weight of carbon, as determined especially by the gas density method.

THE LIMITING GAS DENSITY METHOD

We define the density of a gas, at any pressure p, by

$$\rho_p = w/v, \tag{1}$$

where w is the mass of gas used, and v is the measured volume. Now let

$$L_p = \rho_p/p = w/pv. \tag{2}$$

Then if $p=1$, $L_p=\rho_p$, the density at unit pressure. This is regularly denoted as merely L. Moreover, if we had a perfect gas (pv = constant), L_p would be constant regardless of the value of p. Actually the value of L_p is found, in the case of all real gases, to vary with p. Hence L_p is the density the real gas *would have*, at unit pressure, *if* it acted like a perfect gas between the pressure at which the density ρ_p is actually measured and unit pressure. This is a useful concept, for at $p=0$ any gas becomes asymptotically a perfect gas. Hence the limiting value $L_{\lim}$ of L_p at $p=0$ is the density at unit pressure that the actual

[1] F. A. Jenkins and L. S. Ornstein, Proc. Amsterdam Acad. **35**, 1212 (1932).

gas would have *if* it were a perfect gas. This quantity L_{lim} is of course a function of temperature, but if all work is done at 0°C, then the product of L_{lim} and the normal mole volume R is, by definition, the molecular weight M, i.e.,

$$M = L_{\text{lim}} \cdot R. \tag{3}$$

As previously discussed by one of us,[2] R is the normal mole volume in liter-mole^{-1} units, with $g_{45} = 980.616$ cm·sec.$^{-2}$, the units commonly employed in gas density work.

Eq. (3) is the fundamental equation for the determination of molecular weights by this method. The value of R is derived from the limiting density of oxygen, as will be discussed by one of us in the next article of this series.[3] Then for any other gas one needs to know *only* L_{lim}. This quantity, in turn, can be determined *only* by an *extrapolation* to $p=0$ of values of L_p taken at various different pressures. The problem is then one of extrapolation, with all the uncertainty attending such a process. The uncertainty is of two kinds,—first that connected with the assumed functional form of L_p, and second that connected with the purely experimental errors.

Fortunately in the case of the permanent gases, the first cause of uncertainty is virtually absent. From work over a long range of pressures it is known that the curvature of L_p when plotted against p, between $p=0$ and one atmosphere, is so small as to be quite negligible. We are therefore entirely justified in assuming a linear relation and this has been done in all recent work on these gases.

In the case of easily condensible gases, however, the plot of L_p against p sometimes shows a definite curvature. This makes the problem of extrapolation more difficult, and incidentally greatly increases the number of possible methods. Another addition to the list of possible methods comes from the fact that $1/L_p$ is often plotted against p. This custom arose in the following way. We see from Eq. (2) that pv is inversely proportional to L_p. Hence, except for the constant factor w, a plot of $1/L_p$ is also a plot of pv. If $w=1$, the two become identical. We have ourselves occasionally been confused by the use in the literature of pv for $1/L_p$, and in the present article we shall therefore write pv *only* when p and v are alone known (i.e., w unknown). We shall always write $1/L_p$ for the value of pv with $w=1$.

Because of the reciprocal relation, Eq. (2), of pv and L_p, one gets the following useful relations, which also *define* λ and λ_0[4]

$$L/L_{\text{lim}} = (pv)_0/(pv)_1 = 1+\lambda = 1/(1-\lambda_0), \tag{4}$$

where L_{lim} and $(pv)_0$ refer to zero pressure, and L and $(pv)_1$ to unit pressure. In this article unit pressure is always one atmosphere. It would be much more logical to use L_1 and L_0 in place of L and L_{lim}, but the nomenclature of Eq. (4) is so well established (except that P and V, or p and V, are sometimes used for our p and v), that in order to facilitate comparison with the many articles quoted, we here adopt it. From Eq. (4) it follows immediately that

$$\lambda_0 = \lambda/(1+\lambda) \quad \text{and} \quad \lambda = \lambda_0/(1-\lambda_0). \tag{5}$$

Returning to the possible methods for determining L_{lim}, we then have two general classes. In the first class we plot L_p against p and extrapolate to get the intercept L_{lim} at $p=0$. In the second class we plot $1/L_p$ against p and extrapolate to get the intercept $1/L_{\text{lim}}$ at $p=0$. Each of these classes applies also to pv data. That is, if we have made observations only on p and v, then we may plot the products pv

[2] R. T. Birge, Rev. Mod. Phys. **1**, 1 (1929). See p. 12. (This article will be denoted *G.C.* 1929.)

[3] Thus $R = (M)_{O_2}/(L_{\text{lim}})_{O_2} = 32/(L_{\text{lim}})_{O_2}$.

[4] The quantity λ was introduced originally in connection with a linear function of p, and is particularly appropriate in this case. It is, however, now used for the more general case, and this has led to certain misconceptions that make it desirable to emphasize its correct definition, as given by Eq. (4).

The particular symbol λ is in general use, except among the Germans, who write $1-\alpha$ in place of $1+\lambda$ (see Geiger und Scheel, Handb. d. Physik **2**, 493 (1926)). In *G.C.* 1929 the German nomenclature was adopted and this choice has since been criticized by Batuecas, J. chim. phys. **29**, 26 (1932). The symbol λ_0 is being introduced for the first time, in place of the standard symbol A_0[1], for reasons that will appear in connection with Eq. (57) ahead. Meanwhile we wish to emphasize the fact that in this article λ and λ_0 are defined always and only by Eq. (4), although the actual numerical values obtained for λ and λ_0, from a given set of data, will naturally depend on how the data are treated.

against p, and extrapolate to get the intercept $(pv)_0$. This is, except for the constant factor w, precisely the same as plotting $1/L_p$ against p. Similarly we may plot $1/pv$ against p, which is equivalent to plotting L_p.

If values of L_p had been determined in all investigations, there would be no need to discuss pv values at all. Actually, however, much density work has been done at atmospheric pressure only. This yields the quantity L. Then in order to get $L_{\lim}$ it is necessary only to get values of pv at or near one atmosphere, and at various lower pressures. This is often done in a separate investigation. From these values of pv one obtains, by any one of a variety of methods, $(pv)_0$ and $(pv)_1$. Their ratio by Eq. (4) gives $1+\lambda$. Then, also by Eq. (4)

$$L_{\lim} = L/(1+\lambda) \qquad (4')$$

and by Eq. (3)

$$M = LR/(1+\lambda). \qquad (6)$$

This last equation is the standard form used in the literature, and often, as we have said, the value of L comes from *one* investigation, or set of investigations, and the value of $(1+\lambda)$ from *another* set. We do wish, however, to emphasize the fact that in Eq. (6) $L/(1+\lambda)$ is only a long way of writing the $L_{\lim}$ of Eq. (3) and that the problem of determining M, aside from the value of R, is *solely* that of determining $L_{\lim}$. If values of L_p have been obtained, then $L_{\lim}$ follows directly by extrapolation, and it only obscures the issue to introduce separate values of L and $1+\lambda$. However, in order to compare our results with those given in the literature, we shall indicate how L and $1+\lambda$, as well as $L_{\lim}$, may be obtained from the data.

The importance of the above facts is so great that we here summarize the four general ways in which the data may be handled. In all four cases what is desired is a $f(p)$ and this is obtained most reliably by the method of least squares. By $f(p)$ we mean, however, the adopted analytic representation of the data, regardless of how obtained.

(1) One derives $L_p = f(p)$ from observed values of L_p. The value of $f(p)$ at $p=0$ is $L_{\lim}$, and this completes the problem.

(2) One derives $1/pv = f(p)$ from observed values of pv. The value of $f(p)$ at $p=0$ is $1/(pv)_0$ and at $p=1$ is $1/(pv)_1$. The ratio gives, by Eq. (4), the value of $1+\lambda$. This is all that can be derived from pv data.

(3) One derives $1/L_p = f(p)$. The value of $f(p)$ at $p=0$ is $1/L_{\lim}$ and this completes the problem.

(4) One derives $pv = f(p)$, and as in case (2) the values of $f(p)$ at $p=1$ and $p=0$ give $1+\lambda$, by Eq. (4).

Since L_p and $1/pv$ differ by only a constant factor, whatever is the best *functional* form of $f(p)$ in case (1) is necessarily the best in case (2), for any given gas. The same thing is true of (3) and (4). On the other hand, the best function for (1) and (2) may be different from that for (3) and (4) and regardless of whether it is different or not, the *numerical* value of $L_{\lim}$ derived from (1) will never, except by accident, agree with that derived from (3). If, however, one has set up a really satisfactory $f(p)$ in both (1) and (3), the difference in the two resulting values of $L_{\lim}$ will be found entirely negligible. Exactly similar remarks apply to (2) and (4).

We now come to the much more involved and uncertain problem of the derivation of a suitable $f(p)$, in any one of our four cases. With the exception of an arbitrary graphical extrapolation of the data, by means of some curved line, all methods are equivalent to the assumption of some particular functional form. Of all such possible forms, only two seem to have been used, *viz.*, the first and second degree rational integral functions (r.i.f.) commonly called linear and parabolic solutions. We shall consider specific forms for each of these two functions, and noting again that cases (1) and (2) necessarily require the same function, and similarly (3) and (4), we have the following new four-fold division.

(*a*) L_p or $1/pv$ parabolic
(*b*) L_p or $1/pv$ linear
(*c*) $1/L_p$ or pv parabolic
(*d*) $1/L_p$ or pv linear

Case (a)

We begin with (*a*), the parabolic equation for L_p, *viz.*,

$$L_p = a + bp + cp^2 \qquad (7)$$

where, by definition $a = L_{\lim}$. If now a value of a is obtained by least squares, or by some other

reliable method, this completes the problem. The following discussion, which is unfortunately somewhat involved, is necessary because L_p data have quite regularly been used, in various different ways, to calculate also values of λ or λ_0, and it seems desirable to consider the relative reliability of the values so obtained.

To obtain λ or λ_0 it is necessary to evaluate a, b, and c, and as usual we recommend for this a least squares solution. Then λ and λ_0 are given by Eq. (4), in which *both* L and L_{lim} represent *calculated* values. Very often in the literature, however, the *observed* value of L has been used, and in order to distinguish the two resulting values of λ or λ_0 thus obtained, we shall for the remainder of this section write L_a and L_c for the *adopted* (observed) and *calculated* values of L, respectively.[5] Then, by definition

$$L_c = a+b+c \tag{8}$$

and as noted $L_{\text{lim}} = a$. Hence by Eq. (4)

$$1-\lambda_0 = 1/(1+\lambda) = L_{\text{lim}}/L_c = a/(a+b+c) \tag{9},$$

or

$$\lambda_0 = (b+c)/(a+b+c) \quad \text{and} \quad \lambda = (b+c)/a. \tag{10}$$

Eq. (10) gives the only correct values of λ_0 and λ corresponding to Eq. (7). There is also a simple geometrical relation between λ_0 and Eq. (7) which can be shown as follows. Let us *define*

$$\lambda_p' = (1/L_c)(dL_p/dp) = (b+2cp)/(a+b+c). \tag{11}$$

λ_p' can be thought of as the variable slope of the curve obtained by plotting L_p/L_c against p. The limiting value of this slope, at $p=0$, is

$$\lambda' = b/(a+b+c), \tag{12}$$

and this is not simply related to either λ or λ_0, as is seen by comparing Eqs. (12) and (10). But the value of λ_p' at $p=1/2$ is exactly λ_0, by Eqs. (11) and (10). This and other relations are shown in Fig. 1.[6] In place of the λ_p' of Eq. (11) we might have defined another variable slope, obtained by replacing L_c by L_{lim}. In that case the value of this new variable, at $p=1/2$, is exactly λ. (See Fig. 2.) This interchange of λ_0 and λ, when L and L_{lim} are interchanged, is very general.

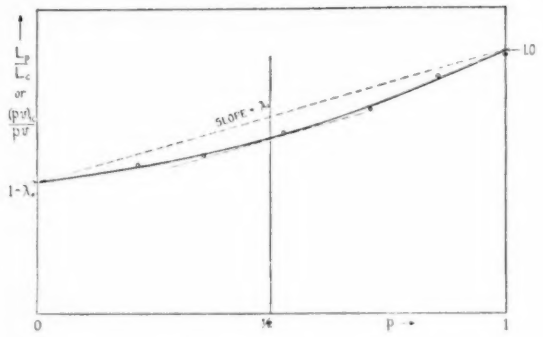

FIG. 1. Schematic diagram, applying to case (a), see Eqs. (11), (12), (24) and footnote 6.

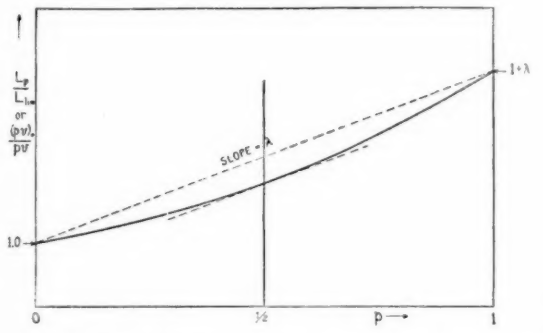

FIG. 2. Similar to Fig. 1, except that L_{lim} replaces L_c (or $(pv)_0$ replaces $(pv)_{1c}$), and λ replaces λ_0. In both figures the intercept values at $p=0$ and at $p=1$ atmosphere are indicated.

Our chief purpose in writing Eq. (11) is to make a comparison with the following Eq. (13), which has been used in the literature. In Eq. (13) the derivative of Eq. (11) is replaced by a special type of finite difference, and for convenience L_a is used in place of L_c. We then have, by definition,

$$\lambda_\Delta' = (1/L_a)(L_a-L_p)/(p_1-p). \tag{13}$$

[5] In the general Eq. (4) any value of L can be used, but it is obvious that the best value of λ or λ_0 will be obtained only when one uses the best calculated value of $L(=L_c)$. When, as is often the case, the value of L is known more accurately than the values at lower pressures, a proper weighting of the various points will obviously lead to a calculated value of $L(=L_c)$ close to the observed value $(=L_a)$. The same remarks apply to $(pv)_1$.

[6] It is easy to show from Eq. (4) that λ_0 is the slope of the secant of the $L_p/L_c : p$ curve, drawn between $p=1$ and 0, and the slope of the secant equals that of a parabola at the middle point.

If now the values of λ_Δ' are considered as a $f(p)$ and are extrapolated by any method to $p=0$, one gets for this limiting value, remembering that p_1 = one atmosphere.

$$\lambda_0=(L_a-L_{\lim})/L_a$$

or

$$1-\lambda_0=L_{\lim}/L_a=1/(1+\lambda). \quad (14)$$

This method then gives a value of λ_0 or of λ, but it is *not* the best value, even if the best possible extrapolation is made, since it uses an arbitrarily adopted value of L, ordinarily the observed value, in place of the best calculated value.

When a nonlinear equation is assumed in gas density work, it is quite customary to reduce it to a dimensionless form, by dividing the $f(p)$ by some common factor. Such a method, however, merely complicates the matter, so far as an evaluation of $L_{\lim}$ is concerned, and leads to a value of λ_0 or λ suffering from the same defect as the value given by Eq. (14). This may be shown as follows. The customary procedure is to divide each observed value of L_p by the observed value of L. We then have, in place of Eq. (7)

$$L_p/L_a=a''+b''p+c''p^2. \quad (15)$$

From Eqs. (7) and (15) we get

$$L_a=a/a''=b/b''=c/c''. \quad (16)$$

The limiting value $L_{\lim}/L_a$ at $p=0$, or a'', is commonly used to get λ or λ_0 as follows:

$$L_{\lim}/L_a=a''=1-\lambda_0=1/(1+\lambda). \quad (17)$$

The desired value of $L_{\lim}$ is evidently $L_a a''$, and it is quite immaterial what numerical value of L_a is used in Eq. (15), so long as the *same* value is used in getting $L_{\lim}=L_a a''$. Moreover, the value of $L_{\lim}$ so obtained is identical with the a of Eq. (7). This is shown directly by Eq. (16). The division and subsequent multiplication by L_a is thus entirely useless, so far as the calculation of $L_{\lim}$ is concerned. On the other hand, the value of λ_0 and λ given by Eq. (17) suffers from the same defect as does that given by Eq. (14), i.e., the observed value of L has been assumed to be the best value. The correct expression for the best value of λ_0 or λ resulting from Eq. (15) is obtained, as usual, by first putting $p=0$ and then $p=1$, and taking the ratio. This gives

$$L_{\lim}/L_c=a''/(a''+b''+c'')$$
$$=1-\lambda_0=1/(1+\lambda). \quad (18)$$

This is identical with Eq. (9), because of the relations of Eq. (16). *If* now, by chance, $L_c=L_a$ we have, by Eq. (15), $a''+b''+c''=1$, and Eq. (18) becomes identical also with Eq. (17).[7]

Let us now consider the parabolic equation in $1/pv$, corresponding to Eq. (7), *viz.*

$$1/pv=a'+b'p+c'p^2. \quad (19)$$

To get the best value of λ or λ_0 we treat this equation just as we did Eq. (7), i.e., we evaluate

---

[7] There are a number of different possible values of λ and λ_0, derivable from the same set of data, that should be distinguished. Taking Eq. (4) as our basis, we note that the value of λ or λ_0 depends on, (1) the value adopted for $L_{\lim}$, and (2) the value adopted for L. In Eq. (7) the value of $L_{\lim}(=a)$, which as just noted is identical with that obtained from Eq. (17), corresponds to a parabola passed freely through the experimental values L_p, preferably by least squares. On the other hand, the value of $L_{\lim}$ in Eq. (14), which comes in turn from Eq. (13), corresponds to some curve (it may be a parabola) that is *required* to pass through the adopted value L_a. Hence the $L_{\lim}$ of Eq. (7) or (17) is preferable to that of Eq. (14). The λ or λ_0 derived from *either* Eq. (17) or (14) is, however, definitely inferior to that derived from Eq. (9) or (18), since in both Eqs. (17) and (14) we assume the adopted L_a, whereas in Eqs. (9) and (18) we assume the calculated L_c value given by Eqs. (7) and (15).

We note also that the non-dimensional L_p/L_a data may be treated by finite differences, just as in the case of Eq. (13). In fact, by merely putting L_a inside the parentheses, Eq. (13) becomes the appropriate equation. We see that the λ_0 of Eq. (14), expressed in this way, is merely the limiting value of the slope of a set of secants, drawn from the adopted $L_a/L_a=1$ value at $p=1$ to the successive experimental L_p/L_a points. See Fig. 3.

Certain further remarks about Eq. (13) may appropriately be made here. It follows immediately from the form of Eq. (13) that if one assumes for λ_Δ' a *linear* equation in p, and gets a least squares solution, then the calculated values of L_p, or of L_p/L_a, that may be derived by Eq. (13) from the calculated values of λ_Δ', satisfy a *parabola*. This calculated parabola, as already noted, necessarily passes through the observed L_a point, but it is *not* the least squares parabolic solution of the L_p data under the condition that the parabola pass through the L_a point. In general if λ_Δ' is assumed as a r.i.f. of the rth degree, this is equivalent to assuming L_p to be a r.i.f. of the $(r+1)$th degree which is required to pass through a definite point.

a', b', and c' by least squares or otherwise. We again differentiate between an adopted and a calculated value of $(pv)_1$, by writing $(pv)_{1a}$ and $(pv)_{1c}$ respectively. Then, by Eq. (4),

$$1-\lambda_0=1/(1+\lambda)=(pv)_{1c}/(pv)_0 = a'/(a'+b'+c'). \quad (20)$$

This corresponds to Eq. (9), and is obviously in agreement with Eq. (9) since, from Eqs. (2), (7) and (19)

$$L_p(pv)=w=a/a'=b/b'=c/c'. \quad (21)$$

Corresponding to Eq. (10) we write, from Eq. (20)

$$\lambda_0=(b'+c')/(a'+b'+c') \quad (22)$$

and

$$\lambda=(b'+c')/a'.$$

Corresponding to Eq. (11) we again get a simple geometrical relation by writing

$$\lambda_p'=(pv)_{1c}\frac{d(1/pv)}{dp}=\frac{b'+2c'p}{a'+b'+c'}=\frac{b+2cp}{a+b+c}. \quad (23)$$

The value of λ_p' at $p=1/2$ is, by Eq. (22), exactly λ_0. In this case λ_p' is the variable slope of the $(pv)_{1c}/pv$ curve, considered as a function of p, but this is identical with the L_p/L_c curve mentioned in connection with Eq. (11) and shown in Fig. 1, since, from the inverse proportionality of L_p and (pv), Eq. (2), we have

$$L_p/L_c=(pv)_{1c}/pv. \quad (24)$$

Accordingly both sides of Eq. (24) are given as the ordinate in Fig. 1. We may now define a new variable slope, by replacing $(pv)_{1c}$ by $(pv)_0$ in Eq. (23). This slope, at $p=1/2$, will give λ (see Fig. 2). We may also treat $1/pv$ data by finite differences, but as noted near the end of footnote 7, we are thus effectively treating the data in a non-dimensional form, and we accordingly take this up first.

Dividing each $(1/pv)$ by an adopted $(1/(pv)_{1a})$ value we get

$$(pv)_{1a}/(pv)=L_p/L_a=a''+b''p+c''p^2. \quad (25)$$

In other words, due to the inverse proportionality of L_p and pv, the non-dimensional Eqs. (15) and (25) are identical. In the case of pv data we cannot of course evaluate $L_{1\text{lim}}$, but the remarks regarding the evaluation of λ or λ_0 from Eq. (15), by means of Eq. (17), apply also to the present case. To be specific,

$$(pv)_{1a}/(pv)_0=L_{1\text{lim}}/L=a'' = 1-\lambda_0=1/(1+\lambda) \quad (17')$$

gives a poor value of λ_0 or λ. If Eq. (25) is properly handled, the value of $(pv)_0$ corresponds to a parabola passed freely through the pv data, but the value of λ_0 or λ in Eq. (17′) suffers from the use of the arbitrarily adopted $(pv)_{1a}$ value. The correct equation is

$$(pv)_{1c}/(pv)_0=L_{1\text{lim}}/L_c=a''/(a''+b''+c'') = 1-\lambda_0=1/(1+\lambda). \quad (18')$$

It is quite common practice to handle the non-dimensional $(pv)_{1a}/pv$ data by means of finite differences.[8] In analogy to Eq. (13), remembering

[8] See A. Guye, J. chim. phys. **17**, 141 (1919), for an extended discussion of this and other special methods for handling the data. For a criticism of some of his conclusions see G. P. Baxter, J. Am. Chem. Soc. **44**, 595 (1922). It is well known that it is convenient to handle finite differences only when the abscissas are equally spaced, and the use of Eq. (26) in the literature is confined to this special case. We should like at this point to make some general remarks on the handling of finite differences. Let us suppose that a difference table shows that the successive second differences are constant, within the limits of experimental error. Then one is justified in adopting a parabolic formula. Common practice is now to take the *average* second difference and apply it to the final first difference and the final observation to get the first extrapolated value, and so on for further extrapolated values. In such a solution *only* the first two and last two observations are used. No other observations have any effect on the result. The parabola passing through each of the extrapolated points has the following properties. It passes exactly through the last two observations and lies on one side of the first two observations by some small but equal amount. This particular solution cannot be obtained by least squares with any set of weights but it does effectively give infinite weight to the last two observations, equal but finite weight to the first two, and zero weight to all the others. A special case is that of three equally spaced observations. In such a case the parabola necessarily passes through each of the three points and the question of weighting does not enter. Also the calculated and observed values of pv coincide and there is necessarily only one possible value of λ_0 or λ. Guye used the method only in this special case. The real question in such a situation is whether, with only three observations, there is any reason to assume a parabolic formula. The deviation from linearity may be due entirely

also the remark in footnote 7, we write

$$\lambda_\Delta' = [1-(pv)_{1a}/pv]/(p_1-p). \qquad (26)$$

That this expression is identical with Eq. (13) is seen from the relation between pv and L_p given in Eq. (25). Hence the limiting value again gives λ_0. In this case λ_0 is the limiting value of a set of secants drawn on the $(pv)_{1a}/(pv)$ curve from unity at $p=1$ to the successive experimental points (compare final paragraph of footnote 7, and see Fig. 3).

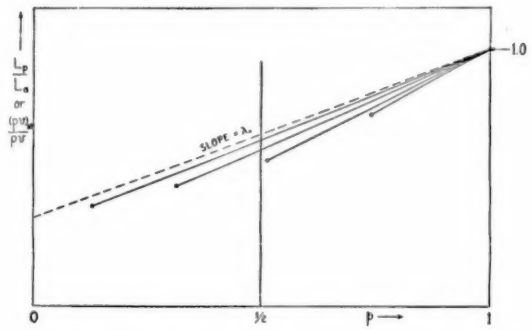

FIG. 3. When L_p/L_a is plotted against p, the limiting value of the slope of a set of secants, drawn from unity at $p=1$ to the experimental points is one (but not the best) estimate of λ_0 (see footnote 7). This is also true if $(pv)_{1a}/pv$ is used as ordinate (see Eq. (26)).

This completes the discussion of case a, which may be summarized as follows. One fits data on L_p to a parabolic function, Eq. (7), and evaluates the coefficients a, b and c, preferably by least squares. Then the best value of the desired $L_{1\text{im}}$ is given by the coefficient a, and the best value of λ or λ_0, if desired, by Eq. (10). λ_0 is geometrically the slope, at $p=1/2$, of the L_p/L_c plot, where L_c is the calculated value at $p=1$ given by Eq. (7). λ is similarly the slope, at $p=1/2$, of the $L_p/L_{1\text{im}}$ plot. A non-dimensional form of the parabola, Eq. (15), leads by a longer process to the same value of $L_{1\text{im}}$ as that given by Eq. (7), but as usually employed, to a less trustworthy value of λ or λ_0, Eq. (17), since an arbitrary value L_a is used in place of the calculated L_c. The best value is given by Eq. (18). A commonly employed finite difference method for handling the data, Eq. (13), not only uses L_a in calculating λ or λ_0, but forces the adopted curve, which may be a parabola, to pass through the adopted L_a point.

In the case of $1/pv$ data one can calculate only λ or λ_0, the best values resulting from the adopted parabola, Eq. (19), being given by Eq. (20) or Eq. (22). The non-dimensional form, Eq. (25), is identical with Eq. (15), and leads to the correct value of λ or λ_0 given in Eq. (18′) or to the poorer value of Eq. (17′). The finite difference method for handling such non-dimensional data, Eq. (26), although often employed, suffers from the same defects as Eq. (13). Some of the relations in the case of the non-dimensional forms are given in Figs. (1) to (3).

Case (b)

The linear case (b) is merely a special form of case (a), in which the coefficient of the second degree term in p has become negligibly small. We therefore *assume* this coefficient to be zero, and thus get a linear equation. Every equation in case (a) can be used for case (b) by setting $c=c'=c''=0$. Thus one takes Eq. (7) in the form

$$L_p = a+bp. \qquad (27)$$

The best value of $L_{1\text{im}}$ is as before merely a, while the best value of λ_0 or λ is given by

$$1-\lambda_0 = 1/(1+\lambda) = L_{1\text{im}}/L_c = a/(a+b) \qquad (28)$$

or

$$\lambda_0 = b/(a+b) \quad \text{and} \quad \lambda = b/a. \qquad (29)$$

In place of a variable slope for the L_p/L_c plot, we now have a *constant* slope

$$\lambda_0 = (1/L_c)(dL_p/dp) = b/(a+b). \qquad (30)$$

We can use Fig. 1 also for this case, if we assume that the secant shown in that figure is now the best representation of the data.

In the case of the linear equation, the more general coefficients of Eq. (27) may conveniently be replaced by λ_0 and L_c. The result is

$$L_p = L_c[1+\lambda_0(p-1)]. \qquad (31)$$

---

to experimental error. An example of this situation is given in the last part of the section on Illustrations.

In a similar way a set of first differences showing no trend justifies the use of a linear equation, but if one uses, for the extrapolation, the average first difference, this is equivalent to passing a straight line exactly through the first and last observations and ignoring all the others.

If in Eq. (30) we replace L_c by $L_{\lim}$ we get

$$\lambda=(1/L_{\lim})(dL_p/dp)=b/a, \qquad (32)$$

i.e., λ is the constant slope of the $L_p/L_{\lim}$ plot, and the secant of Fig. 2 can be taken to represent such a plot. Introducing λ and $L_{\lim}$ in Eq. (27) we get

$$L_p=L_{\lim}(1+\lambda p). \qquad (33)$$

There is no particular advantage in using, for case (*b*), the finite difference Eq. (13), although one *might* adopt for λ_0 the *average* value of the various secant slopes (λ_Δ') thus obtained. Such a value of λ_0 has naturally the same defect discussed in connection with Eqs. (13) and (14).

We may also use the data in the non-dimensional form

$$L_p/L_a=a''+b''p, \qquad (34)$$

but as in the case of Eqs. (15) and (17), the resulting value $L_{\lim}=a''L_a$ is identical with that given by Eq. (27), while the use of a'' as a value of $1-\lambda_0$ is inadvisable since it assumes the correctness of the point L_a. The best value of λ_0 or λ is given by

$$L_{\lim}/L_c=a''/(a''+b'')=1-\lambda_0=1/(1+\lambda) \qquad (35)$$

and Eqs. (35) and (28) are really identical, just as were Eqs. (18) and (9).

The linear equation in $1/pv$ may now be given a similar treatment. We begin with Eq. (19) in the form

$$1/pv=a'+b'p \qquad (36)$$

and note that a trustworthy value of λ_0 or λ can be obtained only by evaluating a' and b' by some good method. The result is

$$1-\lambda_0=1/(1+\lambda)=(pv)_{1c}/(pv)_0 =a'/(a'+b'), \qquad (37)$$

which is really identical with Eq. (28), on account of the general relations given in Eq. (21). Hence

$$\lambda_0=b'/(a'+b') \quad \text{and} \quad \lambda=b'/a'. \qquad (38)$$

By analogy with Eq. (30), we have in place of the variable slope of Eq. (23), the constant slope

$$\lambda_0=(pv)_{1c}[d(1/pv)/dp]=b'/(a'+b') \qquad (39)$$

and the secant of Fig. 1 can be used to represent this constant slope of the $(pv)_{1c}/pv$ plot. Introducing λ_0 and $(pv)_{1c}$ into Eq. (36) we get

$$1/pv=(1/(pv)_{1c})[1+\lambda_0(p-1)]. \qquad (40)$$

If in Eq. (39) we replace $(pv)_{1c}$ by $(pv)_0$, the result is

$$\lambda=(pv)_0[d(1/pv)/dp]=b'/a' \qquad (41)$$

as shown by the secant of Fig. 2. Introducing λ and $(pv)_0$ into Eq. (36) one has

$$1/pv=[1/(pv)_0](1+\lambda p). \qquad (42)$$

As already noted, it is rather common to use pv data in non-dimensional form, and in this linear case Eq. (25) becomes

$$(pv)_{1a}/pv=L_p/L_a=a''+b''p, \qquad (43)$$

which is identical with Eq. (34). The remarks in connection with Eqs. (34) and (35) therefore apply here.

We note finally that Eqs. (30) and (39) are *special* definitions of λ_0, holding only for a linear equation, and similarly Eqs. (32) and (41) are special definitions of λ. These special definitions appear implicitly in the linear Eqs. (31), (33), (40) and (42).

Case (*b*) may be summarized as follows. One fits the data on L_p to a linear function, Eq. (27), and evaluates the coefficients a and b. The best value of the desired $L_{\lim}$ is given by a, and the best value of λ or λ_0, if desired, by Eq. (29). λ_0 is geometrically the constant slope of the L_p/L_c plot, and λ that of the $L_p/L_{\lim}$ plot, as shown explicitly by Eqs. (30) and (32) and implicitly by Eqs. (31) and (33). A non-dimensional form of the data, Eq. (34), is of no practical advantage, and is often used to give a poor value of $1-\lambda_0$ ($=a''$) in place of the correct Eq. (35). In the case of $1/pv$ data, the linear Eq. (36) leads to values of λ_0 and λ given properly by Eq. (37) or Eq. (38). λ_0 is geometrically the constant slope of the $(pv)_{1c}/pv$ plot, and λ that of the $(pv)_0/(pv)$ plot, as shown explicitly by Eqs. (39) and (41), and implicitly by Eqs. (40) and (42). The secants of Figs. 1 and 2 also show these relations.

Case (c)

All of the necessary mathematical forms are included in cases (*a*) and (*b*). To get the analogous formulas for cases (*c*) and (*d*) one merely

substitutes $1/L_p$ for L_p and pv for $1/pv$. This change often results in the replacement of λ_0 by $-\lambda$ or of $1-\lambda_0$ by $1+\lambda$. Aside from changes of this type the equations of cases (*a*) and (*c*) are strictly analogous. The analogy holds also for the assumptions made and for the reliability of the results. Hence it is unnecessary to repeat the greater part of the discussion of case (*a*), and in general we merely list each equation of case (*c*), with the *analogous* equation of case (*a*) indicated in *square* brackets.

The basic parabolic equation is

$$1/L_p=\alpha+\beta p+\gamma p^2, \qquad (44)\ [7]$$

where, by definition, $\alpha=1/L_{1\text{im}}$, and

$$1+\lambda=1/(1-\lambda_0)=(1/L_{1\text{im}})/(1/L_c)$$
$$=\alpha/(\alpha+\beta+\gamma) \qquad (45)\ [9]$$

or

$$\lambda=-(\beta+\gamma)/(\alpha+\beta+\gamma)$$

and (46) [10]

$$\lambda_0=-(\beta+\gamma)/\alpha.$$

For pv data the basic equation is

$$pv=\alpha'+\beta' p+\gamma' p^2. \qquad (47)\ [19]$$

We define

$$\lambda_p''=L_c\frac{d(1/L_p)}{dp}=\frac{1}{(pv)_{1c}}\frac{d(pv)}{dp}$$
$$=\frac{\beta+2\gamma p}{\alpha+\beta+\gamma}=\frac{\beta'+2\gamma' p}{\alpha'+\beta'+\gamma'}. \qquad (48)\ [11]\ [23]$$

Hence λ_p'' is the variable slope of the L_c/L_p or of the $pv/(pv)_{1c}$ plot, and by Eq. (46) equals $-\lambda$ at $p=1/2$. This and other relations are shown in Fig. 4, which is analogous to Fig. 1 of

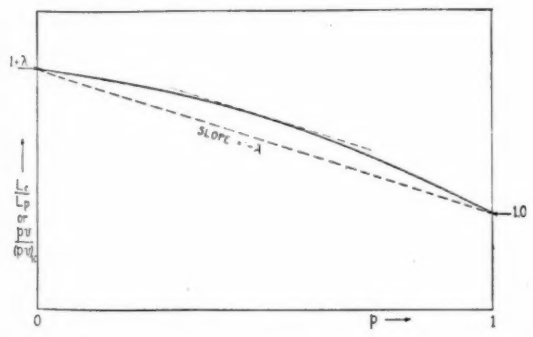

FIG. 4. Illustrative of case (*c*), Eq. (48), and strictly analogous to Fig. 1, of case (*a*).

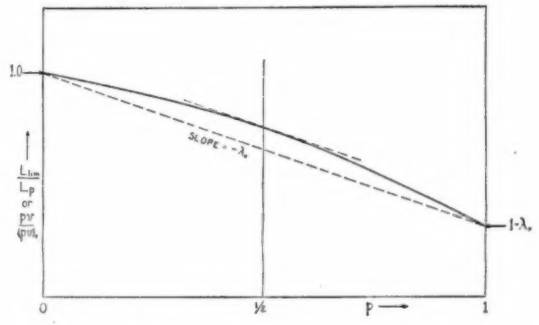

FIG. 5. Illustrative of case (*c*), and related to Fig. 4 in exactly the same way that Fig. 2 is related to Fig. 1, so far as the ordinate is concerned.

case (*a*). Replacing L_c by $L_{1\text{im}}$, or $(pv)_{1c}$ by $(pv)_0$, in Eq. (48) gives a variable slope with a value $-\lambda_0$ at $p=1/2$. This is shown in Fig. 5, which is analogous to Fig. 2.

In non-dimensional form we have

$$L_a/L_p=pv/(pv)_{1a}$$
$$=\alpha''+\beta'' p+\gamma'' p^2 \qquad (49)\ [15]\ [25]$$

and L_a/α'' gives a value of $L_{1\text{im}}$ identical with that obtained from Eq. (44). On the other hand, α'' is a poor value of $1+\lambda$ or of $1/(1-\lambda_0)$, (compare discussion of Eqs. (17) and (17′)). The best value is given by

$$L_c/L_{1\text{im}}=(pv)_0/(pv)_{1c}$$
$$=\alpha''/(\alpha''+\beta''+\gamma'')$$
$$=1+\lambda=1/(1-\lambda_0). \qquad (50)\ [18]\ [18']$$

A common use of the non-dimensional data is in the finite difference form

$$\lambda_\Delta''=\frac{1-(L_a/L_p)}{p_1-p}=\frac{1-pv/(pv)_{1a}}{p_1-p}. \qquad (51)\ [13]\ [26]$$

λ_Δ'' is the slope of the secant drawn from unity, at $p=1$, to any other experimental point, in terms of the L_a/L_p or $pv/(pv)_{1a}$ data, and its limiting value at $p=0$ gives a poor value of $-\lambda$, just as the limiting value of λ_Δ' of Eqs. (13) and (26) gives a poor value of λ_0. This is illustrated in Fig. 6.

Case (*c*) has been given in such condensed form that a summary seems unnecessary.

Case (d)

In a similar manner we write down, for case (*d*), equations analogous to those of case (*b*),

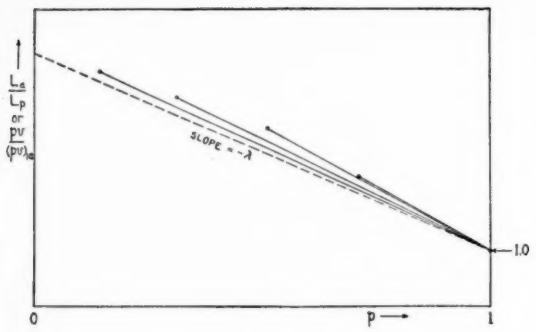

FIG. 6. Illustrative of case (*c*), Eq. (51), and strictly analogous to Fig. 3 of case (*a*).

starting with the assumed special form of Eq. (34), in which $\gamma=0$.

$$1/L_p=\alpha+\beta p. \qquad (52)\ [27]$$

The best value of $1/L_{\lim}$ is α, and the best value of λ or λ_0 is given by

$$1+\lambda=1/(1-\lambda_0)=\alpha/(\alpha+\beta) \qquad (53)\ [28]$$

or

$$\lambda=-\beta/(\alpha+\beta) \quad \text{and} \quad \lambda_0=-\beta/\alpha. \qquad (54)\ [29]$$

For pv data we use the special form of Eq. (47),

$$pv=\alpha'+\beta' p, \qquad (55)\ [36]$$

giving

$$1+\lambda=1/(1-\lambda_0)=\alpha'/(\alpha'+\beta'). \qquad (53')\ [37]$$

λ_p'' of Eq. (48) now equals $-\lambda$, the constant slope of the L_c/L_p or $pv/(pv)_{1c}$ plot, as given by the special definition

$$-\lambda=L_c\frac{d(1/L_p)}{dp}=\frac{1}{(pv)_{1c}}\frac{d(pv)}{dp}$$
$$=\beta/(\alpha+\beta)=\beta'/(\alpha'+\beta'). \qquad (56)\ [30]\ [39]$$

The secant of Fig. 4 can be taken to represent such a plot. If in Eq. (56) we replace L_c by $L_{\lim}$, and $(pv)_{1c}$ by $(pv)_0$ we get

$$-\lambda_0=L_{\lim}\frac{d(1/L_p)}{dp}=\frac{1}{(pv)_0}\frac{d(pv)}{dp}$$
$$=\beta/\alpha=\beta'/\alpha'. \qquad (57)\ [32]\ [41]$$

Hence $-\lambda_0$ is the constant slope of the $L_{\lim}/L_p$ or $pv/(pv)_0$ plot, which may be represented by the secant of Fig. 5. Eqs. (56) and (57) give the best values of λ and λ_0, as obtained from the coefficients α' and β' of Eq. (55). We note also that Eq. (57) is the origin of our symbol λ_0, which bears the same relation to $(pv)_0$ in Eq. (57) that λ does to $(pv)_{1c}$ in Eq. (56).[9]

Putting L_c, $L_{\lim}$, λ and λ_0 into Eq. (52) we get the special equations

$$1/L_p=(1/L_c)[1-\lambda(p-1)] \qquad (58)\ [31]$$

and

$$1/L_p=(1/L_{\lim})(1-\lambda_0 p). \qquad (59)\ [33]$$

Putting $(pv)_{1c}$, $(pv)_0$, λ and λ_0 into Eq. (55) we get the special equations

$$pv=(pv)_{1c}[1-\lambda(p-1)] \qquad (60)\ [40]$$

and

$$pv=(pv)_0(1-\lambda_0 p). \qquad (61)\ [42]$$

We may use the $1/L_p$ or pv data in the non-dimensional form

$$L_a/L_p=pv/(pv)_{1a}=\alpha''+\beta'' p. \qquad (62)\ [34]\ [43]$$

As in Eq. (49), L_a/α'' gives a value of $L_{\lim}$ identical with that obtained from Eq. (52), and as in the case of Eq. (49), α'' is a poor value of $1+\lambda$ or $1/1-\lambda_0$. The best value is given, as in Eq. (50), by

$$L_c/L_{\lim}=(pv)_0/(pv)_{1c}=\alpha''/(\alpha''+\beta'')$$
$$=1+\lambda=1/(1-\lambda_0). \qquad (63)\ [35]$$

There is no particular advantage in using, for case (*d*), the finite difference Eq. (51), although one might adopt for $-\lambda$ the average value of the various secant slopes (λ_Δ'') thus obtained. This value of $-\lambda$ corresponds to a linear graph forced to pass through an accepted point at $p=1$.

This completes the discussion of the four cases, and we now turn to the literature for illustrations of the use of the more important of the preceding equations.

ILLUSTRATIONS

As our first illustration we consider the possible methods of handling a set of L_p data, and for this purpose we choose five values of L_p

[9] On this same ground λ_1 is a more logical symbol than λ, but we do not wish to depart from such a well established nomenclature.

for $(CH_3)Cl$, published by Batuecas.[10] These are listed in Table I.

TABLE I.

p (at.)	1	$\frac{2}{3}$	$\frac{1}{2}$	$\frac{1}{3}$	$\frac{1}{4}$
L_p (g. liter^{-1})	2.3075	2.2895	2.2802	2.2713	2.2664

Each of these L_p values is itself the average of many determinations, all of which appear in the original paper. Batuecas gives a plot of L_p as a $f(p)$. When replotted on a large scale, both L_p and $1/L_p$, as $f(p)$, show a small but perceptible deviation from linearity. This deviation may of course be due to some systematic experimental error, a question to which we revert later. For the moment we accept the data at their face value, and proceed to the analytic derivation of a value of L_{lim}. In this work we use the method of least squares, giving equal weight to each point. In order to indicate certain relations, we have carried out the calculation for all four types of suggested solution, i.e., L_p and $1/L_p$ linear, and L_p and $1/L_p$ parabolic in p. In the following sections, unless otherwise stated, L always means the calculated value L_c.

(1) L_p linear. Eq. (27)

$$L_p=(2.25291\pm0.00012)+(0.05467\pm0.00019)p,$$

$s=1.33\times10^{-4}$ or one part in 17,300 of L.[11]

Hence

$L_{\text{lim}}=a=2.25291\pm0.00012$, $L=a+b=2.30758$,

λ, from Eq. (4) or (29), $=0.024266\pm0.000084$.

(2) $1/L_p$ linear. Eq. (52)

$$1/L_p=(0.443793\pm0.000031)-(0.010454\pm0.000051)p,$$

$s=0.353\times10^{-4}$ or one part in 12,300 of L.

Hence

$L_{\text{lim}}=1/\alpha=2.25330\pm0.00016$,

$L=1/(\alpha+\beta)=2.30766$,

λ, from Eq. (4) or (54), $=0.02412\pm0.00012$.

(3) L_p parabolic. Eq. (7)[12]

$$L_p=(2.25249\pm0.00030)+0.056316p-0.0013042p^2,$$

$s=1.087\times10^{-4}$ or one part in 21,230 of L.

Hence

$L_{\text{lim}}=a=2.25249\pm0.00030$,

$L=a+b+c=2.30751$,

λ, from Eq. (4) or (10), $=0.024424$.

(4) $1/L_p$ parabolic. Eq. (44)

$$1/L_p=(0.443948\pm0.000056)-0.011068p+0.0004891p^2,$$

$s=0.201\times10^{-4}$ or one part in 21,560 of L.

Hence

$L_{\text{lim}}=1/\alpha=2.25252\pm0.00028$,

$L=1/(\alpha+\beta+\gamma)=2.30750$,

λ, from Eq. (4) or (46), $=0.024408$.

The above data show the following significant relationships:

(a) The proportional value of s for the linear and parabolic solutions of L_p is not very different, and the two resulting values of L_{lim} agree as well as is to be expected.[13] On the other hand the proportional value of s for the linear solution of $1/L_p$ is distinctly larger, and the corresponding value of L_{lim} differs from the parabolic solution by more than is to be expected from the probable errors. Hence we conclude that the linear solution of the $1/L_p$ data is unsatisfactory.

(b) Both parabolic solutions lead to almost the same value of L_{lim} and to the same probable error. The latter results from the near equality of the two proportional values of s. We conclude

[10] T. Batuecas, Anales soc. espãn. fís. quím. **24**, 528 (1926).

[11] The standard deviation (S.D.) of a set of observations is $s=(\Sigma wv^2/\Sigma w)^{\frac{1}{2}}$ where $v=$residual$=Obs.\text{-}Calc.$, and w is the weight of each observation. When all observations are given equal weight (unity) as here, s becomes $(\Sigma v^2/n)^{\frac{1}{2}}$, where n is the number of observations. The S.D. differs from the average deviation of the observations from their calculated values only in that the root mean square average is used. The probable error of each coefficient evaluated and of the function itself is proportional to s.

[12] In the case of parabolic solutions it has seemed unnecessary to calculate probable errors except for the important first coefficient giving L_{lim}.

[13] Their difference just equals the sum of their probable errors.

therefore that either parabolic solution is satisfactory, and slightly better than the linear solution of L_p.

(c) In spite of the smaller proportional value of s for the parabolic solutions, as compared with the linear, the corresponding probable errors are much larger. This is an illustration of the fact that as the number of undetermined coefficients in the adopted function is increased, the reliability of any extrapolation very rapidly decreases.[14] We may elaborate this very important point as follows. In the region of *interpolation*, the probable error of any adopted function is a correct indication of the reliability. But in the region of *extrapolation* we are *assuming* the correctness of the adopted function, and any calculated probable error is based on such an assumption. Hence if the assumption is incorrect, the probable error will be quite misleading. So in the present case, the relatively small probable error of L_{lim} for the two linear solutions is a true criterion of the reliability of L_{lim} only if the function is known to be linear. In the case of $(CH_3)Cl$, however, it is possible that the function is not linear, and therefore the probable error of L_{lim}, as calculated by either parabolic solution, is a much more conservative indication of the reliability.

We accordingly adopt, as the best value of L_{lim} obtainable from the data of Table I, the average of the two parabolic solutions, i.e.,

$$L_{\text{lim}} = 2.2525 \pm 0.0003.$$

It will be shown in the second article of this series that the best value of R is 22.4146 ± 0.0003 liter-mole^{-1}. Hence by Eq. (3) $M = 50.4889 \pm 0.0067$ for $(CH_3)Cl$. The international atomic weights for H ($=1.0078$) and Cl ($=35.457$) seem well established and should have negligibly small errors compared to that in M itself. Hence $C = 12.0086 \pm 0.0067$ from the data of Batuecas.[10] In order to compare our results with the calculations of Batuecas, we note that the best value of λ, as obtained from the average of the two parabolic solutions is 0.02442. All four types of solution give a value of L close to the observed 2.3075, and the parabolic solutions give this exactly, to five digits.

Batuecas makes the calculation in a quite different manner. He first plots L_p against p and makes a graphical linear extrapolation, obtaining $L_{\text{lim}} = 2.2527$, compared to our 2.2529 for the same function. Batuecas' article also includes a number of sets of measurements of pv at various pressures, the highest pressure being usually close to one atmosphere. These data have not been considered in our calculations. From such data he calculates λ_Δ'' of our Eq. (51).[15] The values so obtained are found to *decrease* rapidly with decreasing pressure. This corresponds to a pv curve with a negative (and large) coefficient of the second degree term, whereas his $1/L_p$ data lead, as we have just seen, to a *positive* (and small) second degree coefficient. The two sets of data are therefore definitely incompatible, and since the average deviation of the pv data is much larger than for the L_p data, we have discarded the former data entirely. Batuecas, on the other hand, considers that the decrease in the λ_Δ'' values is due to experimental difficulties (surface effects, etc.) and adopts for λ the *highest* λ_Δ'' value in each set. This happens to agree fairly well with his previous determination of λ. The average of all such highest values is 0.0245.

Batuecas now uses his observed value of L and his graphically extrapolated value of L_{lim} to get, by Eq. (4), $\lambda = 0.0243$. This he averages with his other value, 0.0245, and combines the new average λ with his observed L to get finally $L_{\text{lim}} = 2.25254$. By chance this is close to our adopted L_{lim} value, but we fail to see the justification for his handling of the pv data, or for his averaging of the results.[16]

[14] This fact has been well shown by H. Schultz, J. Am. Statistical Assoc. **25**, 139 (1930) (see plots on p. 159). This important article was unfortunately overlooked in a later discussion of the same subject by one of us (R. T. Birge, Phys. Rev. **40**, 207 (1932)).

[15] Batuecas calculates the ratio of the change of pv to that of p, using always the highest pressure (which is *not* one atmosphere) for one of the points. This ratio is then divided by $(pv)_1$, a value he evidently gets by some sort of extrapolation. His resulting λ_Δ'' values are therefore not exactly those defined by Eq. (51), and the limiting value at $p=0$ is not exactly λ, but the theoretical discrepancy is negligible.

[16] In particular one is never justified in combining an observed value of L with a value of λ obtained from pv data in order to calculate L_{lim}, when L is one of a set of

In order to leave no false impression regarding the properties of $(CH_3)Cl$, we may note that later work on this gas has been performed by Crespi.[17] He obtains for L_p at $p=1$, $1/2$ and $1/4$ atmospheres the values 2.30734, 2.27998, and 2.26617 respectively. These lie quite accurately on a linear graph, giving

$$L_p=(2.252489\pm0.000062)+(0.054868\pm0.000093)p,$$

$s=0.43\times10^{-4}$ or one part in 53,600 of L.

Hence $L_{\lim}=2.252489\pm0.000062$,
$\lambda=0.024359\pm0.000041$,
$L=2.30736$,
$M=50.4886\pm0.002$,
$C=12.0082\pm0.002$.

Because of the small number of points, the stated probable errors are rather unreliable, but it would appear that Crespi's work is somewhat more accurate than that of Batuecas, and hence that the curvature in the L_p plot of Batuecas' data is due to some systematic experimental error. Fortunately both agree very well in the resulting values of $L_{\lim}$ and the atomic weight of carbon.

Moles,[18] in summarizing the work on $(CH_3)Cl$, handles the data of Batuecas[10] and Crespi[17] in an entirely different way. Although each of these investigations yields directly a value of $L_{\lim}$, and as just noted, practically the same value, Moles does not attempt to get a value of $L_{\lim}$ from either. Instead he adopts Batuecas' own average value of λ (0.0245), and uses our finite difference Eq. (51) to get from Crespi's data a value $\lambda=0.0244$.[19] The average of these two ($=0.02445$) is then combined with *Crespi's observed* value of L to obtain $L_{\lim}$. The resulting value (2.25227) differs appreciably from the value 2.2525 given directly by each investigation. This well illustrates the danger of working with an observed value of L and a calculated value of λ, rather than with a directly calculated value of $L_{\lim}$. Moles' resulting value $C=12.003$ differs from ours solely because of the difference in the adopted values of $L_{\lim}$.

It seems desirable to interpolate, at this point, a brief description of the method for calculating λ from (pv) data, ordinarily used by Batuecas and others who have been associated with Professor A. Guye. The method is described in detail in a paper by Batuecas, Maverick and Schlatter[20] on the value of $1+\lambda$ for oxygen.

One obtains just three values of pv at different pressures, the first pressure being close to one atmosphere. These are fitted to a linear equation for pv—our Eq. (55)—using a and b for our α' and β'. The value of $1+\lambda$ then follows from our Eq. (53′). The method used is really a variation of the finite difference method, Eq. (51), and is as follows. From points 1 and 2, using Eq. (55), β' is evaluated, i.e., $\beta'=\Delta(pv)/\Delta p$. From points 1 and 3 a second value of β' is obtained. The resulting average value of β' is substituted in Eq. (55) to give, for each experimental point, a value of α'. The three resulting values are averaged. Then our Eq. (53′) is used, with $(\alpha'_{\text{aver}}+\beta'_{\text{aver}})$ in the denominator, but with *each* of the three values of α' in the numerator, to get three values of $1+\lambda$, which are finally averaged. The last two steps are obviously unnecessary. The average $1+\lambda$ is given directly by $\alpha'_{\text{aver}}/(\alpha'_{\text{aver}}+\beta'_{\text{aver}})$.

By making a graphical representation of this method one can see easily that it is equivalent to a least squares solution in which a high weight has been given to point 1 (at the highest pressure), a much smaller weight to point 2 and a still smaller weight to point 3. This is probably a more reasonable method of weighting than

---

L_p values. Such a procedure forces a slope on the L_p plot that may be quite incompatible with that obtained directly from the L_p data. In such a situation the only reliable $L_{\lim}$ value is that obtained directly from the L_p data. In the language of statistics, the value of λ obtained from pv data may be considered as *a priori* information regarding the value of λ to be obtained from the L_p data. A method for incorporating such information into the solution of the L_p data for $L_{\lim}$ could doubtless be devised, but the method would probably not be simple and so far as we know has never been investigated.

[17] Crespi, Anales soc. espăn. fís. quím. **25**, 25 (1927).

[18] E. Moles, Rec. trav. chim. **48**, 864 (1929). The L_p data of Crespi[17] are listed here.

[19] The values of λ_Δ'' are assumed by Moles to vary linearly, and the correct extrapolated value at $p=0$ is then actually 0.02444.

[20] T. Batuecas, G. Maverick and C. Schlatter, J. chim. phys. **22**, 131 (1925). See p. 137.

that of equal weights. Hence we have no real objection to the method, although we feel that it is preferable to make a deliberate weighting of each point rather than to use this concealed and wholly arbitrary system of weighting.[21]

We conclude this section with a discussion of a paper by Dietrichson, Orleman and Rubin,[22] entitled *The Density of Ammonia at Reduced Pressures and its Relation to the Atomic Weight of Nitrogen, the Gas Constant R, and the Limiting Molal Volume, v_0*, which illustrates the confusion on this subject that still remains in the literature and the consequent need of an extended treatment of the theory such as we have just given. These investigators determine the density, ρ_p, of ammonia at $p=1$, $2/3$ and $1/3$ atmospheres.[23] They list and recalculate also previous data[24] on ρ_p at $p=1$, $2/3$, $1/2$, and $1/3$ atmospheres. D.O.R. give values of pv for $w=1$. Hence by our Eq. (2) this is merely $1/L_p$ and in general we shall write $1/L_p$ where they write pv.[25] They also use d_n for our L, v_0 for our R, and R for the gas constant which we shall denote R_0. ($R=R_0T_0$, or $v_0=RT_0$ in their notation.)

D.O.R. first write our Eq. (6) in the form

$$L=M(1+\lambda)/R_0T_0$$

and remark that the accuracy with which M can be determined depends on the accuracy with which λ, R_0 and T_0 are known. We have, however, shown in detail that the value of λ is of only secondary importance. It is $L_{1\text{im}}$ that is needed. But what is more important is that T_0 has nothing to do with the problem. It is only the product $R_0T_0=R$ that is required. This product R is known far more accurately than either factor,[26] and as is shown in the next article of this series, has a probable error of only about one part in 64,000 ($R=22.4146\pm0.0003$). The final error in M is therefore due almost solely to the purely experimental error in $L_{1\text{im}}$.

D.O.R. next describe three different ways in which λ may be calculated, from the same set of data, and label the three different numerical results thus obtained λ', λ'' and λ''' respectively. Their λ' is gotten from our Eq. (62), in which as we have remarked, α'' is a poor value of $1+\lambda$. To get their α'' they make a linear extrapolation of the L_a/L_p data to $p=0$. Their λ'' is gotten from our Eq. (34), in which again a'' is a poor value of $1/(1+\lambda)$. Here also they make a linear extrapolation of the L_p/L_a data.[27] Their first two methods then correspond to our cases (*d*) and (*b*) respectively, i.e., an assumption of $1/L_p$ and L_p linear in p, respectively.

In the third method, D.O.R. say "the authors feel that the coefficient of deviation from Boyle's law should be defined as $(1/pv)_{p\to0}[\partial(pv)/\partial(p)]_T=\lambda'''$." Since they use our Eq. (6) to get M, there is only one possible definition of $1+\lambda$, namely the one given in our Eq. (4). Their definition of λ''', as written, is ambiguous, but we find, by actual trial, that their published result ($\lambda'''=0.015109$) can be obtained *only* if one writes $\lambda'''=-[1/(pv)_0][d(pv)/dp]_{p=1}$. The true definition of λ, by the discussion following our Eq. (48), is however

$$-[1/(pv)_1][d(pv)/dp]_{p=1/2}=0.014516.$$

These results are based on their published equation

$$pv=1/L_p=1.315403-0.017767p-0.001054p^2.$$

[21] The question of weighting, and the actual experimental results of reference 20 will be discussed more fully in the second article of this series.

[22] G. Dietrichson, C. W. Orleman and C. Rubin, J. Am. Chem. Soc. **55**, 14 (1933). To be denoted D.O.R.

[23] Their actual results, which will often be used in this discussion, are $\rho_p=0.77126$, 0.51161, and 0.25458 respectively. These lead by our Eq. (2) to $L_p=0.77126$, 0.767415 and 0.76374 respectively, or $1/L_p=1.296580$, 1.303075 and 1.309346 respectively.

[24] E. Moles and T. Batuecas, Anales soc. espãn. fís. quím **28**, 871 (1930). To be denoted M.B.

[25] They also use 1 cc as the unit of volume and therefore all their values of pv and coefficients in equations for pv as a $f(p)$ must be divided by 10^3 to obtain our $1/L_p$ in liter·atmos. g.$^{-1}$ units. We make such a division in quoting their results.

[26] Actually R_0 is determined from R/T_0 and has therefore practically the same probable error as has T_0, i.e., one part in 9100. ($T_0=273.18\pm0.03$ by *G.C.* 1929.)

[27] We have remarked in footnote 8 on the inadvisability of using any average first difference for such an extrapolation. Quite aside from this question, we are unable to check the results given by D.O.R. In the case of $1+\lambda'$ the two available first differences are 0.00501 and 0.004836, but to get their published 1.014901 one must assume 0.005055 in the extrapolation. Similarly for $1/(1+\lambda'')$ the available first differences are 0.004985 and 0.004765, but 0.005031 is needed to get their published 0.985219 ($=1/1.015003$).

In getting this equation the authors state that each point was weighted in proportion to the pressure and a least squares solution obtained. Since, however, there are three undetermined coefficients and only three points, the correct equation necessarily satisfies each point, regardless of the weighting, and could hardly be called a least squares solution. Their published equation gives a small positive residual for every point. The correct solution, which can be obtained very quickly from a difference table, is

$$1/L_p = 1.315390 - 0.017793p - 0.001017p^2.$$

Having obtained their three different values of λ, which lead in turn to three different values of M, the molecular weight of NH_3, the authors remark "It will be noted that the at.wt. of N . . . was found to show considerable variation. It therefore appears that the gas density method for the determination of atomic weights cannot at present be considered as reliable as that based on gravimetric analyses, not because of insufficient accuracy as regards the gas densities, but rather because of uncertainties in connection with λ, R_0 and T_0 (also $R = R_0T_0$)." But the *variation* in the value of λ, as calculated in different ways, has nothing whatever to do with the value of R, and again we note that it is only the values of R and L_{lim} that concern us in this problem.

Having reached the above conclusion, D.O.R. now proceed to use our Eq. (3) to *calculate* R, from the accepted best value of M for NH_3 (17.0312). In this calculation they use, for the first time, the value of L_{lim} directly calculated from the data. This value they calculate in two ways, (1) $1/L_p$ parabolic, giving their $1/L_{\text{lim}} = 1.315403$ in the equation already quoted, and (2) $1/L_p$ linear, for which they get $1/L_{\text{lim}} = 1.316484$. From these two results they get $R = 22.4032$ and 22.4213, respectively. They make similar calculations for the M.B. data, getting $R = 22.4136$ and 22.4120. As we shall show immediately, the most probable value of L_{lim} obtainable from this work has a probable error of about one part in 12,000 and obviously cannot be used to improve the evaluation of R, which is already known to about one part in 64,000, from the work on oxygen to be discussed in the second paper of this series.

Let us now turn to a consideration of the most probable value of L_{lim}, and of M, resulting from the work of D.O.R. and of M.B. As just noted, D.O.R. have given solutions based on our Eqs. (44) and (52), i.e., $1/L_p$ parabolic and $1/L_p$ linear, respectively. We have made similar calculations, with results somewhat different from those that they publish. We have already given our parabolic solution for the D.O.R. data. The corresponding linear solution with the weighting (proportional to pressure) used by D.O.R., is

$$1/L_p = (1.31582 \pm 0.00011) - (0.01922 \pm 0.00011)p,$$

$s = 0.50 \times 10^{-4}$ or one part in 26,000 of L.

$L_{\text{lim}} = 0.759983 \pm 0.000064$ or one part in 12,000.

λ (from Eq. (53)) $= 0.01482 \pm 0.00010$,

$M = 17.0347 \pm 0.0014$, $\quad N = 14.0113 \pm 0.0014$.

For the reasons to be stated presently, we believe this to be the best result obtainable from the D.O.R. data. Their own equation is

$$1/L_p = 1.316484 - 0.020066p$$

and gives $s = 2.17 \times 10^{-4}$, or 4.3 times that of the necessarily minimum value of the least squares solution.

For the M.B. data we obtain as the linear solution

$$1/L_p = (1.315776 \pm 0.000088) - (0.01991 \pm 0.00012)p.$$

$s = 0.60 \times 10^{-4}$ or one part in 21,600 of L.

$L_{\text{lim}} = 0.760007 \pm 0.000051$,

$\lambda = 0.015371 \pm 0.000089$,

$M = 17.0352 \pm 0.0012$, $\quad N = 14.0118 \pm 0.0012$.

D.O.R. give for the same treatment of the M.B. data

$$1/L_p = 1.315940 - 0.020177p.$$

We find from this equation, $s = 0.96 \times 10^{-4}$, or 1.6 times the true least squares result.

Now a plot of the M.B. data shows no trend whatsoever from linearity. In fact an unweighted

parabolic solution of their data[28] gives $L_{\text{lim}} = 1.315846$, which differs from the linear result by less than the probable error of the latter. On the other hand, the value of s for the D.O.R. linear solution is even smaller than that for the M.B. data, so that unless the former data are by far the more accurate, the deviation from linearity should be ascribed to experimental error. Moreover, the value $1/L_{\text{lim}} = 1.315390$, as already given for the parabolic solution of the D.O.R. data, leads to $M = 17.0403$, a result greater than the accepted value, 17.0312, by one part in 1870, whereas the linear solution gives a result greater by only one part in 4860. Finally, the linear solutions of the D.O.R. and the M.B. data give almost the same value of L_{lim}. We conclude, therefore, that the mean deviation of the D.O.R. data from a linear curve, i.e., one part in 26,000, is to be ascribed to experimental error. We are not in a position to discuss critically the cause of the high resulting value of M. We may note, however, that if the D.O.R. point at $p = 1/3$ is discarded, and a straight line passed through the other two $1/L_p$ values (at $p = 1$ and $2/3$), the result is $L_{\text{lim}} = 0.759841$, or $M = 17.0315$ and $N = 14.0081$. It is therefore possible that systematic errors enter into the determination at $p = 1/3$.[29]

The value of L_{lim}, as published by M.B.[24] is 0.75990, as contrasted with our 0.760007 obtained from a linear $1/L_p$ solution. We have made solutions of their data corresponding to all four of our cases (*a*) to (*d*), but none of the results is as low as theirs.[30] From it, with their usual $R = 22.414$, M.B. obtain $N = 14.009$. It is possible that M.B. obtained their result in a manner similar to that just mentioned in connection with the D.O.R. work, for if one uses only the two $1/L_p$ points at $p = 1$ and $2/3$, the resulting value of L_{lim} is 0.759886, giving, with our value of R, $N = 14.0091$. So again there may be systematic errors at their two lower pressures (1/2 and 1/3 atmospheres). In any case it would appear that ammonia is not a suitable material to use in precision measurements of the at.wt. of nitrogen, by the limiting gas density method.

Conclusions

From the preceding discussion we may conclude that, starting with the fundamental Eq. (3), the best value of L_{lim} is obtained from the intercept of the L_p curve, at $p = 0$, after fitting the L_p data to an analytic function by means of least squares. In the case of the permanent gases, a linear function in p is known to be satisfactory, in the region $p = 1$ to 0 atmospheres, but in the case of the easily condensible gases, it may be necessary to use a parabolic function. Further, if L_p is given by a linear function in p, $1/L_p$ is likely to be an equally satisfactory linear function in p, and this form has often been used in the literature. A similar remark applies to L_p and $1/L_p$ as parabolic functions in p. These four possible functions have been treated in detail in cases (*a*) to (*d*). In each of these cases there are several ways in which the function may be written and handled, thus accounting for the wide variety of methods used in the literature. In each of the cases (*a*) to (*d*) however, we have shown that there is only one method that leads directly to the most reliable value of L_{lim}. Unfortunately some of the more commonly used methods of calculating L_{lim} are by no means the most reliable, and numerical examples of this have been given in the concluding section on Illustrations.

If one has only values of pv, at various pressures, it is possible to calculate only λ or λ_0, as defined by Eq. (4). To get L_{lim} we then need a value for L, the density at one atmosphere, as shown by Eq. (4′). It is, however, questionable procedure to use a value of L obtained from one investigation in combination with a value of λ, or λ_0, obtained in some other investigation. Furthermore, if experimental values of L_p are available, these lead directly to a value of L_{lim}, and the calculation of L and $1+\lambda$ from such

---

[28] We find that the weighted and unweighted linear solutions give values of L_{lim} differing by only one part in 200,000, so that the weighting is here immaterial. All our parabolic solutions have accordingly, to save time, been made with unweighted data.

[29] The observed $\rho_n = 1/3$ is given by D.O.R. as 0.25458 $\pm$0.00001 g. liter^{-1} and the calculated value, on this new assumption, is 0.254536. The discrepancy is 4.4 times the stated probable error, but the data quoted on p. 16 of D.O.R. indicate the possibility of systematic errors of this magnitude.

[30] This value, 0.75990, is quoted by the Inter. At. Wt. Committee, J. Am. Chem. Soc. **53**, 1627 (1931). We do not have available the original M.B. paper.

data, as is often done, only complicates the matter, and has sometimes resulted finally in an untrustworthy value of L_{lim}. These points have also been discussed in connection with cases (*a*) to (*d*), and have been illustrated by examples from the literature. It is, in fact, easily possible to obtain a value of L_{lim}, and hence a molecular weight, that differs by several times its probable error from the most trustworthy value given by the data. Hence for data of the accuracy now obtainable in precision work on gas densities, the best analytic methods are not only suitable, but demanded. The actual application of such methods to the data on oxygen and on carbon will be given in detail in the next two papers of this series.

On the Statistical "Interaction Between Ions and Molecules" in Media of Small Dielectric Constant

OTTO HALPERN, *New York University*, AND PHILIPP GROSS, *University of Vienna*

(Received November 24, 1933)

In this paper the general theory of the interaction between ions and molecules in solution is discussed with particular reference to the theory of Debye on the salting-out effect. Formulae are developed for the free energy of the interaction between ions and dipoles. The formulae are applied to the dissociation equilibrium of an electrolyte in a medium of low dielectric constant.

I. INTRODUCTION. COMPARISON WITH A THEORY OF DEBYE

AS is well known, the solubility of neutral molecules is very frequently changed by the presence of ions (salting-out effect). Debye[1] was the first to ascribe this phenomenon to the local changes in the average dielectric constant of the medium produced by the different attractions exerted upon the molecules of different types in the nonhomogeneous electric fields of the ions. From macroscopic electrostatics we learn that substances of high dielectric constant (high dipole moment) accumulate in regions of a higher field of force, while substances of lower dielectric constant are expelled therefrom. In perfect analogy, the molecules of higher dipole moment will accumulate in the neighborhood of the ions, while those of smaller dipole moment will mostly be found in more distant parts. Since the dipole moments of most solute substances are smaller than that of water these molecules will be repelled by the ions, or in other words the volume accessible to them will become diminished by the presence of charges. This explains qualitatively the reduction of solubility of most solutes in water. Inversely, solutes having a dipole moment larger than that of water show an increase in solubility in the presence of charges, as we can predict by the simple picture, and as has been verified experimentally.[2] (Salting-in effect.)

Debye has succeeded in expressing this picture in the form of a quantitative scheme. For this purpose he considered the influence of the various ions as being independent, and determined the free energy of a mixture the dielectric constant of which varies with the distance from the ion which is assumed as being at the center. In statistical equilibrium, the gradient of the osmotic pressure which is produced by the variable concentrations must be just balanced by the electric forces produced by the ion. He thus derives as a function of the distance from the ion the law of distribution into which the ionic diameter, the dielectric constants of the components, the charge of the ion and the absolute temperature enter as parameters. For practical evaluation some assumptions have to be made as to the variation of the dielectric constant with the relative concentrations of the molecules.

There can be no doubt that the principle of Debye's views is valid and leads to a correct understanding of the phenomena observed. On the other hand, some of the assumptions made for the purpose of calculation do not seem to fit all cases of importance. In aqueous solutions the effect generally is so small that we have to take ionic concentrations which are comparatively high (0.1 N and higher). In such solutions the average distance between the ions becomes so small that we can no longer assume the effect of each ion to be independent of the presence of the

[1] P. Debye and I. McAulay, Phys. Zeits. **26**, 23 (1925); P. Debye, Zeits. f. physik. Chemie **130**, 56 (1927).

[2] Gross and Schwarz, Monatshefte f. Chemie **55**, 287 (1930); Sitzber. Ak. Wien. IIb **139**, 179 (1930); Gross and Iser, ibid. **55**, 329 (1930); IIb **139**, 221 (1930).

others.[3] Furthermore, it is an essential assumption on which Debye's theory is based that we shall have at every point in the mixture a composition corresponding to the equilibrium distribution. This assumption is the more dangerous since the volume elements with which we are concerned are of a molecular order of magnitude, so that fluctuations will invariably play an important part and will influence the free energy of the composition decisively. The following calculations will show that this point is of paramount importance, and it could have been suspected to play a decisive part on *a priori* grounds. In fact, it changes completely the quantitative form of the result for the case of a "salting-in" effect to which the formulae given below can be directly applied.

Without any calculations it is easy to understand the qualitative difference between Debye's treatment and that which we are going to propose, by considering the following example: The energy density of an ion carrying the charge ϵ in a medium of a dielectric constant D in the distance r from the ion is given by the expression

$$\epsilon^2/(8\pi D r^4).$$

The maximum change which can be reached by the presence of molecules of higher dipole moment is precisely equal to the value given above. This maximum change would correspond to an infinite dielectric constant. On the other hand, let us take a molecule with a dipole μ and put it at a distance r from the ion. The work gained by carrying the molecule from infinity to r will increase with the dipole moment. The difference in the results is due to the fact that, in statistical equilibrium for the case of an ideally homogeneous complete mixture, the various dipoles influence each other, and in this way reduce the work which could be gained by the attraction of one single dipole.

To sum up: Debye's treatment would be rigorous if we were dealing with infinitely small molecules carrying infinitely small dipoles so that there is always a complete mixture even in molecular dimensions according to the laws of thermodynamics. We shall on the other hand neglect the "competition for space around an ion" which the different molecules are making each other. The formulas derived in the following paragraph therefore apply directly only to the case of a solute of very low concentration in a medium, the dielectric constant of which is negligibly small compared to the dielectric constant of the solute molecule. This permits us to consider the "fluctuation-terms" which are of decisive importance for dissociation—equilibria.

II. Statistical Calculation of the Free Energy

Let us consider the dilute solution of an electrolyte in a solvent of the small dielectric constant D. The electrolyte shall be partially dissociated, the concentrations expressed in mols per liter of the ions, and the undissociated molecules shall be denoted respectively by c_i and c_M. The charge of the ion, which shall be characterized by the index i, shall be ϵ_i. The total volume of the solution shall be V, so that the volume which can be ascribed on the average to each ion will be equal to

$$v_i = 4\pi R^3/3 = 1000/N\sum c_i,$$

where N = Loschmidts number. The minimum distance between the molecules and the ion i shall be $a \ll R$. We shall assume for the purpose of calculation that the value of the dielectric constant D shall be constant up to the surface of the ion, an assumption to be discussed in detail in due course. We now can divide the total volume into $N\sum c_i$ cells each containing one ion; and it shall furthermore be assumed that on the boundary of this volume the force exerted by the ion shall have become vanishingly small. Each volume v will contain $Nc_M v/1000$ undissociated molecules. The excess free energy ψ_M of each molecule *due to the interaction between ion and molecules* is then given by the following equation

$$v e^{-\psi_M/kT} = 2\pi \int_a^R r^2 dr \int_0^\pi \sin\vartheta d\vartheta e^{\epsilon\mu\cos\vartheta/DkTr^2}. \qquad (1)$$

[3] Gross, Monatshefte f. Chemie **53** and **54**, 445 (1929).

To evaluate this integral we expand the exponential function in a power series, and first carry out the integration over ϑ. We thus arrive at the following expression:

$$ve^{-\psi_M/kT}=4\pi\int_a^R r^2dr\left\{1-\tfrac{1}{2}\sum_1^\infty{}_n\left(\frac{\epsilon\mu}{DkTr^2}\right)^n\frac{\cos\vartheta^{n+1}}{(n+1)!}\Big|_0^\pi\right\}$$

$$=4\pi\int_a^R r^2dr\left\{1+\sum_1^\infty{}_n\left(\frac{\epsilon\mu}{DkTr^2}\right)^{2n}\frac{1}{(2n+1)!}\right\}. \quad (2)$$

This series can be integrated term by term, with the result

$$ve^{-\psi_M/kT}=\left\{\frac{4\pi r^3}{3}-4\pi\sum_1^\infty{}_n\frac{1}{(2n+1)!}\frac{1}{(4n-1)}\left(\frac{\epsilon\mu}{DkT}\right)^{2n}r^{-4n+1}\right\}\Big|_a^R$$

$$=\left\{\frac{4\pi r^3}{3}-2\pi\sum_1^\infty{}_n\frac{r^3}{(2n+2)!(1-7/2(2n+2))}\left(\frac{\epsilon\mu}{DkTr^2}\right)^{2n+2}\cdot\left(\frac{DkTr^2}{\epsilon\mu}\right)^2\right\}\Big|_a^R. \quad (3)$$

We will now discuss the value of the integrated power series separately for the two boundaries. For $r=R$ the first term gives $(4\pi/3)R^3=v$ while all following are smaller by a factor of the order of $(\epsilon\mu/DkTR^2)^2$. It is therefore sufficient to limit ourselves to the first term.

The lower boundary necessitates a more elaborate treatment. For practical reasons we are mostly interested in such values of the dipole moment and ionic diameter for which $\epsilon\mu/DkTa^2$ becomes large compared to 1, since only then can an appreciable effect be expected. If we now rewrite the expression for our power series at the lower boundary in the following form

$$\frac{2\pi a^3}{\sigma^2}\sum_1^\infty{}_n\frac{\sigma^{2n+2}}{(2n+2)!(1-7/2(2n+2))}$$

$$(\sigma=\epsilon\mu/DkTa^2)$$

we notice that it differs from the power series for the exponential function e^σ for three reasons. The first four terms are missing, the factorials in the denominator have the additional factor $1-7/2(2n+2)$ and every second term has dropped out. If now σ is a large number compared to 1, as assumed, the value of the exponential function is almost exclusively determined by those terms in its power series the index of which is almost equal to σ. In this case the first few missing terms do not contribute anything appreciable, and the additional factor in the denominator can be replaced by a constant factor $1-7/2(2\sigma+2)$. (It will appear later on that it is without influence in any case.) For the missing terms we can account by introducing the factor $\frac{1}{2}$. Keeping this in mind we can sum the power series for the lower boundary also, and thus arrive at the final expression

$$ve^{-\psi_M/kT}=v+\frac{\pi a^3e^\sigma}{\sigma^2(1-7/2(2\sigma+2))}, \quad (4a)$$

$$\psi_M=-kT\log\left\{1+\frac{\pi a^3e^\sigma}{v\sigma^2(1-7/2(2\sigma+2))}\right\}. \quad (4b)$$

Since

$$v=1000/N\sum c_i$$

we arrive at the following expression for the additional free energy of each molecule

$$\psi_M=-kT\log\left\{1+\frac{N\pi a^3\sum c_ie^\sigma}{1000\sigma^2(1-7/2(2\sigma+2))}\right\}. \quad (5)$$

For sufficiently low ionic concentrations we can expand the logarithm, and we thus obtain the following expression for the additional free energy of the total solution:

$$\Psi_1=Nc_M\psi_M=-\frac{\pi a^3kTN^2c_M\sum c_ie^\sigma}{1000\sigma^2(1-7/2(2\sigma+2))}. \quad (6)$$

III. Remarks and Applications

The most objectionable point in our derivation seems to be the use of the microscopic dielectric constant of the solvent up to the surface of the ion. For all practical applications where ionic diameter and the dipole of the molecule will be constants which must be determined empirically we have to keep in mind that the values thus obtained are not strictly correct, but might be considerably influenced by the probably wrong assumption as to the value of the dielectric constant. At the present stage we do not think that matters can be improved in this respect.

The application to the change of solubility is quite obvious. The equilibrium condition for the molecule in solution can be simply obtained by differentiating Ψ_1 with respect to Nc_M and adding the resulting expression ψ_M to the free energy of the solute. The dissolved molecules have an activity coefficient $e^{\psi_M/kT}$ the logarithm of which is proportional to the concentration of the ions, and which depends in a very sensitive way on the dielectric constant of the solvent.

A more important application, for which our treatment would seem to be particularly appropriate, is the dissociation equilibrium, and its dependence on concentration. In media of low dielectric constant the effect calculated above will be of great importance, and might account, as we have anticipated, for a number of observed anomalies. The equilibrium condition between ions and non-dissociated molecules can be written in the form

$$f_i^2 c_i^2 / f_M c_M = K \tag{7}$$

f_M stands for the activity coefficient of the molecule, f_i for that of the ion. f_i is due to the interionic effects as well as to the interaction between ions and molecules. We *shall here omit the interionic contribution* to the activity coefficient, since it can always be inserted easily, provided that the theory of ionic interaction has been developed for the solvent under consideration. The contribution to the activity coefficient resulting from the ion-molecule interaction is obtained by differentiating Ψ_1 with respect to Nc_M and Nc_i. Inserting these expressions into (7), we arrive at the following equilibrium condition

$$\log \frac{c_i^2}{c_M} = \log K + \frac{kT\pi a^3 M e^{\sigma}}{1000\sigma^2(1-7/2(2\sigma+2))}(c_M - \sum c_i). \tag{8}$$

In the special case of *slight* dissociation (8) simplifies to

$$\log \alpha^2 c = A + Bc \tag{9}$$

(α = degree of dissociation and c = analytic concentration of solute).

This equilibrium condition shows interesting features, insofar as the dissociation sometimes increases with increasing concentration, because of the presence of the term Bc on the right-hand side. The concentration for which the dissociation does not change with concentration is given by the relation

$$d\alpha/dc = 0,$$

which can be written in the form

$$1/c_{\min.} = B. \tag{10}$$

If we substitute this expression for B in (9) we notice that the change of dissociation with concentration is very unsymmetrical on both sides of the point $c_{\min.}$, and that more particularly the dissociation increases very rapidly if we pass $c_{\min.}$

We shall make use of the formulae here derived in the following paper, to explain conductivity phenomena in media of low dielectric constant.

On Electrolytes in Media of Small Dielectric Constant

PHILIPP GROSS, *University of Vienna*, AND OTTO HALPERN, *New York University*

(Received February 15, 1934)

The authors give a general summary of some recent theoretical views concerning the characteristic features of electrolytes in media of small dielectric constant. After a discussion of conductivity observations in water-dioxane mixtures, previous attempts for their theoretical interpretation are criticized. It is shown that in agreement with previously proposed views of the authors the experimental data can be qualitatively and partly quantitatively understood by considering the activity-coefficient arising from ion-dipole interaction. (See preceding paper.)

I. Recent Conductivity Observations and Their Interpretations

THE behavior of electrolytes in solvents of low dielectric constant is known to show a number of anomalies when compared with aqueous solutions. The electrolytes are apparently of high molecular weight when judged by osmotic phenomena. At the same time these seemingly highly associated electrolytes show comparatively high electric conductivity. This conductivity does not depend on concentration in the way to which we are accustomed in the case of water, or media of considerable dielectric constant. Here the equivalent conductance decreases with increasing concentration, in accordance with Ostwald's law of dilution or with the theory of the conductivity coefficient (interionic forces). The authors[1] have some time ago (1925) given a general discussion in which these various contradictory phenomena are brought into harmony. By assuming interaction forces between the ions and between the ions and molecules they provided a suitable explanation for the apparent contradiction between "high association" on the one hand and anomalous conductivity on the other. The most powerful tool for treating these problems was offered by the conditions for thermodynamic stability.[2]

Quite recently, several papers have appeared which are of importance for the problem under consideration. An investigation by V. K. La Mer and Harold C. Downes[3] has again drawn attention to the appearance of anomalous conductivity of acids in benzene. These authors explain their results by making use of the views which have been given by the writers. Still later in a paper by Kraus and Fuoss[4] the conductivity of tetraisoamylammonium nitrate (and some other salts) has been studied with a solvent composed of dioxane and water in shifting proportions. Furthermore in several theoretical investigations the activity coefficients which are due to interaction between dipoles and ions have been studied by Fuoss and Kraus.[5] In this paper we shall mostly be concerned with the theoretical interpretation of the experimental results obtained by Fuoss and Kraus.

[1] Phys. Zeits. **26**, 636 (1925).

The authors wish to make use of this opportunity to correct a point in their previous presentation. In the paper quoted above they made use of an expression for the activity coefficient of the ions as given by Debye's theory of electrolytes. This application is certainly untenable, since the behavior of ions in media of small dielectric constant cannot even approximately be described by Debye's formula.

[2] Rodebush (Rodebush and Ewart, J.A.C.S. **54**, 419 (1932)) claims that the ideas presented above have been anticipated in a paper by himself and Latimer (J.A.C.S. **42**, 1419 (1920)). We readily admit that Rodebush and Latimer have in a general way mentioned the influence of electric forces the existence of which was in fact obvious. The determining influence of the activity coefficient on anomalous conductivity, the connection between anomalous conductivity and small osmotic pressure, and the general thermodynamic relations were not mentioned.

[3] La Mer and Downes, J.A.C.S. **53**, 891 (1931).

[4] Kraus and Fuoss, J.A.C.S. **55**, 21 (1933).

[5] Fuoss and Kraus, J.A.C.S. **55**, 476 (1933).
Fuoss and Kraus, J.A.C.S. **55**, 1019 (1933).
Fuoss and Kraus, J.A.C.S. **55**, 2387 (1933).
Fuoss, Zeits. f. Elektrochemie **39**, 513 (1933).

The experimental results obtained by these two authors can perhaps be simply summarized as follows: The conductivity of tetraisoamylammonium nitrate is rather small at most concentrations, if pure dioxane or mixtures with a small percentage of water are used as solvents. If the solvent contains a large percentage of water the conductivity (i.e., the dissociation) increases very rapidly. Keeping the solvent constant the equivalent conductivity shows a minimum with increasing concentration, and increases fairly rapidly after passing this minimum. The location of this minimum shifts markedly to a higher concentration with increasing dielectric constant (i.e., higher water percentage of the solvent). For sufficiently high dielectric constant the equivalent conductivity shows no more minima, and changes only slightly with concentration.

Fuoss and Kraus have attempted to explain these observed facts by making use of the concept of "ionic association" which has been introduced into the theory of electrolytes by Bjerrum.[6] According to this author ions which are at a distance R from each other smaller than $\epsilon_i\epsilon_k/2DkT$ (ϵ_i, ϵ_k charge of ion, D, dielectric constant, k, Boltzmann's constant, T, abs. temp) shall be considered as forming a neutral molecule which contributes neither to the interionic forces nor according to Fuoss and Kraus to the electrical conductance. As Bjerrum already mentioned, and as actually worked out by Fuoss and Kraus, in their paper IV, this formation of complexes was not considered to cease with molecular formation, but should proceed to complexes of higher type (triple ions, quadruple ions, and so on). Thus, for example, a dipole carrying molecule and an ion were considered to form a "triple ion," provided the distance R' between them is less than a quantity R' defined by the relation

$$1/R' = 2DkT/\epsilon^2 + R'/(R'+\delta)^2,$$

where δ = dipole moment μ divided by ϵ.

With the help of Bjerrum's formulae Fuoss and Kraus calculated the "dissociation constant" for the various equilibria

$$c_J^2 f_J^2/c_M = K_1,$$

$$c_M c_J f_J/c_{J'} f_{J'} = K_2.$$

(c_J, c_M, $c_{J'}$ denote respectively the concentrations of free ions, "molecules" and triple-ions; f_J and $f_{J'}$ are the ionic activity coefficients due to *interionic* forces.) Into these formulae, parameters enter which denote the minimum distance between two ions, between an ion and a molecule, and so on. These were so determined as to give the best fit with their observation. In this way the authors were able to account for the increase of the dissociation with increasing dielectric constant, for the minimum in the conductivity-concentration curve, and for the shift of this minimum to higher values of the concentration with increasing dielectric constant. The authors furthermore made use of the Debye formula for the activity coefficient of the ions arising from the interionic forces; since the ionic concentration is very small it would follow (assuming correctness and applicability of this formula) that the *interionic* effect is of secondary importance only.[7]

The main points which Fuoss and Kraus consider as experimental verifications of Bjerrum's ionic association may be enumerated as follows: (a) With a suitably chosen value a_1 for the minimum distance of approach between the ions it is possible to calculate the variation of the logarithm of the molecular dissociation constant for changes in the dielectric constant of the medium; the following relation is found to hold:

$$\log K_1 \sim 1/D.$$

(b) By introducing *another* molecular diameter

[6] Bjerrum, Copenhagen, Akad. fys. Medd. **7**, 9 (1926).

[7] Into the formula for the activity coefficient there enters the actual ionic concentration to be determined from the analytic concentration with the aid of the law of dilution which itself contains the activity coefficients. The authors Fuoss and Kraus quote, as their sources, papers by Davis, J. Phys. Chem. **29**, 977 (1925).

Sherill and Noyes, J.A.C.S. **48**, 1861 (1926).

MacInnes, J.A.C.S. **48**, 2068 (1926).

It may be mentioned that a discussion of the influence of the activity coefficient and the law of dilution for weak electrolytes has been given in a paper by Gross and Halpern, Phys. Zeits. **25**, 393 (1924).

a_2 they calculated a dissociation constant for the equilibrium

$$c_J f_J c_M / c_{J'} f_{J'} = K_2.$$

This dissociation constant K_2 permits the determination of the shift of the minimum in the conductance-concentration curve with changing dielectric constant of the solvent. The authors furthermore claim that there exists a range in which the product $D^3/c_{\min.}$ is constant according to their theory of interaction between molecules and ions (triple ion formation). This they consider to be a theoretical explanation of an empirical law previously found by Walden.

For the reasons given in the following discussion we do not consider an explanation given on the basis of Bjerrum's theory of ionic association to be tenable.

II. Bjerrum's Concept of Ionic Association and Its Application to Conductivity Phenomena

In a previous paper[8] by one of the writers a discussion of Bjerrum's "ionic association" has been given to which the reader should refer for details. It has there been shown that the Helmholtz-relation between energy and free energy of the ions is not satisfied in Bjerrum's theory. This result is due to the fact that the maximum distance at which two ions are considered as forming a molecule depends on the temperature according to the relation $R = \epsilon_i \epsilon_k / 2DkT$. Notice that R depends on T and D only in the form $R = f(D \cdot T)$; since this is a general consequence of statistical mechanics elimination of the temperature-dependence by some modification of the expressions for R would likewise eliminate the influence of a variation of D and thereby completely invalidate the application of the theory to media of low dielectric constants. The same objections must of course be raised against the calculations of higher complexes (triple-ion equilibria etc.).

A correction which is of slight importance in the case of aqueous solutions (or in the mathematically equivalent case of van der Waals forces in non-ideal gases[9]) becomes of decisive importance for media of small dielectric constant. Here we are referring to the determination of the volume which is accessible to the free ions. According to the general concept of ionic association an ion is considered to be free if its distance from the closest ion of opposite sign is larger than R. For determining the free energy of the ions one therefore has to consider them as contained in a volume which is equal to the total volume minus the "volume occupied by the molecules." (This corresponds to the correction for the proper-volume in van der Waals theory). The "molecules" in Bjerrum's theory of ionic association have a "radius" R which for media of low dielectric constant (e.g., dioxane $D = 2.2$) takes a value 1.3×10^{-6} cm. Since almost all the salt dissolved is forming "molecules" the volume accessible to the "free ions" becomes very much reduced (sometimes even negative); the free energy of the ions therefore is very much increased as compared with the value it would take if the total volume were accessible to the ions.

To illustrate this fact let us consider an actual case of practical interest: a normal solution of tetraisoamylammonium nitrate in dioxane ($D = 2.2$). With the value R we obtain for the *volume per liter* occupied by the "molecules" 5000 cc. There is no rational way of correcting for these quite enormous errors. They are fundamentally associated with the unsound basis of the theory which treats long range (Coulomb) forces like short range (van der Waals) forces.

Furthermore Fuoss and Kraus have to assume that these associated ions do not contribute anything to the conductivity of the solution. They have not given any reasons to support this contention, nor is it by any means intuitively obvious why two ions with some forty molecular layers of liquid between them and negative potential energy ($2kT$) only slightly in excess of their average kinetic energy should not participate in electric conduction. On the other hand, they have to assume for example that a molecule and an ion are bound to a triple ion even though the binding energy in some cases is smaller than kT, that is to say to less than two-thirds of the *average* kinetic energy.

The idea in the papers of Fuoss and Kraus of explaining conductivity curves by partial dissociation is not new. What is new is only the

[8] O. Halpern, J. Chem. Phys. **2**, 85 (1934).

[9] Cf. e.g., R. H. Fowler, *Statistical Mechanics*, § 9.6.

interpretation of partial dissociation as ionic association in Bjerrum's sense. This method of computation we have already criticized from a theoretical point of view. The fact that the logarithm of the dissociation constant varies proportional to $1/D$, and that this variation is implied in Bjerrum's picture cannot be thought to corroborate the latter. *Every model* will show the same dependence, because the work necessary to remove two ions from each other varies as $1/D$. Deviation from this simple relation could only be expected if the ions had a different solvation energy in the various media. Since some traces of water appear to be always present, the ions would be mostly surrounded by water dipoles (salting-out effect), so that the energy of solvation probably varies but slightly. This view is supported by experimental evidence gained through observations of the index of absorption of ions. The index of absorption of the anion of picric acid dissolved in pure ethyl alcohol ($D=26$) shifts to the value which it shows for aqueous solutions if only a small amount of water (0.7 m/lit.) is added to the alcohol.[10]

Remembering the difficulties introduced by the contradiction with thermodynamics, by the impossibility of a correct statistics (volume-correction) and by the crude assumptions of widely distant but nevertheless nonconducting ion-pairs, we feel justified in rejecting the quantitative application of the hypothesis of ionic association.

III. The Influence of the Activity-Coefficient Arising from the Ion-Dipole Interaction

As mentioned in the introduction, it has been pointed out by the authors that anomalous conductivity can be explained by the influence of the activity coefficient due to the interaction of the ions with each other and with neutral molecules. The ion-dipole interaction we have treated in the preceding note; the formulae for the dissociation-equilibrium and for the concentration of minimum dissociation apply directly to the present case.

The evaluation of the activity-coefficient due to interionic forces is at present impossible. It has been shown[8] that in media of small dielectric constant the Debye-formula for the activity-coefficient *does not give the right order of magnitude even at the lowest concentrations which are accessible to observation.* From the curves given below we learn that it is possible to reproduce quantitatively several features of the conductivity phenomena by tentatively neglecting the interionic effects and merely considering the ion-dipole interaction. This very crude procedure cannot of course claim any accuracy; but it is significant that the agreement is best for very low dielectric constants and near the minimum of dissociation, in which cases the ionic concentration becomes very small.

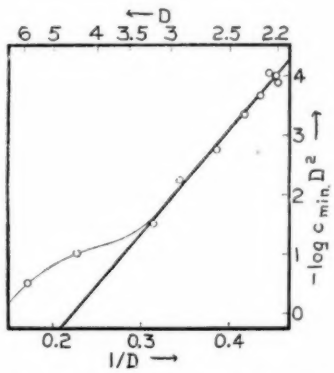

FIG. 1. Test of Eqs. (8, 9, 10) of the preceding paper. The connection between minimum-conductance concentration ($c_{min.}$) and dielectric constant of the medium. Tetraisoamylammonium nitrate dissolved in various dioxane-water mixtures.

Fig. 1 has been constructed with the aid of

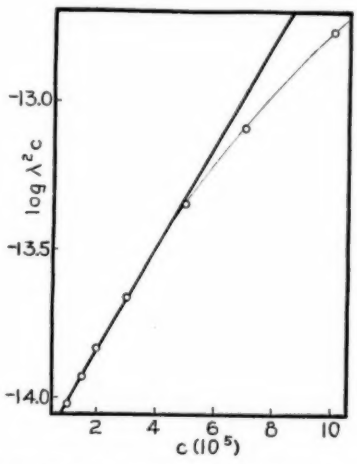

FIG. 2. $\log \Lambda^2 c$ as a function of the concentration c of tetraisoamylammonium nitrate dissolved in pure dioxane.

[10] Ph. Gross, Zeits. f. Elektrochemie **36**, 789 (1930).

formulae (8), (9) and (10) of the preceding paper. The degree of dissociation is replaced by the equivalent conductivity λ to which it is here assumed to be (nearly) proportional. For values of the constants we have taken $a=4.2\times10^{-8}$ cm and $\mu=5.8\times10^{-18}$ cm e. s. u. In Fig. 2 the observed values of $\log \lambda^2 c$ are compared with the theoretical values given by (8) and (9) of the preceding paper.

This agreement is much less satisfactory than it appears, and is partly misleading, since we are not able to reproduce theoretically by means of (8) of the preceding paper the whole conductivity-concentration curve for all media. Our formula gives satisfactory results principally for the region close to the minimum-conductivity and for the case of very small dielectric constants. Otherwise the activity coefficient due to interionic forces becomes important. We have furthermore already pointed out in the preceding paper that the meaning of the dielectric constant at the surface of the ion becomes somewhat ambiguous.

The formulae of Kraus and Fuoss can only be considered to be empirical laws. Their claim to have provided a theoretical basis for Walden's

$$D^3/c_{\text{min.}}=\text{const.}$$

does not seem tenable, since this law relates to ionic concentrations which are so high that the interionic forces become dominant.

Acoustical Studies. III. The Rates of Excitation of Vibrational Energy in Carbon Dioxide, Carbon Disulfide and Sulfur Dioxide[1]

WILLIAM T. RICHARDS AND JAMES A. REID, *Princeton University*

(Received January 6, 1934)

Measurements on these three gases at various pressures, temperatures and frequencies are reported. In all cases double collisions provide the predominant mechanism of excitation. The van der Waals or capillary forces follow the acoustical cycle without lag under the conditions of the experiments. The velocity of sound at 9 kc in carbon dioxide shows that a part of the heat capacity has already disappeared from the adiabatic elasticity at this frequency, and comparison with the measurements of other investigators leads to the belief that this term is missing even at considerably lower frequencies at ordinary temperatures. The remaining vibrational energy terms disappear together from the acoustical cycle, their rates of excitation being sensibly equal. There is a considerable activation energy necessary to excite the deformation vibration. The velocity of sound at 9 kc in carbon disulfide agrees well with that obtained by calculation from the results of band spectral analysis and hence no important energy terms appear to be lacking at this frequency. The symmetrical linear (S←C→S) and the deformation (S↓C↑S↓) vibrations leave the acoustical cycle together at high frequencies or at low pressures. A study of the dispersive region caused by this disappearance shows that the rates of excitation of the various energy states are identical within limit of error, and consequently that the activation energy of collision is uniform throughout the dispersive region. The velocity of sound at 9 kc in sulfur dioxide conforms reasonably well to the somewhat conflicting band-spectral data for the equilibrium heat capacity. There is a serious discrepancy between the results of the velocity measurements in the dispersive region here reported and the current interpretation of the few existing absorption measurements. A tentative argument is given whereby this discrepancy may be removed. Several theoretical questions which require further elucidation are discussed.

I. METHOD OF EXPERIMENT AND OF PRESENTATION

A. Apparatus

The measuring instruments were modifications of the sonic interferometer devised by Pierce.[2] Since they have already been described in a communication from this laboratory,[3] only the briefest sketch is here necessary. Magnetostriction oscillators, cut from nichrome steel, were mounted in cylindrical tubes of Pyrex glass and driven by valve-tube circuits. Points of maximum reaction in the vibrating column of gas were explored with plane-ground Pyrex reflectors, and detected by means of a microammeter in the plate circuit of the driving oscillator. The displacements of the reflecting pistons were measured to 0.05 mm from 9 to 92 kc and to 0.005 mm from 94 to 451 kc. The frequency was measured to 0.05 percent at all temperatures; it is not necessary to quote here its exact value in each case. Determinations at 9 and 92 kc were made exclusively in Pyrex tubes of 2.5 cm internal diameter and of 1 mm wall-thickness. Determinations at 94 and 451 kc were made exclusively in Pyrex tubes of 1.0 cm internal diameter and 1 mm wall-thickness. The pressure and temperature control were suitable to reproduce the velocity of sound in a non-absorbing gas to ± 0.05 m sec.$^{-1}$.

The use of tubes of small diameter greatly simplifies the process of measurement, but necessitates a tube-correction to compensate for the retarding influence of the walls on the compressional wave. The tube corrections for this apparatus have already been defined by measurements in pentane and air at 9 and 92 kc and in pentane, propane and air at 94 and 451 kc. A number of measurements were made on other gases, but since they do not alter the previous values they will not be printed. In the meantime

[1] An advance notice of this work appeared in Nature **130**, 739 (1932). A few of the earlier conclusions have here been modified owing to the introduction of a more quantitative method for the analysis of experiment.

[2] Pierce, Proc. Am. Acad. Sci. **61**, 1 (1928).

[3] Richards and Reid, J. Chem. Phys. **1**, 114 (1933).

a paper has appeared by Kaye and Sherratt[4] and an investigation has been undertaken in the laboratory of Professor Pierce by Mr. G. A. Norton[5] which very strongly support the Helmholtz-Kirchhoff reduction formula, and place measurements of the velocity of sound in small tubes in an extremely strong position.

As before the measurements at 9 and at 92 kc have been made compatible by a tube correction, and the measurements at 94 and 451 kc have been similarly adjusted to give mutual concordance. No attempt has been made to correlate the 92 and 94 kc measurements since a difference of a few tenths of a meter in the absolute velocities is considered of no importance. The tube corrections have already been applied to all the measurements quoted below.

B. "Idealization" of the measured velocity of sound

The velocity of a plane sinusoidal wave of infinitesimal amplitude propagated in an ideal, non-absorbing gas of molecular weight M and heat capacity at constant volume C is given by

$$V_{\text{ideal}} = \{(RT/M)(1+R/C)\}^{\frac{1}{2}}. \qquad (1)$$

This will be spoken of below as the *ideal velocity of sound*.

In interpreting measurements on the free-space velocity of sound in real gases it has been customary to make use of this expression, and consequently to neglect two sets of corrections. The first set deals with the acoustical conditions, and includes corrections for the finite amplitude of the wave, viscosity and heat conduction of the gas, and the like. No attempt to apply corrections of this character will be made, since it is believed that they are of secondary importance for the interpretation of the type of dispersive effect which is here discussed. The second set of corrections result from non-ideal behavior of the gas. Since it is expedient, in order to economize space, to plot measurements at various pressures and frequencies, or at various temperatures and frequencies, on a single Cartesian surface, corrections of the second type become imperative. They will be introduced by means of a factor w which is to be applied in the sense $w = V^2_{\text{ideal}}/V^2_{\text{real}}$. It has been obtained by the following argument.

If the van der Waals equation

$$(P+a/v^2)(v-b) = RT \qquad (2)$$

is used for the description of a real gas of density ρ the velocity of sound is found to be

$$V = \left\{\frac{RT+P(b-2a/RT)}{M-\rho b} + \frac{R}{C}\cdot\frac{RT}{M-2\rho b}\right\}^{\frac{1}{2}} \qquad (3)$$

if appropriate derivatives for substitution into the equation $V=(\partial P/\partial\rho)^{\frac{1}{2}}_{\text{adiab}}$ are evaluated, neglecting terms in ρ^2. Eq. (3) is suitable for the description of the velocity of sound at low frequency in a real gas, and may easily be adapted for use with a dispersive gas in which a part of the heat capacity C_0-C_∞ fails to follow the adiabatic acoustical cycle at high frequencies, if the assumption is made that the van der Waals forces remain in equilibrium. Since according to (2) $(\partial C_v/\partial v)_T=0$, the heat capacity and the density remain independent variables, and the usual derivation according to the method of Einstein is not seriously disturbed. This yields

$$V_\omega\mu^{\frac{1}{2}} = \left\{\frac{RT+P(b-2a/RT)}{M-\rho b} + \frac{R(C_0+\omega^2\vartheta^2C_\infty)}{(C_0^2+\omega^2\vartheta^2C_\infty^2)}\cdot\frac{RT}{(M-2\rho b)}\right\}^{\frac{1}{2}} \qquad (4)$$

and is suitable for the description of a real dispersive gas which has a heat capacity of C_0 at equilibrium, of C_∞ at frequencies so high that $\omega^2\vartheta^2 \geqq \infty$, and in which the energy states contributing C_0-C_∞ to the heat capacity have identical approximate relaxation times ϑ. The factor μ is determined by the absorption.[6]

It is, therefore, the ratio of the squared velocity according to (1) and that calculated from (3) which determines the van der Waals correction factor w for the low frequency velocity of sound. Corresponding values of w in

[4] Kaye and Sherratt, Proc. Roy. Soc. **A141**, 123 (1933).
[5] G. A. Norton, private communication.
[6] The significance of μ and of ϑ have been discussed by Richards in J. Phys. Chem. **1** (1933) on pages 865 (Eq. 1.8) and 876 (Eqs. 5.5 and 5.6), respectively.

the dispersive region may readily be obtained from the customary ideal dispersion equation developed from (1) and from its corrected equivalent (4). Measured velocities of sound which have been multiplied by a calculated quantity w^1 will be spoken of as *idealized measured values*.

A considerable advantage is gained by idealizing measured velocities if the energy levels of the molecule are known from band-spectral analysis. In this case (1) contains no unknown quantities, and the ideal value of the velocity of sound at very low frequency is defined with great accuracy. Any lack of correspondence with experiment at low frequencies becomes, therefore, of immediate interest.

In an ideal gas, the energy adjustments of which are effected by double collisions only, an increase of the acoustical frequency has the same effect on the velocity as a numerically equal decrease of pressure. This is, of course, the result of the fact that the number of double collisions per molecule is directly proportional to the pressure. Hence a given value of ν/P, where ν is the acoustical frequency, defines the velocity at any given temperature. A plot of V^2 against $\log_{10} \nu/P$ is a symmetrical S-curve if the gas has the dispersive properties described by (4). This is easily constructed and any experimental deviations from the regular function will be readily apparent.

C. The effect of traces of gaseous impurities

If there is a steric or energetic hinderance in the adjustment of vibrational energy by collisions between like molecules, very small traces of impurities may greatly affect the transition probability which is inferred from experiment. Since irregularities are reported below which appear to have this cause, it is perhaps worth while to cite a simplified specific example.

Let us consider a pure gas A at such a temperature and pressure that each molecule suffers on an average 10^{10} double collisions per second. Let us further suppose that on an average only one collision in 10^6 is effective in bringing about a given energy transition. This means that, for the transition in question, f_{AA} is 10^4 sec.$^{-1}$. Let us now introduce 0.1 percent of a gas B which has approximately the same molecular weight and heat capacity as A and hence does not appreciably alter the measured value of the velocities at very low and at very high frequencies. The probability that the energy transition may be effected is now $f_{AA}+f_{AB}$. The number of collisions with B molecules suffered by an A molecule is about 10^7 per second. If each one of these is effective f_{AB} is 10^7 sec.$^{-1}$ and is so far greater than f_{AA} which remains 10^4 sec.$^{-1}$ that the dispersive region in the gas will shift to frequencies which are higher by almost three orders of magnitude. If, on the other hand, the efficiency of an AB collision is equal to or less than the efficiency of an AA collision f_{AB} becomes numerically far inferior to f_{AA} and the presence of the trace of gas B will cause no noticeable effect.

Traces of accidentally included impurities are, therefore, not likely to cause an apparent diminution of f_{AA} but may cause an enormous apparent increase. The lowest value observed for f_{AA} is, therefore, most likely to be correct if the gas is known to be reasonably pure.

Since an ordinary glass surface retains water in the adsorbed condition which will evaporate slowly into any pure gas in contact with the surface, irregularities are to be expected if water is an effective agent in bringing about energy transitions in the pure gas. Evidence is already at hand which indicates that collisions between water molecules and carbon dioxide molecules or oxygen molecules give rise to this effect.[7] In such cases wholly trustworthy values of the AA probabilities may evidently be obtained only by the use of high vacuum technique.

II. Measurements on Carbon Dioxide

The carbon dioxide was prepared from calcium carbonate and a guaranteed brand of hydrochloric acid. It was passed through a drying train of calcium oxide and phosphorous pentoxide, and was, therefore, reasonably pure when admitted to the evacuated apparatus. An oil pump of conventional design was used for evacuation, and the apparatus was washed several times with pure gas before a series of measurements was

[7] Carbon dioxide, Rogers, Phys. Rev. **41**, 369 (1932); Eucken and Becker, Zeits. f. physik. Chemie **B20**, 467 (1933); oxygen, Kneser, J. Acous. Soc. Am. **5**, 122 (1933).

made. It is significant that, even with these precautions, it was difficult to obtain reproducible results. Evidently traces of some substance which is extremely effective in adjusting the transverse vibration were not eliminated by this preliminary treatment.

A. The velocity of sound at 9 kc

The measured velocity of sound at 9 kc, 30°C, and 774 mm was 271.8 m sec.$^{-1}$, and at 403 mm was 272.2 m sec.$^{-1}$ at the same temperature. When idealized these yield an average of 272.5 m sec.$^{-1}$ at 9 kc, and show no trace of dispersion in this frequency and pressure region. The ideal velocity of sound at very low frequency from (1) may in this case be calculated with some precision, since the energy levels of the CO_2 molecule have been extensively studied. Strictly speaking the unperturbed Planck-Einstein φ-function for the vibrational energy

$$C_0/R = 5/2 + 2\varphi(\Theta_1/T) + \varphi(\Theta_2/T) + \varphi(\Theta_3/T) \quad (5)$$

must be modified, since the second energy state corresponding to the characteristic temperature $\Theta_1(O\downarrow C\uparrow O\downarrow)$ is so close to the first energy state of $\Theta_2(O\leftarrow C\rightarrow O)$ that a perturbation occurs in one of the three degenerate levels of the second state of the Θ_1 vibration. The heat capacity is somewhat larger than that given by (5) in consequence. The error is, however, small, and there is reason to believe it inappreciable at 30°C from the recent analysis of Adel and Dennison,[8] and the approximate agreement at low temperatures of the measured heat capacity of carbon dioxide with that calculated from the Planck-Einstein function found by Eucken and Mücke.[9] The value of C_0/R will, therefore, be considered to be 3.5116 at 30°C, which is the figure resulting from (5) if $\Theta_1 = 956°$, $\Theta_2 = 1841°$, and $\Theta_3 = 3331°$. This corresponds to an ideal low frequency velocity of 271.2 m sec.$^{-1}$, and is significantly lower than the corresponding idealized experimental values at 9 kc. The discrepancy strongly suggests that a part of the heat capacity has already disappeared from the adiabatic cycle at acoustical frequencies considerably less and at frequencies of molecular impact considerably greater than those of the 9 kc measurements here reported.

A certain amount of corroborative evidence for this conclusion is already at hand. *The International Critical Tables* give two empirical formulae for the velocity of sound in carbon dioxide over a range of temperatures, which were set up from the measurements of Buckendahl[10] and of Dixon, Campbell and Parker[11] at atmospheric pressure. Both these agree that at 30°C and 760 mm the velocity of sound is 271.8 m sec.$^{-1}$, which corresponds to an idealized velocity of 272.5 m sec.$^{-1}$ under these conditions, and agrees satisfactorily with the 9 kc measurements reported above. The frequencies at which these measurements were made were evidently well within the audible range, and the conclusion follows that the missing energy terms have already disappeared at frequencies even below 9 kc at atmospheric pressure. Furthermore, Eucken and Mücke,[9] on the basis of heat capacity measurements at equilibrium, were led to the conclusion that the term corresponding to the symmetrical linear $(O\leftarrow C\rightarrow O)$ vibration was absent from the measurements on the velocity of sound at 3–4 kc made by Partington and Schilling and by Dixon. The missing term was believed to make a gradual reappearance only at high temperatures. On this assumption the ideal velocity at 9 kc should be 272.1 m sec.$^{-1}$ at 30°C, which agrees fairly well with the idealized measured value of 272.5 m sec.$^{-1}$. In view of considerations later to be discussed the conclusion of Eucken and Mücke will not be unconditionally supported, it being merely agreed that a term corresponding to about 1300 wave numbers is lacking at 9 kc and ordinary temperatures.

B. A revision of the customary notation

In view of the fact that several dispersive regions, which occur in quite separate ranges of frequency, must be distinguished, a point of notation arises. In writing V_0 for the velocity of sound corresponding to the equilibrium heat

[8] Adel and Dennison, Phys. Rev. **43**, 716 (1933).

[9] Eucken and Mücke, Zeits. f. physik. Chemie **B18**, 186 (1932).

[10] Buckendahl, Diss. Heidelberg (1906). This paper was unfortunately not available, and the frequency at which the measurements were made is, therefore, unknown to us.

[11] Dixon, Campbell and Parker, Proc. Roy. Soc. **A100**, 1 (1921).

capacity C_0, and V_∞ corresponding to a high frequency heat capacity C_∞ it has already been stressed that the subscripts do not indicate zero and infinite acoustical frequencies, but are intended only to specify whether $\omega^2\vartheta^2 \leqq 0$ or whether $\omega^2\vartheta^2 \leqq \infty$ from the point of view of experiment. Since the values of the relaxation times of the excited states of the various modes of vibration may apparently be separated by many orders of magnitude, additional subscripts unfortunately become necessary in order to avoid ambiguity. For example the transverse (O↑C↓O↑) vibration may maintain substantially its equilibrium distribution in the acoustical cycle at frequencies so high that the symmetrical linear (O←C→O) vibration is wholly absent from the effective heat capacity. In order to avoid multiple subscripts the following convention has been adopted, the terms "in" and "out" signifying equilibrium distribution and complete disappearance from the acoustical cycle respectively.

	Mode of vibration		
Symbol	O↑C↓O↑	O←C→O	O→←C→O
V_∞	out	out	out
V_6	"	"	in
V_5	in	"	out
V_4	out	in	"
V_3	"	"	in
V_2	in	"	out
V_1	"	out	in
V_0	"	in	"

These velocities designate a number of the possible terminal velocities of a colinear triatomic molecule, and may also be employed, by the usual conventions, to specify the corresponding quantities for any triatomic molecule. In this language the 9 kc velocity reported above corresponds approximately to both V_1 and to V_5 since the unsymmetrical linear (O→←C→O) vibration is not appreciably excited at room temperatures.

C. The variation of the velocity of sound with pressure and temperature in the dispersive region

A detailed study was made of the variation of the velocity of sound with frequency and with pressure in the upper limit of the main vibrational dispersive region. This was undertaken because there is reason to believe that the 0→1 transition is somewhat less probable than the 1→2 transition,[12] and the transverse vibration, which predominates in this dispersive region, has an appreciable fraction of its molecules in the second excited state at 30°C. The results of this study are presented in Table I, together with the appropriate van der Waals factors obtained from the constants $a = 3.61 \times 10^6$ cm^6 atm. mole^{-1} and $b = 42.6$ cc mole^{-1}. The idealized measurements have been graphed in Fig. 1 by plotting V^2 in cm^2 sec.$^{-2} \times 10^{-8}$ as ordinates against $\log_{10} \nu/P$, where ν is the acoustical frequency in cycles per

TABLE I. *Measurements of the velocity of sound in carbon dioxide at 30°C and various pressures and frequencies.*

				At 450.7 kc				
P in mm Hg	70.5	116	237	408	431	602	604	774
V in m sec.$^{-1}$	283.7	283.6	283.6	283.4	283.5	283.2	283.4	283.0
w	1.0005	1.0007	1.0015	1.0026	1.0028	1.0039	1.0039	1.0050
P	776	777	778	800	880	935	1012	1180
V	283.1	282.9	283.1	282.8	282.8	282.9	282.7	282.4
w	1.0050	1.0050	1.0050	1.0052	1.0057	1.0060	1.0065	1.0076
P	1336	1640						
V	282.2	281.5						
w	1.0087	1.0108						
				At 94.0 kc				
P	70.5	116	237	408	602	604	774	776	778
V	283.6	283.4	282.9	282.2	281.3	281.5	280.4	280.2	280.0
w	1.0005	1.0007	1.0016	1.0027	1.0040	1.0040	1.0052	1.0052	1.0052
P	800	880	935	1012	1180	1336	1474	1640	
V	280.3	280.0	279.7	279.3	278.4	277.0	276.7	275.6	
w	1.0054	1.0060	1.0063	1.0068	1.0080	1.0091	1.0102	1.0114	

[12] See for example, Richards, J. Chem. Phys. **1**, 872 (1933).

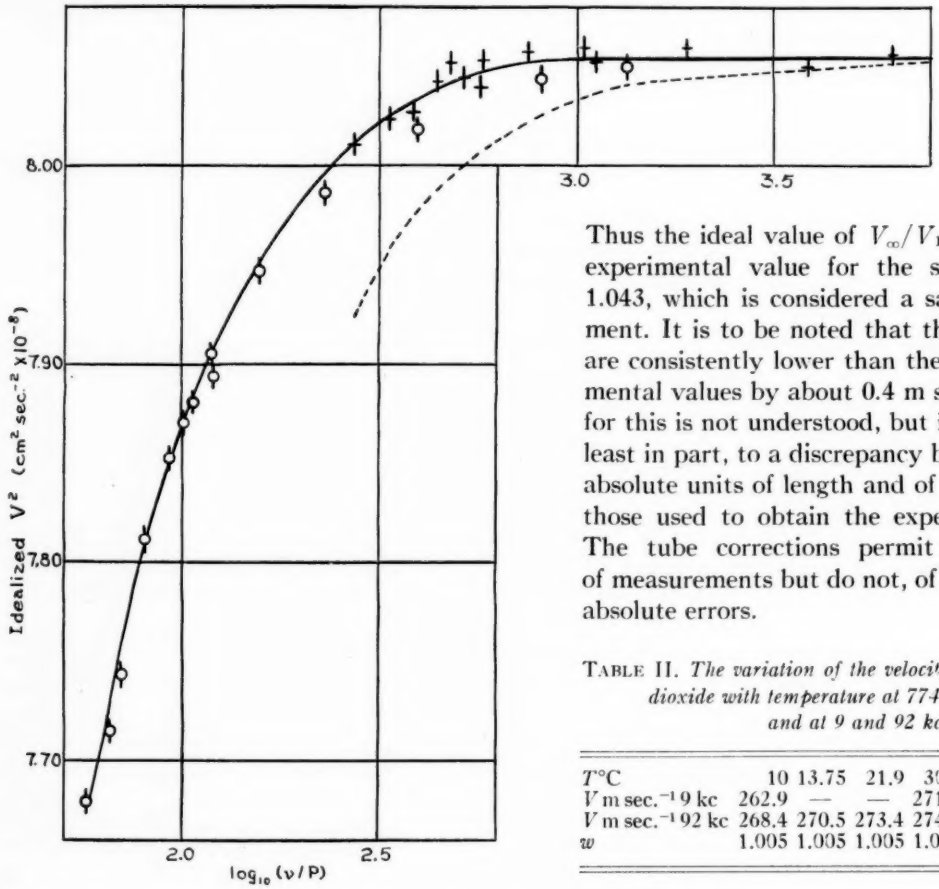

FIG. 1. The variation of the velocity of sound in carbon dioxide with frequency and pressure at 30°C. Experimental points are indicated by plus signs at 451 kc, and by circles with lines through them at 94 kc, the extension of the vertical line being equivalent to ±0.1 m sec.$^{-1}$. The continuous line is drawn from theory, and the dotted line indicates the course of the experimental points at 451 kc if they are uncorrected for van der Waals forces.

second and P the pressure in mm of mercury, as abscissae. The solid line in Fig. 1 is the theoretical V^2, log ν/P curve for an ideal gas in which $V_\infty/V_1=1.042$, $f_{10}=f_{21}$ etc. $=2.23\times10^5$ per molecule per second at 760 mm, and in which the excitation is brought about wholly by double collisions. The dotted line shows the course of the 45 kc measurements if they are uncorrected for departures of carbon dioxide from ideal behavior.

The idealized measured velocities average to give 283.7 m sec.$^{-1}$ as the terminal velocity. The ideal terminal velocity using an apparent heat capacity ratio of 1.400 is 283.2 m sec.$^{-1}$. Thus the ideal value of V_∞/V_1 is 1.041 and the experimental value for the same quantity is 1.043, which is considered a satisfactory agreement. It is to be noted that the ideal velocities are consistently lower than the idealized experimental values by about 0.4 m sec.$^{-1}$. The reason for this is not understood, but it may be due, at least in part, to a discrepancy between the exact absolute units of length and of temperature and those used to obtain the experimental figures. The tube corrections permit intercomparison of measurements but do not, of course, eliminate absolute errors.

TABLE II. *The variation of the velocity of sound in carbon dioxide with temperature at 774 mm pressure, and at 9 and 92 kc.*

T°C	10	13.75	21.9	30.0	50.0	70.0	90.0
V m sec.$^{-1}$ 9 kc	262.9	—	—	271.8	279.2	286.9	295.0
V m sec.$^{-1}$ 92 kc	268.4	270.5	273.4	274.6	279.9	—	—
w	1.005	1.005	1.005	1.005	1.004	1.004	1.004

Measurements were made on the velocity of sound at 770–776 mm between 10°C and 90°C at 9 kc and between 10°C and 50°C at 92 kc. These are summarized in Table II, the van der Waals factors having been obtained from constants already given. The idealized measured velocities are plotted against temperature in Fig. 2. It is to be noted that the velocity at 30°C and 92 kc is 274.6 m sec.$^{-1}$ in Table II and at 94 kc and the same pressure is 280.2 according to Table I. Only a small part of this discrepancy is accounted for by the difference in frequency. This is unfortunate, for it indicates that the purity of the carbon dioxide used for the study of the temperature coefficient was not as great as that used for the study of the pressure coefficient. This is confirmed by the unsystematic character of the points in the dispersive region of the former study, as illustrated in Fig. 2. Calculation shows that the probability of the 1→0 transition has been increased by a factor of about 3.

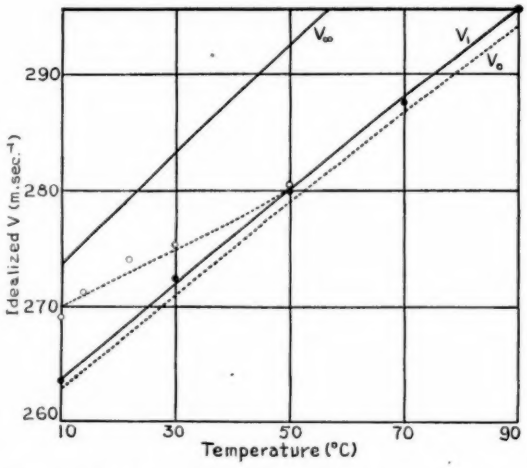

FIG. 2. The variation of the velocity of sound in carbon dioxide with temperature and frequency at 773 mm pressure. The various continuous and dotted lines conform to the convention explained in Section IIB with the exception of the dotted line connecting the 92 kc points, which have been indicated by circles. 9 kc points are indicated by black dots.

Whatever the impurity present, however, its effect on the 9 kc velocity was too slight to be experimentally manifest, for the 9 kc measurements could be reproduced quantitatively without difficulty.

D. Conclusions from the study of the velocity of sound in carbon dioxide

(1) The van der Waals forces follow the acoustical cycle quantitatively throughout the regions of pressure, temperature and frequency which were studied. This is based on the course of the dotted line in Fig. 1 and similar uncorrected constructions which have not been given to avoid confusing the diagrams.

(2) The mechanism by which excitation and de-excitation of the vibrational energy is effected is wholly that of double-collisions within the limit of error of experiment. This conclusion is based on the agreement of the 94 and 451 kc measurements at low pressures, and on the conformity of both to the fragment of a symmetrical S-curve drawn in Fig. 1. As a corollary it may be stated that the radiation life-time of the first excited state of the transverse vibration is greater than 10^{-4} seconds.[13]

[13] An argument communicated to us privately by Professor E. U. Condon indicates that this lifetime is between 1 and 100 seconds.

(3) The velocity of sound at 9 kc and 774 mm pressure between 10°C and 90°C conforms closely to that calculated on the assumption that the symmetrical linear (O←C→O) vibration is absent from the heat capacity under these conditions. The reason for this conclusion has been discussed at some length above in connection with the 30°C velocity at 9 kc, at other temperatures it follows from a consideration of Fig. 2.

(4) The velocity of sound at the highest frequencies and lowest pressures employed in this study corresponds to a heat capacity in which the rotational terms are fully active and are classically excited. It is maintained constant for at least one order of magnitude of frequency or of pressure change. This statement is justified by measurements at large values of $\log \nu/P$ in Fig. 1. The magnitude of this terminal velocity corresponds to that measured by Kneser,[14] Pielemeier,[15] and Eucken and Becker,[16] although none of these authors have demonstrated its constancy over so wide a range of conditions.

(5) The probability of the 1→0 transition of the transverse vibration is 2.23×10^5 per molecule per second at 760 mm and 30°C. This is reasonably in accord with the somewhat less carefully defined values given by Pierce,[17] Kneser[14] and Pielemeier.[15] The chemical purity of the gas is so acutely important in determining the absolute value of this constant that exact agreement between different investigators is not to be expected at present.

(6) The probability of the 2→1 transition is equal to this within a factor of about 5. This follows[6] from the correspondence of the experimental points and the continuous line in Fig. 1. A slight tendency for the points to fall under the continuous line may perhaps be imagined at large values of $\log \nu/P$, but it is certainly insufficient to justify quantitative conclusions.

(7) The temperature coefficient of the dispersion is adequately accounted for if it be assumed that the 1→0 transition of the transverse mode is effected only by molecules able to

[14] Kneser, Ann. d. Physik **11**, 777 (1932); **12**, 1015 (1932).
[15] Pielemeier, Phys. Rev. **41**, 833 (1932).
[16] Eucken and Becker, Zeits. f. physik. Chemie **B20**, 467 (1933).
[17] Pierce, Proc. Am. Acad. Sci. **60**, 271 (1925).

supply an activation energy of 6000 cal. mole^{-1}. On this assumption the relative translational energy for the 0→1 transition must evidently exceed 8000 cal. mole^{-1}. The probable error, of this determination is great, and an accuracy better than ±2000 cal. mole^{-1} may not be claimed. The slope of the V_{92} curve against temperature is difficult to determine from the experimental points, and the presence of a trace of impurity may evidently also somewhat have obscured the result.

(8) The activation energy of the 2→1 transition can evidently not be far inferior to this figure, since no flattening of the S-curve in Fig. 1 is observed at large values of log ν/P.

(9) The effective collision diameter is found to have about one-fifth of its value for ordinary kinetic processes from the data given above. This conclusion is highly qualitative since the experimental determination of the activation energy is not exact.

III. Measurements on Carbon Disulfide

The carbon disulfide was obtained from the best certified commercial source. It was fractionated through phosphorous pentoxide, only the middle third being retained for study. The apparatus was pumped out and washed several times with pure vapor before each determination. It is apparent from the scattering of points in the dispersive region that this method of preparation was not wholly adequate. Additional difficulty in obtaining accurate measurements in the dispersive region was occasioned by the enormous acoustical absorption of carbon disulfide vapor. Absorption reduced the intensity of the electrical reaction to about 1 percent of its value after 5 wave-lengths in the center of the dispersive region. This is a somewhat greater effect than is to be expected from the magnitude of the acoustical absorption coefficient, although so large a part of the heat capacity disappears from the acoustical cycle with a hundred-fold change in frequency that outstanding absorptive properties must result.

Table III summarizes the measurements made at 30°C and various frequencies and pressures; they are presented graphically in Fig. 3, after being corrected for deviations from perfect behavior. The correction constants employed were $a=11.61\times10^6$ cc^2 atm. and $b=76.8$ cc per mole. The high frequency terminal velocity is in some doubt, since no oscillator above 451 kc was available, and it was found impossible to make reproducible measurements at pressures below 80 mm. That indicated in the figure, which corresponds to an apparent heat capacity including rotational terms and terms due to the unsymmetrical linear (S→←C→S) vibration in their equilibrium distributions, appears to accord well

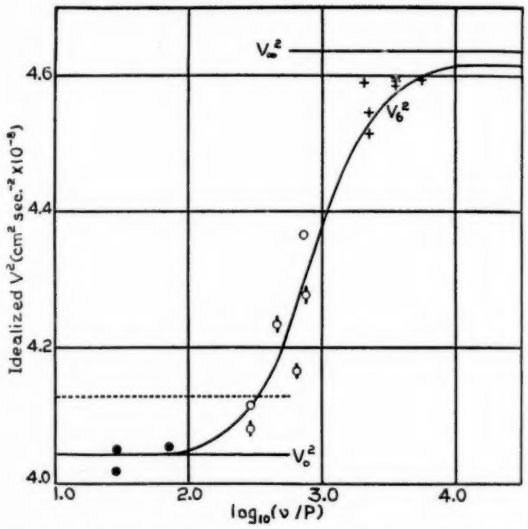

FIG. 3. The variation of the velocity of sound in carbon disulfide with frequency and pressure at 30°C. 451 kc measurements are indicated by plus signs, 94 kc by circles with lines through them, 92 kc by circles and 9 kc by black dots. The continuous line has been drawn from theoretical considerations. The measurements are not sufficiently accurate, however, to define unequivocally the high frequency terminal velocity, and the upper part of the *S*-curve must therefore be considered tentative.

TABLE III. *The velocity of sound in carbon disulfide at 30°C and various frequencies and pressures.*

				451 kc			
P mm	215	200	200	128	128	128	80
V m sec.$^{-1}$	213.6	212.0	212.7	213.9	214.0	213.9	214.1
w	1.006	1.005	1.005	1.004	1.004	1.004	1.002
				94 kc			
P mm	321	200	128	128			
V m sec.$^{-1}$	201.0	205.1	203.6	206.4			
w	1.010	1.006	1.004	1.004			
	92 kc			*9 kc*			
P	309	128		314	309	128	
V	201.8	208.5		200.3	199.5	201.0	
w	1.010	1.004		1.010	1.010	1.004	

TABLE IV. *The velocity of sound in carbon disulfide at various temperatures.*

At 200 mm and 451 kc							
T°C	20.0	20.0	30.0	30.0	40.0	40.0	
V m sec.$^{-1}$	210.0	209.8	212.0	212.7	214.7	214.7	
w	1.006	1.006	1.005	1.005	1.005	1.005	
At 309–314 mm and 92 kc							
T°C	25.0	26.0	27.5	30.0	34.0	37.6	50.0
V m sec.$^{-1}$	200.6	200.7	201.8	201.8	202.9	203.9	206.4
w	1.012	1.012	1.011	1.010	1.010	1.009	1.008
At 309–314 mm and 9 kc							
T°C	25.0	30.0	30.0	50.0	60.0	70.0	80.0
V m sec.$^{-1}$	198.7	200.3	199.5	206.5	209.6	212.5	215.6
w	1.012	1.010	1.010	1.009	1.008	1.008	1.007

with the measurements. The velocities at 9 kc correspond well with those calculated from band-spectral analysis for equilibrium conditions.[18]

Table IV summarizes in a similar manner measurements made on the temperature coefficient of the velocity under various conditions. Fig. 4 represents graphically the result of the measurements at 9 and 92 kc and 309–314 mm only.

These data are the justification of the following conclusions.

(1) The van der Waals forces follow the acoustical cycle without lag throughout the region experimentally investigated. This follows from the mutual discordance of measurements before the w correction has been applied.

(2) The transverse (S↑C↓S↑) and symmetrical linear (S←C→S) vibration leave the acoustical cycle at the same frequencies of sound, and their characteristic adjustment rates are identical within limit of error. This follows from the conformity of the experimental points to the symmetrical S-shaped V^2 against log ν/P curve which is illustrated by Fig. 3.

(3) The mechanism by which the excitation of these states is effected is one of double collisions only over the range and within the error of

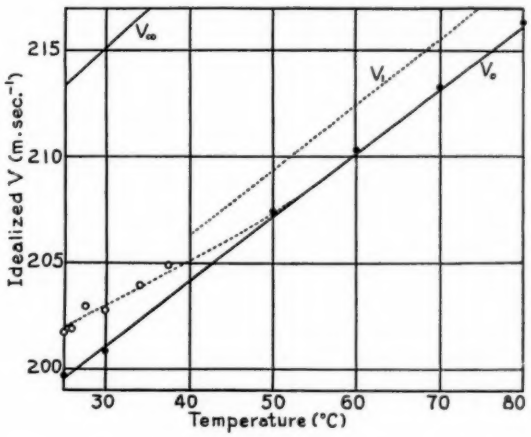

FIG. 4. The variation of the velocity of sound in carbon disulfide with temperature and frequency at 310 mm pressure. The conventions are the same as in Figs. 2 and 3.

experiment. Here, again, conformity to the S-curve in Fig. 3 is sufficient proof.

(4) The activation energy of collision for that process of excitation which dominates in the low frequency part of the dispersive region is about 5400 cal. mole^{-1}. The effective cross section appears to be of normal magnitude for this excitation process, although the error of the experiments is great enough to make this statement somewhat questionable. The activation energy and cross section have been obtained, as usual, from the slope of the line connecting 92 kc points in Fig. 4.

(5) The activation energy of collision and effective cross section for the excitation process which determines the upper part of the dispersive region are identical with those dominating the lower part within limit of experimental error.

There are two methods for justifying this statement. The measurements at 200 mm and 451 kc quoted in Table IV are in accord with the 92 kc measurements graphed in Fig. 4, but uncertainty concerning the high frequency terminal velocity somewhat obscures their significance. Also, the conformity of the 451 kc measurements plotted in Fig. 3 with the symmetrical S-curve may be used as a powerful supporting argument. A difference of 2000 cal. mole^{-1} in the activation energy of collision between the processes determining the lower and higher parts of the dispersive region would result, with normal cross sections, in a difference of nearly thirty-fold

[18] The fundamental molecular frequencies were obtained from Villars, Chem. Rev. **9**, 369 (1932). The empirical formula given in the *Int. Crit. Tables* for the velocity of sound does not agree either with our measurements or with the band-spectral results. Since the values are consistently too high, it may be assumed that a trace of some unknown impurity has been unintentionally included in the construction of the formula. Air, for example, owing to its smaller density and heat capacity could produce such an error if present even in very small quantities.

in rate. This difference would be manifest by a marked tendency of the S-curve to flatten in the high frequency region, and the measurements although inexact, are ample to demonstrate that no such effect is present.

(6) The probabilities of the $1\rightarrow 0$, $2\rightarrow 1$, etc., transitions of the deformation vibration are evidently about 7.8×10^5 per molecule per second at 30°C and 310 mm pressure. This is significantly greater than the corresponding probabilities for carbon dioxide which are 9.1×10^4 per molecule per second under these conditions.

IV. Measurements on Sulfur Dioxide

Relatively little attention has here been devoted to sulfur dioxide because the band spectral analysis appears to be controversial. The measurements reported below were, indeed, obtained merely during the process of defining the tube-correction. They are printed to permit a rough comparison with the absorption coefficients measured by Grossmann.[19]

The sulfur dioxide was obtained from tanks of the usual commercial product. It was dried by phosphorus pentoxide, but not further purified. The absolute values of the velocities are, therefore, not unassailable, and a scattering of experimental points is to be expected.

Table V. *The velocity of sound in sulfur dioxide at 30°C and various frequencies and pressures.*

	At 451 kc			
P in mm	770	770	425	200
V in m sec.$^{-1}$	222.4	222.6	223.9	224.9
w	1.013	1.013	1.007	1.003
	At 94 kc			
P	770	770	425	200
V	221.9	221.1	222.8	223.7
w	1.013	1.013	1.007	1.003

Table V summarizes the measurements at 30°C at 94 and at 451 kc. The van der Waals factor was obtained from the constants $a=6.7\times 10^6$ cm^6 atm. mole^{-1}, $b=56$ cm^3 mole^{-1}. A measurement at 9 kc, 30°C, and 480 mm gave a velocity of sound of 222.3 m sec.$^{-1}$, and requires multiplication by a factor of $(1.008)^{\frac{1}{2}}$ in order to give the corresponding idealized velocity.

[19] Grossmann, Ann. d. Physik **5**, 681 (1932).

The ideal velocity at very high frequencies of sound will be $(1.3333\,RT/M)^{\frac{1}{2}}$ or 229.0 m sec.$^{-1}$ at 30°C if no vibrations contribute to the heat capacity, and if the rotations are classically excited and follow the wave without lag. At very low frequencies the heat capacity ratio from band spectra is 1.269 if the analysis of Bailey, Cassie and Angus,[20] which gives the fundamental frequencies of 610, 1164 and 1369 cm^{-1} is employed, and 1.263 using the more recent values of 510, 1150, and 1370 cm^{-1} due to Chow[21] and Smyth.[22] Thus the ideal velocity of sound at very low frequencies should lie between 223.5 and 222.9 m sec.$^{-1}$ at 30°C. This accords with the idealized measured 9 kc velocity.

In Fig. 5 the experimental data are summarized graphically in the usual way. Several conclusions are clearly indicated by this diagram.

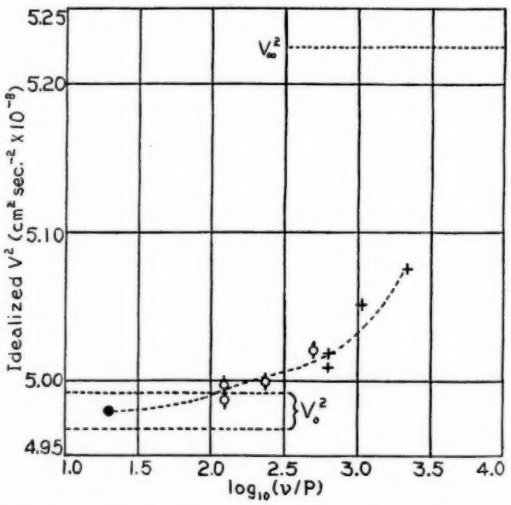

Fig. 5. The variation of the velocity of sound in sulfur dioxide with pressure and frequency at 30°C. The two dotted lines at low values of V^2 represent the low frequency velocity of sound according to two different band-spectroscopic analyses. The curved dotted line connecting experimental points is based on an unproved hypothesis which is tentatively advanced in the text.

(1) The van der Waals forces follow the adiabatic cycle quantitatively at 30°C to frequencies of 450 kc and 400 mm pressure. This follows from a plot, which has not been repro-

[20] Bailey, Cassie and Angus, Proc. Roy. Soc. London **A130**, 142 (1930).

[21] Chow, Phys. Rev. **44**, 638 (1933).

[22] Smyth, Phys. Rev. **44**, 690 (1933).

duced, of log ν/P against the non-idealized measured velocities.

(2) The dispersive region must be due, at least in part, to sluggishness in the adjustment of the energy states characterized by the fundamental frequency 510 cm^{-1}. Supposing that the two high frequency molecular vibrations disappear from the adiabatic cycle, leaving only the lowest in equilibrium, the ideal velocity of sound would be about 224.3 m $sec.^{-1}$ at very high frequencies, and this is significantly lower than the highest idealized measured value of 225.3 m $sec.^{-1}$.

(3) The position of the dispersive region in sulfur dioxide leads to the expectation that the absorption maximum will be in the neighborhood of log $\nu/P=3.5$ or about 2400 kc at atmospheric pressure.

The last of these conclusions permits a comparison with Kneser's prediction,[23] from the absorption measurements of Grossmann, that the absorption maximum must occur at about 20°C (the temperature is not exactly specified) and atmospheric pressure at about 1000 kc. A combination of these two figures yields an activation energy of 15,000 cal. $mole^{-1}$ by the approximate formula[24]

$$\omega_{max}/\omega'_{max}=e^{-(A(T'-T)/RTT')}.$$

So large an activation energy of collision cannot seriously be considered, since it implies a fantastically large effective molecular cross section in view of the rapid rate at which transitions occur. It is, therefore, necessary to supply an explanation for the discrepancy.

The argument given in the following paragraph is presented for this purpose, but it must be considered to be highly tentative in character.

If the dispersive or absorptive region is due to the concomitant dropping out from the acoustical cycle of a group of energy states which have identical rates of adjustment, the effect is normally complete in a frequency range the upper limit of which is a hundred times the lower limit. If, for example, dispersion first becomes manifest at 10 kc the high frequency terminal velocity will usually have been sensibly attained at 1000 kc at constant temperature and pressure. It will be noticed by consulting Fig. 5 that although the velocity at log $\nu/P=2.0$ is sensibly greater than that at low frequencies, the dispersive region will not be complete at log $\nu/P=4.0$. Furthermore, a function of the type of the dotted line appears better suited to describe the experimental points than the conventional S-shaped curve. This suggests that one of the series of energy states corresponding either to 1160 cm^{-1} or to 1370 cm^{-1} is somewhat less readily adjusted by collisions than those states corresponding to the 510 cm^{-1} vibration. This is supported by the slight fall of the absorption coefficient measured by Grossmann at the beginning of the vibrational absorptive region. If this hypothesis is granted, the absorption maximum predicted by Kneser must be shifted to higher frequencies at 20°C and atmospheric pressure, and the magnitude of the activation energy of collision which must be assumed is very greatly diminished. Neither the velocity nor the absorption measurements are of sufficient accuracy to define the matter more exactly, but there appears at present no convincing ground for believing them incompatible.

Since the terminal velocity at high frequencies may be measured at 451 kc and 30°C only at pressures below 70 mm no quantitative statement of the transition probabilities of the various vibrational energy states may here be made. The predominant adjustment rate at 30°C is evidently about five times that of carbon disulfide, and about 15 times that of carbon dioxide.

V. Discussion

It is apparent that at least one dispersive region in the range of acoustical frequencies now experimentally available is to be expected with polyatomic gases in which the vibrational heat capacity is appreciable. It is of little interest, therefore, merely to multiply the number of examples of dispersive gases, and attention is rather to be directed to the information which they provide concerning the mechanism of the transformation of kinetic to vibrational energy. Unfortunately, however, attempts to correlate experiment and theory must at present be highly speculative, since the descriptions of these

[23] Kneser, Ann. d. Physik **16**, 337 (1933).

[24] This is made on the basis of Eq. (15) of page 740, Richards and Reid, J. Chem. Phys. **1** (1933). The approximations are $f_{01}=f_{12}=\cdots=0$, $(T/T')^{\frac{1}{2}}=1$, and $B_0/B_\infty Q=B_0'/B_\infty'Q'$.

phenomena in terms of quantum mechanical processes are so general that they do not lend themselves to the treatment of specific physical examples. In view of the predominantly experimental character of this study no theoretical discussion will here be attempted. The following paragraphs have been included to point out that our measurements are not at present unequivocal in their significance, and to indicate directions for further investigation.

Carbon dioxide and carbon disulfide so closely resemble each other in structure that it is surprising to find an appreciable part of the heat capacity failing to participate in the velocity of sound at audible frequencies in the former, whereas in the latter all of the heat capacity remains fully active well into the ultrasonic range. It is natural, in considering carbon dioxide alone, to follow Eucken and Mücke in supposing that the symmetrical linear vibration is that with the extremely low rate of adjustment. In searching for a kinetic mechanism by which such a mode of vibration may be excited a fortunate triple-collision of the type $A \rightarrow OCO \leftarrow A$ suggests itself; any bond-softening process or other double-collision mechanism seems inefficient in comparison. This supplies an excellent qualitative explanation for the behavior of carbon dioxide, but fails completely to account for that of carbon disulfide.

An examination of the quantitative differences in the structure of the energy levels of the two molecules serves only to make their difference in behavior more puzzling. It is probable, for example, that the various energy states in the symmetrical linear vibration and the deformation vibration "communicate" during the time that two colliding carbon disulfide molecules are effectively in contact. The equality of the rates of adjustment of these states, which has experimentally been established, can reasonably be explained only on the supposition that vibrational equilibrium between them has essentially been reached on every effective collision. Under these conditions all the "communicating" vibrations will, of course, fall out of the acoustical cycle with the rate of adjustment of the most readily excited member of the group, and the steric and energetic factors which are measured characterize the most probable transition. (This is sharply in contrast to the behavior of nitrous oxide,[25] and may also differ from that of sulfur dioxide, where it appears that each of the vibrational modes is dropping out with a separate characteristic rate.) It is further apparent that the probability of "communication" between two vibrational modes increases greatly as the number of excited states in each is increased, since the matrix component connecting two widely separated energy levels is necessarily small. Since carbon disulfide contains a greater number of excited vibrational states at any given temperature than carbon dioxide, and since the duration of a collision between the heavier molecules is also probably greater, it would be natural to attribute their difference in acoustical behavior to the effect of "communication" alone. A serious difficulty to this interpretation results, however, from the perturbation of the first state of the linear vibration by one of the three levels corresponding to the second state of the transverse vibration. Perturbation indicates that one of these states may transform itself into the other during the course of a few vibrations without the intervention of a collision. It is, therefore, difficult to believe that the linear vibration alone drops out of the acoustical cycle at low frequencies while the deformation states remain in equilibrium well into the ultrasonic range.

It would be convenient, if it were possible, to discredit entirely the measurements at 9 kc on carbon dioxide, which are here reported, and obliterate the difference in behavior on *a priori* grounds. Unfortunately, however, they corroborate a considerable body of independent evidence, and only the case of carbon dioxide is difficult to interpret. It is necessary, therefore, to confess that the low frequency dispersive region in carbon dioxide is not understood by the writers, and to leave the matter in this highly unsatisfactory condition.

The situation is hardly more satisfactory when an explanation of the so-called activation energy of collision is sought. Three alternative hypotheses are at hand, and none of these may be eliminated with confidence.

(1) A bond-softening process has been suggested as the mechanism by which the excited state is reached. In this case the collision energy

[25] Kneser and Zühlke, Zeits. f. Physik **77**, 649 (1932).

must necessarily be greater than the energy available for the bond-softening process. This implies that the activation energy shall decrease roughly in proportion to the ratio between the energy of the state to be excited and the zero point energy. The experimental evidence fails to show this effect either with carbon dioxide or with carbon disulfide, since in neither gas is the symmetry of the S-shaped V^2, log ν/P curve appreciably disturbed. If, however, equilibrium between the vibrational states may be established during the time of a collision, as has been supposed above, this difference cannot be detected by experiment.

(2) Heil has suggested that, because of the comparatively small rigidity of the bonds attaching the oxygen atoms to the carbon, a broadside collision of the type $\rightarrow\cdots\vdots\leftarrow$ would result in the transference of only about a third of the relative translational energy of the molecules into the vibration if the requirements of the law of conservation of linear momentum are to be satisfied. On this basis he has successfully predicted the order of magnitude of the activation energy of collision and the effective cross section of carbon dioxide from Kneser's measurements at atmospheric temperatures. A similar argument applies equally well to carbon disulfide: the available energy is smaller, but the rigidity of the bond is also less, and an activation energy of about the same magnitude is to be expected. The situation is somewhat complicated, however, by the rotation of the molecules during a collision. The activation energy represents, of course, predominantly the minimum potential energy which must be available in order to de-excite a given state, and there appear to be several configurations of rotating molecules more favorable for the process than that which Heil has described. An explanation based on a dynamic mechanism of this kind has, however, the advantage that it implies approximately equal activation energies for the various states of a vibrational mode, and this is in accord with experiment.

(3) It is also possible that a molecule which is vibrating has an advantage over a molecule which contains only its zero point energy in bringing about transformations of the relative kinetic energy into vibrational energy by collision. If, for example, it is supposed that only the states 0 and 1 are present, and that a molecule in the state 1 is far more effective per collision in causing the transitions $1\rightarrow0$ and $0\rightarrow1$ than a molecule in the state 0, the transition probability f_{10} will not be proportional to the total number of collisions but to the number of 1–1 collisions. The relation between the number of molecules in the 0 and in the 1 states is of course $n_1 = n_0 e^{-h\nu_0/kT}$ and consequently, for gases like carbon dioxide and carbon disulfide at ordinary temperatures, n_1 will increase exponentially with temperature, and an apparent activation energy will be observed which has no relation to the activation energy ordinarily discussed in chemical kinetics. This possibility may also seem remote, but it is difficult to devise an experiment by which it may convincingly be eliminated.

Acoustical Studies. IV. The Collision Efficiencies of Various Molecules in Exciting the Lower Vibrational States of Ethylene, Together with Some Observations Concerning the Excitation of Rotational Energy in Hydrogen

WILLIAM T. RICHARDS AND JAMES A. REID, *Princeton University*

(Received February 7, 1934)

The velocity of sound in pure ethylene has been determined at various pressures, temperatures and frequencies. It is concluded that equilibrium is attained between the various states of the vibrational energy on every effective collision, but that a considerable activation energy of collision is required for the conversion of translational into vibrational energy. Collisions with argon, helium, and nitrogen molecules have no appreciable effect on the vibrational energy of the ethylene molecule. Collisions with hydrogen molecules are about ten times as effective as ethylene-ethylene collisions in producing transitions in the lower vibrational energy states of ethylene. Hydrogen shows a dispersive region at ultrasonic frequencies which is apparently due to the failure of the rotational energy transitions to follow the acoustical cycle. It has been found necessary to suppose that ethylene-hydrogen collisions are about twenty times as effective as hydrogen-hydrogen collisions in exciting the rotational energy of hydrogen molecules.

INTRODUCTION

ONE of the outstanding unsolved problems in chemical kinetics is the mechanism of activation by collision. It has become increasingly apparent that great differences exist in the relative activation efficiencies of various types of molecules, but the theoretical approach to the problem is difficult, and it is apparently impossible at present to make quantitative predictions. The multiplication of suitably chosen experiments becomes therefore highly desirable.

Measurements on the dispersion and absorption of sound provide ready access to data concerning a somewhat analogous process: the excitation by collision of the lower vibrational energy states. This differs from the chemical activation of the molecule in several respects, but is even harder to describe from a theoretical standpoint because the interaction of the molecules must here be attacked by quantum mechanics, whereas there is every indication that in chemical activation the problem will ultimately yield to a classical dynamical treatment. Any final description of the mechanism by which translational energy is converted into vibrational energy must, however, be sufficiently general to embrace transitions between both the lower and higher vibrational states. A study of the collision efficiencies of various molecules in adjusting the heat capacity cannot fail, therefore, to have ultimate bearing upon the chemical problem.

The first research of this character was undertaken by Abello,[1] who measured the absorption of ultrasonic energy in mixtures of carbon dioxide, hydrogen and nitrogen. The theoretical equipment necessary to interpret his results was provided shortly thereafter by Bourgin.[2] In 1932 Rogers[3] reported briefly concerning the effect of water vapor on the absorption of sound in carbon dioxide, and an advance notice of the present work was published.[4] During the past year Kneser has interpreted existing measurements on air and on oxygen-water-vapor mixtures,[5] and Eucken and Becker[6] have published conclusions from a few measurements on the velocity of sound in binary mixtures containing as one constituent either carbon dioxide or chlorine. This appears to complete the meager list of measurements which have been published to date.

[1] Abello, Proc. Nat. Acad. Sci. **13**, 699 (1927).
[2] Bourgin, Nature **122**, 133 (1928); Phil. Mag. **7**, 821 (1929); Phys. Rev. **34**, 521 (1929).
[3] Rogers, Phys. Rev. **41**, 369 (1932).
[4] Richards and Reid, Nature **130**, 739 (1932).
[5] Kneser, Ann. d. Physik **16**, 337 (1933); J. Acous. Soc. Am. **5**, 122 (1933).
[6] Eucken and Becker, Zeits. f. physik. Chemie **B20**, 467 (1933).

I. Pure Ethylene

A. The purity of the ethylene gas employed

The ethylene gas was obtained in compressed cylinders, which are supplied by the U. S. Industrial Chemical Company, and rated as about 99 percent pure. Four of these cylinders were employed, and of these three gave fairly reproducible results. The fourth gave values which varied from day to day, and all measurements on gas from this cylinder have been discarded. The cylinders were cooled to -20°C to liquefy the ethylene, and then "blown off" to remove any traces of non-condensing gases. Ethylene was then evaporated through phosphorus pentoxide into evacuated acoustical chambers of a design which has already been described.[7] The apparatus was washed with gas several times before each measurement.

The measurements, combined by means of smoothed curves, permit comparison for theoretical purposes with an accuracy somewhat greater than 0.1 percent. It is not possible, however, to estimate here their absolute accuracy.

B. The low frequency terminal velocity

A measurement of the velocity of sound at 9 kc, 30°C, and 770 mm gave 332.8 m sec.$^{-1}$. In order to idealize this quantity it was multiplied by a factor of 1.0035, which was obtained from the van der Waals constants $a=4.47\times10^{6}$ cm^{6} atm. mole^{-1} and $b=57.14$ cm^{3} mole^{-1}. The resulting figure is 333.9 m sec.$^{-1}$, which disagrees gravely with 336.1 m sec.$^{-1}$ calculated in a similar manner from the empirical equation given in the *International Critical Tables*. We cannot account for this discrepancy. It should be noted, however, that the equation given in the *International Critical Tables* results from a combination of the measurements of six different observers, who are in violent mutual disagreement.

No wholly satisfactory data on the heat capacity appear to be available. The most recent study has been made by Haas and Stegeman,[8] who give values which are slightly lower than those reported by previous writers. Their results are quoted without specification of the pressure, and are considered to vary linearly with temperature from 3° to 67°C; both of these approximations leave much to be desired from the standpoint of the present work. If their empirical equation for the temperature coefficient is valid $(1/C_v)(dC_v/dT)=2.5\times10^{-3}$, and if it is considered that the empirical equation refers to the heat capacity of the gas at zero pressure C_0 at 30°C is 8.20 cal. mole^{-1} deg.$^{-1}$. The corresponding ideal velocity is 334.2 m sec.$^{-1}$, whereas the idealized experimental velocity at 9 kc is 333.9 m sec.$^{-1}$. The agreement is better than that to be expected considering the various possibilities for error, and it is concluded that no important part of the heat capacity of ethylene is lacking in the adiabatic compressibility at 9 kc, 760 mm pressure and 30°C. No band spectral analysis of sufficient scope to confirm or to modify this conclusion is known to us.

C. The variation of the velocity of sound with pressure and frequency

The results of a study of the variation of the velocity of sound in the dispersive region with pressure at 30°C are reported in Table I. A large number of determinations were made at 790 mm because this measurement served as a test of the purity of the ethylene. The spread of points is great, being ±0.45 m sec.$^{-1}$ for the 94 kc and ±0.75 m sec.$^{-1}$ for the 451 kc points. It is to be noted, however, that the difference $V_{451}-V_{94}$ has a maximum variation of ±0.35 m sec.$^{-1}$, which is less than half that of the 451 kc measurements.

Table I. *The variation of the velocity of sound in ethylene with pressure and frequency at 30°C.*

			At 451 kc			
P in mm	790	472	236	83	60	60
V in m sec.$^{-1}$	335.4*	337.6	341.4	345.7	344.8	345.7
w	1.007	1.004	1.002	1.001	1.001	1.001
			At 94 kc			
P	790	472	236	83		
V	333.1*	333.9	334.5	339.5		
w	1.007	1.004	1.002	1.001		

* These figures are the average of the following determinations each pair of which was made on a separate sample of gas.

450 kc	335.9	335.6	335.8	335.3	334.7	335.4	336.2	334.9
94 kc	333.4	333.6	333.1	333.1	332.9	332.7	333.3	332.7

[7] Richards and Reid, J. Chem. Phys. **1**, 114 (1933).

[8] Haas and Stegeman, J. Phys. Chem. **36**, 2127 (1932).

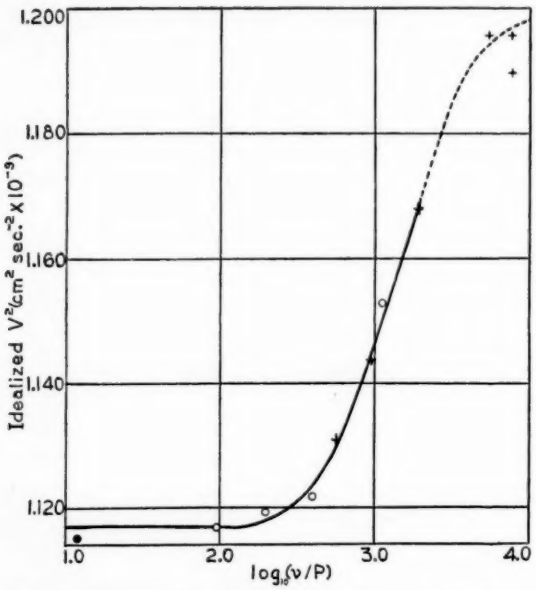

FIG. 1. The variation of the velocity of sound in ethylene with frequency and pressure at 30°C. 9 kc measurements indicated by black dots, 94 kc by circles, and 451 kc by plus signs. The line connecting the points is drawn from theoretical considerations discussed in the text.

Fig. 1 summarizes graphically the results of Table I by plotting, in the usual way, the square of the idealized velocity against the logarithm of the ratio of the acoustical frequency in Herzian cycles and the pressure in mm Hg equivalents. Several points in connection with this diagram should be noted. The S-curve has been drawn, according to the customary three-state approximation, from the points corresponding to $C_0 = 8.20$ cal. deg.$^{-1}$ mole^{-1} and $C_\infty = 5.96$ cal. deg.$^{-1}$ mole^{-1}. The experimental values in the neighborhood of the supposed high frequency terminal velocity were made at very low pressures, and, because of the small mass reaction of the gas on the oscillator under these conditions, were of conspicuously less accuracy than the other determinations. An oscillator of higher frequency was not available, and no search for a constant velocity in the upper part of the dispersive region could therefore be undertaken. The moment of inertia of the hydrogen atoms around the carbon-carbon axis is so small that ethylene may enter a rotational dispersive region, analogous to that exhibited by hydrogen,[9] before the dispersive region due to the vibrations is wholly complete. The upper part of the S-curve has been drawn as a broken line to emphasize this uncertainty. No evidence for complexity of the dispersive region is, however, revealed by the measurements, since they fall uniformly on the S-curve within limit of experimental error.

D. The variation of the velocity of sound with temperature

A study of the temperature coefficient of the velocity at 94 and at 451 kc gave a series of measurements which are reported in Table II. The temperature coefficient was studied with somewhat more than the usual care, since by means of it certain conclusions may be reached which are directly serviceable in Section II.

TABLE II. *The velocity of sound in ethylene at 790 mm pressure and various temperatures.*

				At 451 kc			
T°C	15.0	15.3	22.5	25.0	27.8	30.0	32.5
V m sec.$^{-1}$	328.3	328.7	331.8	333.5	334.2	335.4*	336.3
T	35.0	35.0	37.5	40.0	40.0	42.0	45.0
V	336.8	337.1	338.6	340.1	340.0	340.5	341.7
				At 94 kc			
T	15.0	15.3	20.0	22.5	25.0	27.8	30.0
V	325.5	325.7	328.1	329.4	330.7	332.0	333.1*
T	35.0	35.0	40.0	40.0	42.0	45.0	45.0
V	335.2	335.5	337.4	337.5	338.5	340.1	340.0

* Each of these values is the average of the eight determinations on different samples of ethylene gas which are quoted in Table I.

The continuous line connecting the 94 kc measurements is drawn from the data for the heat capacity quoted in B of this section, and from the equation $V_0 = \{(RT/M)(1+R/C_0)\}^{\frac{1}{2}}$. It is to be noted that the disagreement of the points with the theoretical line is never greater than 0.3 m sec.$^{-1}$, which is well within a reasonable limit of absolute error for the velocity determinations. The theoretical line is, however, almost rectilinear, whereas a slight consistent tendency for the points to fall under this is observable both below and above 30°C. A dotted line has been drawn between the 451 kc measure-

[9] Abello is apparently the discoverer of this dispersive region. Bourgin and Herzfeld and Rice (Phys. Rev. **31**, 691 (1928)) have attributed it to the failure of rotational energy adjustment; Kneser has recently supported this interpretation.

ments to give the most probable value of the velocity at this frequency at 790 mm pressure. The deviations of the experimental points from this average value is naturally somewhat greater than in the case of the 94 kc measurements.

E. Conclusions from the velocity of sound in pure ethylene

Owing to the lack of adequate band-spectral data it is not possible at present to describe the velocity of sound in the dispersive region in fundamental terms. The results may, however, be expressed in terms of numbers which will take on an exact meaning when the energy levels of the molecule are unequivocally defined.

From the ideal velocity of sound at a given temperature and various pressures and frequencies a characteristic time, ϑ, may be computed by the relationship

$$\vartheta = (C_0/\omega C_\infty)\{(V_\omega^2 - V_0^2)/(V_\infty^2 - V_\omega^2)\}^{\frac{1}{2}}, \quad (1)$$

in which C_0 and C_∞ are the heat capacities when $\omega^2\vartheta^2 \leqq 0$ and $\omega^2\vartheta^2 \leqq \infty$, respectively, V_0 and V_∞ the corresponding ideal velocities, and V_ω the velocity at a circular frequency ω. This expression is approximate in several respects: notably a correction for the absorption has been neglected, and the time ϑ is without quantitative meaning in terms of specific transitions. The variations of ϑ with pressure and temperature, nevertheless, permit certain conclusions.

The conformity of experimental points to a symmetrical S-curve illustrated in Fig. 1 demonstrates, for example, that double collisions are the only appreciable means by which the various energy states which cause the dispersive region are excited. Similarly, since ϑ has been found to be independent of frequency and directly dependent upon the numerical density, the transition probabilities are sensibly equal from an acoustical standpoint for all of the contributing states. This strongly suggests that the vibrational energy attains equilibrium on every effective collision. The maximum acoustical absorption at 760 mm and 30°C evidently occurs at about 1.0×10^6 cycles sec.$^{-1}$. At this temperature and pressure the time ϑ has a value of 2.38×10^{-7} sec.

The activation energy of collision is evidently not great since the increase in $V_{451} - V_{94}$ is only 1.2 m sec.$^{-1}$ between 45° and 15°C (Fig. 2). In

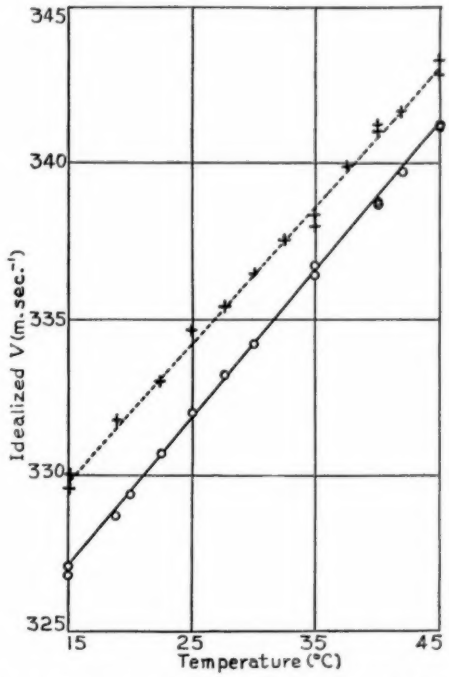

FIG. 2. The variation of the velocity of sound in ethylene with temperature at 780 mm. The line connecting the 94 kc points, which are indicated by circles, is the calculated ideal velocity. The dotted line connecting the 451 kc points, which are indicated by plus signs, assumes an activation energy of collision of 2800 cal. mole^{-1}.

such cases it is probable that the variation of the effective molecular cross section with temperature must be taken into account in the kinetic analysis of the transition probabilities. However, an upper limit for the activation energy of collision A may be simply obtained by writing, at temperatures T and T',

$$\vartheta'/\vartheta = (T'/T)^{\frac{1}{2}} e^{-(A(T'-T)/RTT')} \quad (2)$$

which involves the approximations that the cross section of the molecule is independent of the temperature, and that $(1+e^{-x})/(1+e^{-x'}) = 1$, where $x = h\nu_0/kT$. Since ϑ is 1.93×10^{-7} sec. at 45°C and 2.73×10^{-7} sec. at 15°C, the activation energy of collision is evidently about 2800 cal. mole^{-1}. If this value is substituted into the usual kinetic expression, it is found that the least separation of ethylene molecules on an effective collision is about 2×10^{-8} cm, which is only about a half of that found in ordinary kinetic processes. Since the measurements of the temperature coefficient of the velocity are unusually precise

and concordant, it is believed that the agreement of these two quantities is significant, and that no serious stearic difficulty can be responsible for the failure of the vibrational energy to maintain its equilibrium distribution in the sound wave at high frequencies. A line drawn on the supposition that the activation energy of collision is 2800 cal. mole^{-1} is identically the dotted line of Fig. 2.

II. Binary Mixtures of Ethylene with Other Gases

The velocity of sound in a binary mixture of a gas A and a gas B will be approximately[10]

$$V^2=\frac{P}{\rho_A m+\rho_B(1-m)}\left\{1+R\frac{C_{0A}m+C_{0B}(1-m)+\omega^2\vartheta^2[C_{\infty A}m+C_{0B}(1-m)]}{[C_{0A}m+C_{0B}(1-m)]^2+\omega^2\vartheta^2[C_{\infty A}m+C_{0B}(1-m)]^2}\right\}, \tag{3}$$

where ϑ is the characteristic time in the particular mixture, P, C and ρ refer to pressure, heat capacity, and density at P respectively, and m is the concentration of A expressed as a mole fraction. This expression is approximate in that it neglects absorption, and in that the characteristic time represents only roughly the reciprocal of the sum of the various transition probabilities involved in that part of the heat capacity $(C_{0A}-C_{\infty A})$ which causes the dispersive region.

The velocity of sound in binary mixtures of ethylene with nitrogen, argon, helium and hydrogen has been measured, and the results and conclusions are reported below. The two gases were mixed under pressure in a reservoir and subsequently fed into the acoustical apparatus at a pressure of 780 mm. The gases were dried with phosphorus pentoxide, but not otherwise purified. The mixture was analyzed at the end of an experiment by absorbing the ethylene in fuming sulfuric acid, and measuring the residual volume of gas. This procedure was not of great accuracy, and a reproducibility of the measurements comparable to that obtained in the previous section is not to be expected. The temperature was uniformly maintained at 30°C.

Since the P, v, T relations of these mixtures have not been extensively studied, the procedure of idealizing the measured velocities of sound by the use of an acoustical equation which includes the second virial coefficient is not practicable. As an alternative the actual properties of the various gases, from data given in the *International Critical Tables*, were used for substitution into (3). They are summarized in Table III.

Table III. *The acoustical constants of several gases.*

Gas	A	C_2H_4	He	H_2	N_2
ρ in g cm^{-3} at 30°C and 780 mm	1.649 $\times10^{-3}$	1.166 $\times10^{-3}$	1.651 $\times10^{-4}$	8.407 $\times10^{-5}$	1.157 $\times10^{-3}$
C_0/R at 30°C	1.5	4.115	1.5	2.46	2.504

A. Ethylene-argon, nitrogen, and helium mixtures

The various measurements at 94 and 451 kc are summarized in Table IV. In the case of nitrogen the results may be numerically reproduced by (3) only if ϑ is taken as being identical with ϑ obtained from the study of pure ethylene at a corresponding partial pressure. The agreement between the calculated and observed velocities is within experimental error, as a

Table IV. *The velocity of sound at 780 mm and 30°C in various binary gaseous mixtures containing ethylene as one constituent.*

				Argon mixtures				
m	0.952		0.850		0.625		0.445	
V_{451}	333.2		330.1		324.3		322.0	
V_{94}	331.3		327.0		319.9		316.8	
				Nitrogen mixtures				
m	0.970	0.959	0.895	0.870	0.851	0.800	0.635	0.500
V_{451}	335.7	335.8	337.5	337.7	337.7	339.2	342.6	346.2
V_{94}	333.8	334.1	335.2	335.3	335.8	343.1	339.5	—
				Helium mixtures				
m	0.940		0.900		0.852		0.760	
V_{451}	343.5		348.6		356.4		373.1	
V_{94}	—		345.0		352.4		368.5	

[10] This type of expression was first developed by Bourgin. The one here printed has been obtained from Einstein's treatment of the dispersion theory. See Richards, J. Chem. Phys. **1**, 877 (1933).

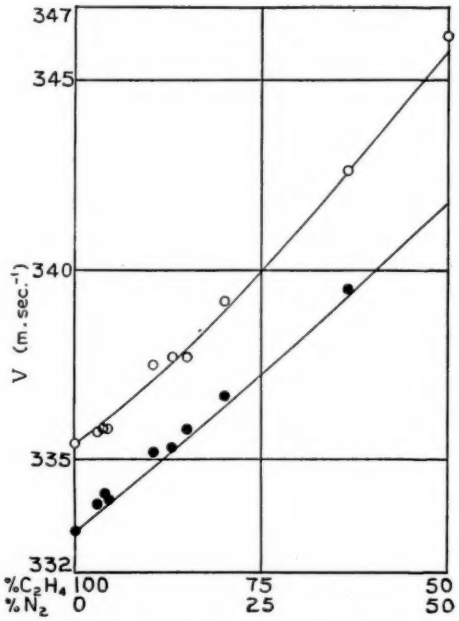

FIG. 3. The velocity of sound in nitrogen-ethylene mixtures at 780 mm and 30°C. The lines are calculated from the data in Table III; black dots indicate 94 kc and circles 451 kc.

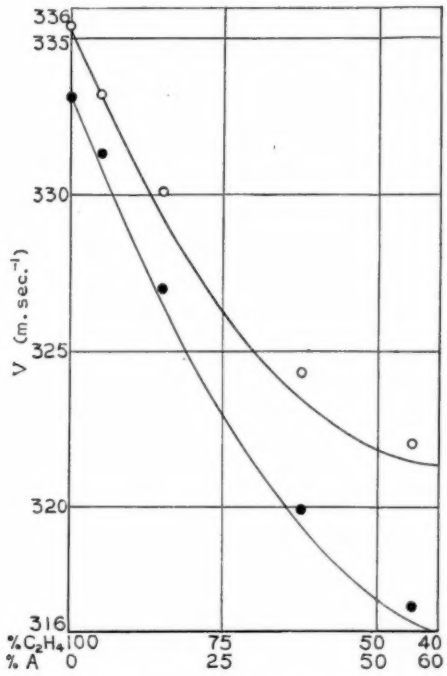

FIG. 4. A comparison of the measured and calculated velocities of sound in ethylene-argon mixtures at 780 mm and 30°C.

glance at Fig. 3 demonstrates. With argon the agreement is not so satisfactory, since the experimental points lie increasingly above the calculated line with increasing concentrations of argon. A measurement on a sample of the argon employed gave a velocity of sound of 325.3 m sec.$^{-1}$ both at 451 and at 94 kc. Since this is conspicuously higher than the value 324.1 m sec.$^{-1}$ obtained from (3) when $m=0$ the discrepancy may safely be attributed to impurity of the argon.

With the helium measurements it is apparent that an even greater error due to impurity is present. At $m=0.75$, V_{451} calculated using the ϑ obtained from pure ethylene, is 386.7 m sec.$^{-1}$ and $V_{451\ \mathrm{obs.}}$, read from a smoothed curve through the experimental points, is 375.0 m sec.$^{-1}$. Similarly, at $m=0.75$, $V_{94\ \mathrm{calc.}}$ is 382.5 whereas $V_{94\ \mathrm{obs.}}$ is only 370.3. It is to be noted, however, that $(V_{451}-V_{94})_{\mathrm{calc.}}$ is 4.2 m sec.$^{-1}$ which agrees reasonably well with $(V_{451}-V_{94})_{\mathrm{obs.}}$ which is 4.7 m sec.$^{-1}$. Similarly at $m=0.90$ the calculated difference is 3.0 m sec.$^{-1}$ and the experimental 3.6 m sec.$^{-1}$. There can be little question, therefore, that the cause of error is the inclusion in the helium of a few percent of some denser impurity. Since *a priori* this is extremely likely, no serious concern is felt because of the lack of absolute agreement between the experimental and theoretical velocities.

Within experimental error, therefore, collisions of argon, nitrogen, and helium molecules fail entirely to bring about vibrational energy transitions in ethylene. It may roughly be estimated that their collision efficiencies must be less than a tenth that of the ethylene-ethylene collision.

B. Mixtures of hydrogen and ethylene

Measurements on hydrogen-ethylene mixtures are reported in Table V. It should be noted that the determinations at 94 kc which result in a velocity of sound greater than 400 m sec.$^{-1}$ are of

TABLE V. *The velocity of sound in hydrogen-ethylene mixtures at 780 mm and 30°C.*

m	0.950	0.940	0.890	0.780	0.51	0.306	0
V_{451}	342.5	345.3	354.0	376.4	462.9	584.2	1409
V_{94}	341.6	344.7	353.1	376.1	461.5	578.8	1319

considerably less accuracy than those below this figure. This is both because the tube-correction has not been determined for the apparatus at large velocities, and because the dimensions of the apparatus did not permit the detection of many points of maximum reaction when the wave-length was large. The agreement of the velocity at very low frequency calculated from (3) and that determined by experiment at 94 kc is in all cases satisfactory, however, and little hesitation is felt in basing approximate conclusions on the entire range of measurements.

It is at once apparent from an inspection of Table V that two independent tendencies are at work, since $\Delta V(=V_{451}-V_{94})$ nearly vanishes in a mixture for which $m=0.75$, and increases markedly on either side of this composition. This behavior is plausibly explained if it is supposed that hydrogen-ethylene collisions are more efficient than ethylene-ethylene collisions in exciting the vibrational energy of ethylene, and that, conversely, ethylene-hydrogen collisions are more efficient than hydrogen-hydrogen collisions in exciting the rotational energy of hydrogen. A somewhat complicated situation results, which may most simply be described by the expression[11]

$$V^2=\frac{P}{\rho}\left\{1+\frac{R(1-\omega^2\vartheta_A\vartheta_B)(C_0-C_\infty\omega^2\vartheta_A\vartheta_B)+R\omega^2(\vartheta_A+\vartheta_B)[C_\infty(\vartheta_A+\vartheta_B)+C_A\vartheta_B+C_B\vartheta_A]}{(C_0-C_\infty\omega^2\vartheta_A\vartheta_B)^2+\omega^2[C_\infty(\vartheta_A+\vartheta_B)+C_A\vartheta_B+C_B\vartheta_A]^2}\right\}. \quad (4)$$

In (4) subscript A refers to ethylene and subscript B refers to hydrogen, and

$$C_0=C_{0A}m+C_{0B}(1-m),$$
$$C_\infty=C_{\infty A}m+C_{\infty B}(1-m),$$
$$C_A=(C_{0A}-C_{\infty A})m, \quad C_B=(C_{0B}-C_{\infty B})(1-m),$$

the heat capacities being expressed per mole and m indicating the mole fraction of A. As before $\rho_A m+\rho_B(1-m)=\rho$, ρ_A and ρ_B being, of course, the densities of A and of B at P. Finally

$$\vartheta_A=\vartheta^\circ_{AA}/[m+\epsilon_B(1-m)],$$
$$\vartheta_B=\vartheta^\circ_{BB}/[(1-m)+\epsilon_A m],$$

where ϵ_B is the relative efficiency, at *unit concentration*, of the ethylene-hydrogen collision and the ethylene-ethylene collision, and ϵ_A is the relative efficiency, at *unit concentration*, of the ethylene-hydrogen and the hydrogen-hydrogen collision. ϑ^0_{AA} is the "relaxation time" of the ethylene-ethylene collision, and ϑ^0_{BB} that of the hydrogen-hydrogen collision, both expressed at a numerical density corresponding to P. These are determined from the properties of the pure gases, and appropriate values of ϑ_A and ϑ_B found from gaseous mixtures containing small percentages of A and of B respectively.

In order to relate ϑ_A and ϑ_B to the relative efficiency of $A-B$ and $A-A$ or $B-B$ collisions, expressed *per collision*, it is further necessary to consider the velocity and cross section of the A and B molecules. Ordinary kinetic considerations show that, at equal numerical densities, the factor relating number of collisions to concentration is $(\sigma_A+\sigma_B)^2(M_A+M_B)^{1/2}/2^{5/2}\sigma_A{}^2M_B{}^{1/2}$, where σ indicates the kinetic diameter and M the molecular weight. By using σ_A (ethylene) = 4.3

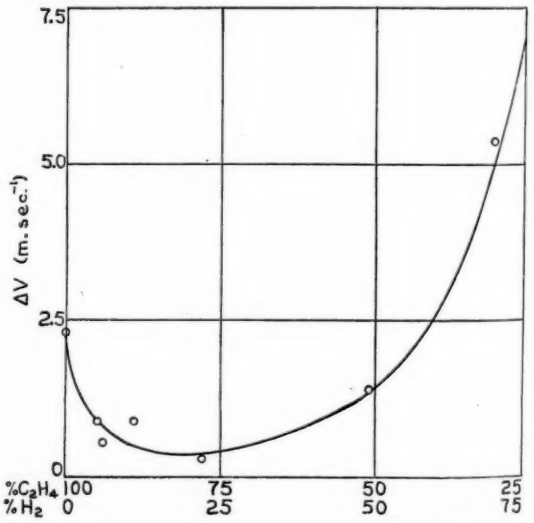

FIG. 5. A comparison of the measured difference in velocity of sound at 451 and at 94 kc. (ΔV) with that calculated on the assumption that an ethylene-hydrogen collision is twenty times as effective in causing transitions in the rotational energy of hydrogen as a hydrogen-hydrogen collision, and ten times as effective in causing transitions in the vibrational energy of ethylene as an ethylene-ethylene collision.

[11] This corresponds to Eq. (6.1) Richards, J. Chem. Phys. 1, 877 (1933).

$\times 10^{-8}$ cm and σ_B (hydrogen) $= 2.2 \times 10^{-8}$ it is found that a molecule suffers 1.53 times as many collisions in a given concentration of hydrogen as in a given concentration of ethylene.

The results of the measurements at 780 mm and 30°C indicate that a hydrogen-ethylene collision is about 10 times as effective as an ethylene-ethylene collision in exciting the vibrational energy of ethylene, and that an ethylene-hydrogen collision is about 20 times as effective in giving rotational energy to hydrogen as a hydrogen-hydrogen collision. The correspondence of these assumptions with experiment is indicated by Fig. 5, where the heavy line indicates ΔV calculated from (4) on this basis and the circles are the experimental points. The agreement is within experimental error, and justifies the assumption, which is implicit in (4), that the adjustment of rotational energy in hydrogen is effected by a double-collision mechanism. It remains to attempt to reach an understanding of these findings.

III. Discussion

It has been concluded in the previous sections that collisions with hydrogen are extremely effective in bringing about transitions between the lower vibrational energy states of ethylene, whereas collisions with argon, helium and nitrogen are virtually without effect. This raises the question which has been discussed in connection with the maintenance of the unimolecular decomposition rates of the paraffins by hydrogen. What advantage has the hydrogen molecule over other molecules (with the exception of the vibrating molecule itself and its close chemical analogs as, for example, its decomposition products) in effecting the conversion of translational energy into vibrational energy? We cannot attempt to answer this question here. A very brief review of several methods of attack will, however, be given in order to emphasize the necessity for further experiment.

It does not appear that the small mass of the hydrogen molecule can be of primary importance in this connection. If the laws of molecular impact are formulated in a purely classical manner, after the method initiated by Oldenberg,[12] it is possible to imagine that a single hydrogen atom could give a part of its translational energy to a single more massive atom of some other molecule, and that all of the energy so imparted should appear as vibrational energy after the termination of the collision. The necessity for the conservation of linear momentum allows hydrogen a maximum advantage of a factor of less than two over helium in such a process. The experimental data, which indicate that this factor is in excess of 20, clearly demand another explanation.

The quantum mechanical approach to the problem leads to more promising conclusions. Zener[13] and Rice[14] have attempted solution by these means. Franck and Eucken[15] have reduced this treatment to a qualitative picture which is more suitable for discussion here. It is supposed that the forces which ultimately make themselves felt by atomic exchange reactions are, with low relative translational energies, capable of causing small displacements of the nuclei in the colliding molecules. The efficiencies of various collisions are thus in a sense conditioned by the chemical reactivity of the participating molecules. In this respect hydrogen differs profoundly from helium, and a qualitative explanation for its advantage is found. A somewhat similar variant of the quantum mechanical treatment was suggested in Part II[16] of this series when a mutual "bond-softening" of the colliding molecules was discussed. The great disadvantage of these methods of treatment is that they cannot, at present, supply numbers which may be compared with those obtained from actual measurement. The necessity for estimating the duration of the collision by the formulation of some dynamical mechanism of approach and separation of the molecules is a source of difficulty. It is not

[12] Oldenberg, Phys. Rev. **37**, 194 (1931); Heil, Zeits. f. Physik **14**, 31 (1932).

[13] Zener, Phys. Rev. **38**, 277, 556 (1931).

[14] Rice, Phys. Rev. **38**, 1943 (1931); J. Am. Chem. Soc. **54**, 4558 (1932).

[15] Franck and Eucken, Zeits. f. physik. Chemie **B20**, 460 (1933).

[16] Richards, J. Chem. Phys. **1**, 874 (1933).

possible, therefore, to accept this type of explanation without reserve in spite of its great plausibility.

Yet a third distinctive property of the hydrogen molecule, which has not been greatly stressed in this connection, arises from the smallness of its moment of inertia. As a result the rotational quanta for hydrogen are immense, and it has failed to attain a classical distribution of rotational energy even at room temperature. The occurrence of a dispersive region due to the failure of the rotational transitions to follow the acoustical cycle is surely due to this property; Zener has, indeed, essentially predicted such behavior.[13] It is suggestive that, since ethylene is conspicuously more successful than hydrogen in giving rotational energy to hydrogen, it must also be that hydrogen can give its rotational energy to ethylene with relative ease. It appears at least possible that the magnitude of the rotational quanta which are so exchanged may be connected with the conspicuous effectiveness of the hydrogen molecule in exciting vibrational energy. If approximate "matching" or resonance occurred between a hydrocarbon vibrational quantum and a hydrogen rotational quantum a fresh basis on which to build an explanation would appear.

Owing to the ill-defined condition of the present theoretical background it appears wiser to await an expansion of the very meager experimental material before attempting an explanation of the phenomena which have here been discussed. Comparative measurements of light and of heavy hydrogen at once suggest themselves as likely to provide desirable information. The chemical characteristics of the two are practically identical, and hence their behavior from the Franck-Eucken standpoint should be similar. The mass of the molecule of the heavy isotope is very near to that of helium, and any purely mass effects should, therefore, be readily separable. The larger moment of inertia of heavy hydrogen should on the other hand, profoundly alter any distinctive behavior which is due to rotational energy, and its smaller vibrational quantum should enhance any effects due to vibrational resonance. In this direction we hope for immediate progress.

LETTERS TO THE EDITOR

This section will accept reports of new work, provided these are terse and contain few figures, and especially few halftone cuts. The Editorial Board will not hold itself responsible for opinions expressed by the correspondents. Contributions to this section must reach the office of the Managing Editor not later than the 15th of the month preceding that of the issue in which the letter is to appear. No proof will be sent to the authors. The usual publication charge ($3.00 per page) will not be made and no reprints will be furnished free.

Raman Spectra of HCl in Non-Ionizing Solvents

In the course of study of the nature of dissolved molecules we have investigated the Raman effect of HCl dissolved in various solvents. The results here communicated are for the vibration frequency of HCl in some non-ionizing solvents. Woodward[1] has reported his inability to observe the Raman spectrum of HCl dissolved in carbon tetrachloride, benzene and xylene, pointing out, however, that the negative result was probably to be ascribed to the low solubility of HCl in these solvents. This difficulty we have circumvented by the obvious device of examining the scattered spectra at a temperature at which the solubility of HCl in the various solvents was adequate, the mol. fraction of HCl in the solutions being about 0.2 and the temperature −65°C. By ν in Table I is indicated the frequency difference between the exciting line (Hg 4047) and the long wave side of the HCl band, which, if the latter is an unresolved Q branch with the same relation of rotational lines as in the gas, corresponds approximately to the vibrational frequency of the molecule in the lowest state. $\Delta\nu$ describes the difference between ν in solution and ν observed by Wood and Dieke and by Salant and Sandow for the gas (2886).

TABLE I.

Solvent	Electric moment $\times 10^{18}$	Diel. Const. at −65°	ν cm^{-1}	$\Delta\nu$
Silicon tetrachloride	0		2860	26
Phosphorus trichloride	0.90	10.3	2824	62
Chloroform	1.03	7	2826	60
HCl liquid (Salant and Sandow)[2]	1.08	8.8(−90°C)	2800	86
Sulphur dioxide	1.63	25	2798	88
Ethyl bromide	1.83	14	2797	89
Acetyl chloride	2.7	20.5	2804	82

The electric moments listed are for the solvents in the gaseous state or in dilute solution in nonpolar solvents. When ν is plotted against the electric moment of the solvents, a straight line is obtained, within the accuracy of the measurement of ν, ± 5 cm^{-1}, up to the value of μ for ethyl bromide. It is not at all surprising that the shift in frequency should cease to be proportional to the electric moment of solvent molecules of high electric moment as measured in the attenuated state, for it is well known that the polarization of complicated molecules of large electric moment may diminish very markedly with concentration. The approximate proportionality of the frequency shift with the electric moment of the molecules of the solvent would seem to indicate that a large part of the shift is due to dipole interactions between solvent and solute molecules, and as the frequency of liquid HCl is of the same order as in solvents of the same electric moment as HCl, the shift between gas and liquid in this case can also be largely attributed to dipole action, as indeed is suggested by the fact that the frequency difference between gas and liquids for the nonpolar mols H_2, O_2, N_2, CH_4 is much smaller than for polar molecules.

The results have some bearing on the nature of the ionization process in HCl molecules. The diminution in vibration frequency with increasing dipole moment of the solvent indicates a diminution of the force constant for the vibration, i.e., a diminution of the strength of binding between the hydrogen and chlorine nuclei. The HCl molecule in a polar environment may be regarded in a state of incipient dissociation, and the diminution of binding strength is in a sense the effect recognized by Nernst and J. J. Thomson in their correlation between ionizing power and the dielectric constant of solvents; but it is also very obvious from our results that electrolytic dissociation by pure dipole interaction would require a solvent of enormously greater electric moment than any yet found. Where electrolytic dissociation of HCl actually occurs in the solvents in what it has been observed, many of which, like water, alcohol, ether, have electric moments lower than some of these investigated by us, the essential process is probably, as has often been stated, the attach-

[1] Woodward, Phys. Zeits. **32**, 777 (1931).

[2] R. W. Wood and G. H. Dieke, Phys. Rev. **35**, 1355 (1930); E. O. Salant and A. Sandow, Phys. Rev. **37**, 373 (1931).

ment of a H^+ by valence forces to the oxygen atom of the solvent molecules.

It is also of some interest to inquire if the increase of the electric moment of HCl from a value of 1.08×10^{-18} e.s.u. in the gas to about 1.3×10^{-18} in benzene, hexane and carbon tetrachloride, reported by F. Fairbrother[3] could be accounted for by the stretching of the molecule in solution.

Assuming the constancy of the expression νr^2 where r is the internuclear distance, one finds that the greatest change in ν, in highly polar solvents, corresponds to an increase in r of some 3 percent and in nonpolar solvents it would be much less. An increase of 20 percent, to 30 percent in the electric moment of HCl dissolved in nonpolar solvents cannot be attributed to the elongation of the molecule which takes place on solution.

The investigation is being extended to the other hydrogen halides both by the study of Raman and infrared spectra.

Wm. West
Paul Arthur

Department of Chemistry,
Washington Square College,
New York University,
February 20, 1934.

[3] F. Fairbrother, J. Chem. Soc., p. 43 (1932).

On the Calculation of the Probability of the Spontaneous Decomposition of Linear Triatomic Molecules

In his paper *Lifetimes of Unstable Molecules*,[1] N. Rosen has calculated the probability of spontaneous decomposition of the "quasi-molecule" HO_2 into the molecule O_2 and atom H.

His method of calculation is as follows: When we treat the molecule HO_2 as linear, the wave equation of the system may be represented in the following form:

$$\left\{-\frac{h^2}{8\pi^2}\left[\frac{1}{\mu_1}\frac{\partial^2}{\partial r_1^2}+\frac{1}{\mu_2}\frac{\partial^2}{\partial r_2^2}-\frac{2}{m_2}\frac{\partial^2}{\partial r_1\partial r_2}\right]+V_1(r_1)+V_2(r_2)\right\}$$

$$\times\psi(r_1, r_2)=E\psi(r_1, r_2), \quad (1)$$

where $r_1=x_2-x_1$, $r_2=x_3-x_2$ (x_1, x_2 and x_3 are the distances of atoms m_1, m_2 and m_3 from a certain fixed point), $\mu_1=m_1m_2/(m_1+m_2)$, $\mu_2=m_2m_3/(m_2+m_3)$ and $V_1(r_1)$, $V_2(r_2)$ are the potential energies of the two end-atoms with the middle one (the interaction between the end-atoms is neglected).

The term,

$$T=(h^2/4\pi^2m_2)(\partial^2/\partial r_1\partial r_2)=(1/m_2)p_1p_2 \quad (2)$$

is considered by Rosen as the perturbation energy; in this case the variables in the Eq. (1) can be separated and the probability of spontaneous decomposition of the molecule is defined in the usual way through the matrix elements of (2).

The perturbation method can be applied, however, only in that case, when the matrix elements of the perturbation energy are sufficiently small compared with the energy differences of the states under consideration, i.e., when:

$$|T_{n,\,n^1}|\ll|W_n-W_{n^1}|. \quad (3)$$

For the sake of simplicity we approximate the wave functions of the unperturbed problem referring to the discrete states by the wave functions of two harmonic oscillators (which is certainly valid for not too large values of the quantum numbers, n_1 and n_2). The nonvanishing matrix elements of the perturbation energy are in this case those corresponding to transitions $n_1\to n_1\pm1$, $n_2\to n_2\pm1$. We shall restrict ourselves to the case of two opposite jumps corresponding to the smallest values of the difference $W_n-W_{n^1}$. We get in this case:

$$T_{n_1n_1^1;\,n_2,\,n_2^1}=(1/m_2)p_{n_1,\,n_1^1;\,n_2,\,n_2^1}$$
$$=hA[n_1(n_2+1)]^{\frac{1}{2}}, \text{ if } n_1^1=n_1-1,\ n_2^1=n_2+1$$
$$=hA[n_2(n_1+1)]^{\frac{1}{2}}, \text{ if } n_1^1=n_1+1,\ n_2^1=n_2-1,$$

where $A=(1/2m_2)(\mu_1\mu_2\nu_1\nu_2)^{\frac{1}{2}}$, ν_1 and ν_2 being the frequencies of the respective bonds. The condition (3) assumes the following form:

$$\left.\begin{aligned}A[n_1(n_2+1)]^{\frac{1}{2}}&\ll|\nu_1-\nu_2|\\A[(n_1+1)n_2]^{\frac{1}{2}}&\ll|\nu_1-\nu_2|\end{aligned}\right\}. \quad (3')$$

Now it can easily be seen that this condition is *not* fulfilled either for the "quasi-molecule" HO_2 or for linear triatomic molecules known.

For the "quasi-molecule" HO_2 we have $A=0.6\times10^{13}$, $|\nu_1-\nu_2|=6\times10^{13}$ for the values of $n(n_1=4,\ 3,\ 2,\ 1;\ n_2=16,\ 17,\ 19,\ 21)$ used by Rosen both sides of the inequality (3') are of the same order of magnitude. For the molecule N_2O, we have: $A>|\nu_1-\nu_2|$, ($A=1.63$; $|\nu_1-\nu_2|=1.36$). For the symmetrical molecules CO_2 and CS_2 $|\nu_1-\nu_2|=0$, the term $A[n(n+1)]^{\frac{1}{2}}$ is, however, >0.

It follows that by dropping in Eq. (1) the "perturbation energy" (2) we do not obtain any approximations to the actual stationary states of the molecules, so that Rosen's perturbation method cannot be applied.

T. Kontorova
V. Sorokin

Leningrad,
Institute of Chemical Physics,
February 8, 1934.

[1] N. Rosen, J. Chem. Phys. **1**, 319 (1933).